

Osteogenic Effects of Pigment Epithelium Derived Factor on Mesenchymal Stem Cells

Mina Elahy

College of Health and Biomedicine Victoria University

**Submitted in fulfillment of the requirements of the degree of doctor of
philosophy**

July 2015

Abstract

The field of bone tissue engineering has expanded in the recent decade to meet the increasing need to replace bone tissue in skeletal disease, congenital malformation, trauma, and tumours. Stem cell encapsulation has become a promising method in the future of this field. Alginate is a natural polymer that has been used widely for stem cell transplantation due to its biocompatibility. Pigment epithelium-derived factor (PEDF) is known for its anti-cancer properties due to its anti-angiogenic and anti-proliferative properties, particularly against osteosarcoma, a type of primary bone cancer. This study investigated the osteogenic effect of PEDF on mesenchymal stem cells (MSCs) in monolayer cell cultures and encapsulated in alginate beads *in vitro* and *in vivo*. Stem cells were isolated from the bone marrow of mouse long bones, and PEDF was used as an osteogenic supplement to differentiate MSCs to osteoblasts in both monolayers and in alginate beads (3D structure). Differentiation to osteoblasts was evaluated by qualitative and quantitative methods such as immunocytochemistry, mineralisation staining, and immunoblotting for the *in vitro* part of the study. The *in vitro* study shows that PEDF can stimulate MSCs to differentiate into osteoblasts in both monolayers and alginate beads. Furthermore, alginate beads containing PEDF degraded significantly in comparison to alginate beads alone, indicating that PEDF could be used as an agent to modify alginate and make it suitable for stem cells to interact and proliferate inside the beads. These results then have been taken further to an *in vivo* ectopic model. The findings from immunohistochemistry for several bone markers as well as

microcomputed tomography (μ CT) analysis indicate that PEDF in a physiological dose is able to induce bone formation *in vivo* with and without co-encapsulation with MSCs. These findings can be useful in order to introduce a new biological model for future use in clinical bone tissue engineering.

Student declaration

Doctor of Philosophy Declaration

“I, Mina Elahy, declare that the PhD thesis entitled “osteogenic effects of pigment epithelium derived factor on mesenchymal stem cells” is no more than 100,000 words in length including quotes and exclusive of tables, figures, appendices, bibliography, references and footnotes. This thesis contains no material that has been submitted previously, in whole or in part, for the award of any other academic degree or diploma. Except where otherwise indicated, this thesis is my own work”.

Signature

Date 25/05/2015



Preface

The following work presented in this study was carried out in collaboration with other researchers:

(i) Tissue processing, Alcian blue, and H & E staining were performed at the CELL Central School of Anatomy, Physiology & Human Biology, University of Western Australia, 35 Stirling Highway, Crawley, WA, 6009.

(ii) The micro-CT analyses of mouse limbs were performed in the Department of Biomedical Engineering, University of Alberta, Canada.

Acknowledgement

I would firstly like to acknowledge my family, and in particular my parents Saeid and Mehri. Thank you for your unconditional love and support, and offering so much wisdom. I am eternally grateful for everything. My sisters Taraneh and Elahe for their love, support, and understanding, which helped me tremendously.

To my supervisor Professor Crispin Dass, thank you for introducing me to the field of bone research and taking my ideas on board and letting me fly higher and bringing me back to reality again. Thank you for your patience in proof reading and help with publications. Your advice throughout this process kept me focused on this topic and without your guidance this study would not have been possible. I am so grateful.

Dr. Swati Baidur-Hudson, Thank you for your time and suggestions. Thank you to Nikola Popovik and all the staff at the Building 6 -St. Albans campus, Victoria University and all the staff at the CHIRI Biosciences Research Precinct at Curtin University, who generously provided time, expertise, and research equipment for the final part of my study. Thanks are due to Professor Gregory Blatch and Professor Terence McCann for facilitating my relocation from Melbourne to Perth.

I also want to thank Professor Philip Newsholme, who embodied the figure of a kind professor and welcomed me to his research group and gave me valuable advices. I am also indebted to Professor John Mamo, who inspired me to take pride in my research and encourage my crazy ideas and gave me the opportunity to be part of his research group. During my research I was very fortunate to receive training for micro-CT imaging

by Associate Professor Michael Doschak. Thank you for your time and generosity.

Finally Thanks to Doctor Frank Arfuso for proofreading my thesis manuscript.

Abbreviations

| | |
|-------------------|--|
| ARS | alizarin red staining |
| ALP | alkaline phosphatase |
| RGD | arginine-glycine-aspartic acid |
| ACD | asymmetric cell division |
| Ba ²⁺ | barium |
| BMUs | basic multicellular units |
| BMPs | bone morphogenetic proteins |
| BV | bone volume |
| BSA | bovine serum albumin |
| β- GP | β-glycerophosphate |
| Ca ²⁺ | calcium |
| CaCl ₂ | calcium chloride |
| CD markers | cluster of differentiation markers |
| Col-I | collagen I |
| CFU-f | colony forming unit – fibroblast |
| CSD | critical-size bone defect |
| DMEM | Dulbecco's modified Eagle medium |
| DAB | 3, 3'-diaminobenzidine |
| DAPI | 6-diamidino-2-phenylindole dihydrochloride |
| ESCs | embryonic stem cells |

| | |
|----------------|--|
| EDTA | ethylenediamine tetraacetic acid |
| ECM | extracellular matrix |
| FGF | fibroblast growth factor |
| FBS | foetal bovine serum |
| HSC | haematopoietic stem cell |
| H & E staining | haematoxylin and eosin staining |
| HA | hydroxyapatite |
| ISCT | International Society for Cellular Therapy |
| MMPs | matrix metalloproteinase |
| MMP13 | matrix metalloproteinase-13 |
| MMP14 | matrix metalloproteinase-14 |
| MMP2 | matrix metalloproteinase-2 |
| MT1-MMP | membrane type 1 matrix metalloproteinase |
| MSCs | mesenchymal stem cells |
| NCPs | non-collagenous proteins |
| OCN | osteocalcin |
| OPN | osteopontin |
| PAR | protein partitioning-defective protein |
| PBS | phosphate buffered saline |
| PEDF | pigment epithelium-derived factor |
| PDGF | platelet-derived growth factor |

| | |
|------------------|--|
| PLGA | polylactic-co-glycolide |
| PCL | polycaprolactone |
| PGA | polyglycolic acid |
| PHEMA | polyhydroxyethylmethacrylate |
| PLA | polylactic acid |
| PLG | polylactic-coglycolide |
| PMMA | polymethylmethacrylate |
| PTFE | polytetrafluoroethylene |
| RCL | reactive centre loop RCL |
| RT-PCR | reverse transcript polymerase chain reaction |
| (rh) BMP-2 | recombinant human bone morphogenetic protein-2 |
| ROP | ring-opening polymerisation |
| Sr ²⁺ | Strontium |
| SC | subcutaneously |
| TV | tissue volume |
| TGF-β | transforming growth factor- beta |
| VEGF | vascular endothelial growth factor |

List of Publications and Awards

Original papers

1. **Elahy M**, Dass C.R. Dz13: c-Jun downregulation and tumour cell death. *Journal of Chemical Biology and Drug Design*, 2011. Dec;78(6):909-12. doi: 10.1111.
2. **Elahy M**, Baidur-Hudson S, Dass C R. The emerging role of PEDF in stem cell biology. *Journal of Biomedicine and Biotechnology*, 2012:239091. doi: 10.1155/2012/239091
3. **Elahy M**, Baidur-Hudson S, Cruzat VF, Newsholme P, Dass C, R. Mechanisms of PEDF mediated protection with respect to ROS damage and inflammation in diabetic retinopathy and neuropathy. *Journal of Endocrinology*, 2014. Sep; 222(3):R129-39. doi: 10.1530/JOE-14-0065.
4. **Elahy M**, Doschak M, Hughes J, Baidur-Hudson S, Dass C R. Alginate bead-encapsulated PEDF induces ectopic bone formation in vivo in the absence of co-administered mesenchymal stem cells. *Journal Current Drug Target (in Press)*.
5. Alcantara M; Nemazannikova N; **Elahy M**; Dass C R. Pigment epithelium-derived factor upregulates collagen I and downregulates matrix metalloproteinase 2 in osteosarcoma cells, and colocalises to collagen I and heat shock protein 47 in foetal and adult bone. *Journal of Pharmacy and Pharmacology*. 2014 Nov; 66 (11):1586-92. doi: 10.1111/jphp.12289.
6. Tan M.L, Shao P, Moorst M, Friedhuber A M, **Elahy M**, Indumathy S, Dunstan D.E, Wei Y, Dass C R. The potential role of free chitosan in bone trauma and bone cancer management. *Biomaterials*. 2014 Sep; 35(27):7828-38. doi: 10.1016

Conference Papers

1. **Elahy M**, Baidur-Hudson S, Dass C.R. Osteogenic differentiation of mesenchymal stem cells by PEDF in monolayer culture and encapsulated in alginate microbeads Oral presentation 1st PHARMA conference 2013, Singapore
2. **Elahy M**, Baidur-Hudson S, Dass C.R. Osteogenic differentiation of mesenchymal stem cells by PEDF in monolayer culture and encapsulated in alginate microbeads. Poster presentation 25th Lorne conference 2012, Australia

3. Elahy M, Baidur-Hudson S, Dass C R. PEDF can differentiate mesenchymal stem cells to osteoblasts *in vitro* and *in vivo*. Accepted for_Oral presentation, Bone Tech conference 2013, Singapore.

4. Elahy M, Baidur-Hudson S, Dass C R. Effect of co-encapsulation of mesenchymal stem cells (MSCs) and Pigment epithelium- derived factor (PEDF) in alginate beads on ectopic bone regeneration. Oral presentation-Australian Society for medical research (ASMR) Scientific symposium -2014, Perth.

Table of Contents

| | |
|---|-------------------------------------|
| Title | <i>Error! Bookmark not defined.</i> |
| Abstract | <i>ii</i> |
| Student declaration | <i>iv</i> |
| Preface..... | <i>v</i> |
| Acknowledgement | <i>vi</i> |
| Abbreviations | <i>viii</i> |
| List of Publications and Awards | <i>xi</i> |
| Table of Figures | <i>xvi</i> |
| List of Tables | <i>xix</i> |
| 1. Literature review..... | 21 |
| 1.1. Stem cells..... | 21 |
| 1.1.1. Stem cell definition | 21 |
| 1.1.1.1. Stem cell division | 22 |
| 1.1.2. Murine bone marrow-derived stem cells..... | 25 |
| 1.2. Bone tissue engineering | 26 |
| 1.2.1. Bone structure and function | 26 |
| 1.2.2. Bone extracellular matrix (ECM) | 28 |
| 1.2.3. Healing, a natural process | 29 |
| 1.2.4. Bone grafts | 34 |
| 1.2.4.1. Autografts | 35 |
| 1.2.4.2. Allografts..... | 36 |
| 1.2.4.3. Xenograft | 36 |
| 1.2.4.4. Prosthesis..... | 37 |
| 1.2.4.5. Alternative solution: tissue engineering..... | 37 |
| 1.2.5. Scaffolds | 38 |
| 1.2.5.1. Scaffold requirements | 38 |
| 1. 2.5.2. Scaffold materials | 40 |
| 1. 2.5.2.1. Synthetic polymers..... | 41 |
| 1.2.5.2.2. Natural polymers..... | 42 |
| 1.2.5.2.3. Composites..... | 42 |
| 1.2.5.2.4. Blends | 43 |
| 1.2.6. Natural polymers: alginates | 44 |
| 1.2.6.1. Structure and sources..... | 44 |
| 1.2.6.2. Cell encapsulation and interaction | 46 |
| 1.2.6.3. Stem cell encapsulation in alginate for bone regeneration..... | 47 |

| | |
|---|-----------|
| 1.2.7. Growth factors as osteogenic supplement | 48 |
| 1.2.7.1. Bone morphogenetic proteins (BMPs) | 48 |
| 1.2.7.2. Platelet-rich plasma (PRP) | 50 |
| 1.2.8. PEDF | 50 |
| 1.2.8.1. PEDF and mesenchymal stem cells (MSCs)..... | 52 |
| 1.3. Aims and Objectives | 53 |
| 2. Material and Methods | 56 |
| 2.1. In vitro study | 56 |
| 2.1.1. Cell culture | 56 |
| 2.1.2. Stem cell isolation and expansion..... | 56 |
| 2.1.3. Immunocytochemistry | 58 |
| 2.1.4. Flow cytometry analysis..... | 58 |
| 2.1.5. Tri-lineage differentiation | 59 |
| 2.1.5.1. Adipogenic differentiation..... | 59 |
| 2.1.5.2. Chondrogenic differentiation | 60 |
| 2.1.5.3. Osteogenic differentiation..... | 61 |
| 2.1.6. Fabrication of alginate beads with MSC encapsulation | 61 |
| 2.1.7. Viability of MSCs (PEDF and beads) | 62 |
| 2.1.8. Osteogenic differentiation of MSCs | 62 |
| 2.1.9. Fluorescence immunocytochemistry | 63 |
| 2.1.10. Alizarin red staining (ARS) | 64 |
| 2.1.11. von Kossa staining..... | 65 |
| 2.1.12. Immunoblotting | 66 |
| 2.1.13. Alkaline phosphatase activity..... | 67 |
| 2.1.14. Statistical analysis | 67 |
| 2.2. In vivo study | 68 |
| 2.2.1. Animals..... | 68 |
| 2.2.2. Procedure..... | 68 |
| 2.2.3. Microtomography (μ -CT) and bone volume analysis..... | 69 |
| 2.2.4. Immunohistochemistry and histological staining | 70 |
| 2.2.4.1. Immunohistochemistry..... | 70 |
| 2.2.4.2. Alcian Blue staining..... | 71 |
| 2.2.4.3. Haematoxylin and eosin staining (H & E staining) | 72 |
| 3. Results | 74 |
| 3.1. In vitro studies | 74 |
| 3.1.1. Stem cell isolation, identification, culture, and viability | 74 |
| 3.1.1.1. Immunocytochemistry, FACS analysis and trilineage differentiation..... | 75 |
| 3.1.1.2. Stem cell viability | 79 |
| 3.1.2. Osteogenic differentiation of MSCs in monolayer culture..... | 81 |
| 3.1.2.1. Fluorescence immunocytochemistry..... | 81 |
| 3.1.2.2. von Kossa staining..... | 87 |

| | |
|--|------------|
| 3.1.2.3. Alizarin red staining (ARS)..... | 90 |
| 3.1.2.4. Immunoblotting..... | 93 |
| 3.1.2.5. ALP activity..... | 95 |
| 3.1.3. Osteogenic differentiation of MSCs encapsulated in alginate beads | 97 |
| 3.1.3.1. Alginate bead degradation and cell release | 97 |
| 3.1.3.2. Alizarin red staining | 99 |
| 3.1.3.3. von Kossa staining..... | 100 |
| 3.2. In vivo study..... | 103 |
| 3.2.1. Macroscopic findings | 103 |
| 3.2.2. Micro-CT..... | 105 |
| 3.2.3. Haematoxylin and eosin (H & E staining) | 108 |
| 3.2.4. Alcian blue staining | 112 |
| 3.2.5. Immunohistochemistry | 114 |
| 4. Discussion | 125 |
| 4.1. In vitro study..... | 125 |
| 4.2. In vivo study..... | 129 |
| 5. Conclusions, limitation and future directions..... | 136 |
| 5.1 Conclusion..... | 136 |
| 5.2 Limitation and future directions: | 137 |
| 6. References | 139 |

Table of Figures

| | |
|--|----|
| Figure 1. Asymmetric cell division (ACD) | 24 |
| Figure 2. Differentiation capacity of mesenchymal stem cells into mesenchymal lineage. adapted from Caplan <i>et.al</i> [21] | 25 |
| Figure 3. The remodelling of compact bone | 28 |
| Figure 4. Matrix changes during endochondral ossification. | 30 |
| Figure 5. Alginate structure..... | 45 |
| Figure 6. PEDF is expressed in the epiphyseal cartilage (growth plate) and in the areas of active bone remodelling. | 54 |
| Figure 7. Morphological features of the isolated mesenchymal stem cells (MSCs) | 74 |
| Figure 8. Immunocytochemical identification of harvested mesenchymal stem cells (MSCs) by light microscopy. | 77 |
| Figure 9. Flow cytometric identification of harvested mesenchymal stem cells (MSCs). | 78 |
| Figure 10. Differentiation capacity of mesenchymal stem cell..... | 79 |
| Figure 11. Viability of mesenchymal stem cells (MSCs) in the presence of pigment epithelium- derived factor (PEDF). | 80 |
| Figure 12. Viability of mesenchymal stem cells (MSCs) in the presence of pigment epithelium- derived factor (PEDF). | 81 |
| Figure 13. Immunocytochemistry of osteopontin (OPN) marker in monolayer culture of differentiated mesenchymal stem cells (MSCs) under conditions A – F (key below) at days 7, 14, and 21..... | 83 |
| Figure 14. Immunocytochemistry of osteocalcin (OCN) marker in monolayer culture of differentiated mesenchymal stem cells (MSCs) under conditions A – F (key below) at days 7, 14, and 21..... | 84 |
| Figure 15. Immunocytochemistry of collagen I (Col I) in monolayer culture of differentiated mesenchymal stem cells (MSCs) under conditions A – F (key below) at days 7, 14, and 21. | 85 |
| Figure 16. Immunocytochemistry of alkaline phosphatase (ALP) marker in monolayer culture of differentiated mesenchymal stem cells (MSCs) under conditions A – F (key below) at days 7, 14, and 21..... | 86 |

| | |
|---|-----|
| Figure 17. von Kossa staining results of mesenchymal stem cells (MSCs) grown on normal plate surface..... | 88 |
| Figure 18. von Kossa staining results of mesenchymal stem cells (MSCs) grown on osteogenic plates..... | 89 |
| Figure 19. The mineral concentration of mesenchymal stem cells (MSCs) grown on normal (non-bone-matrix-coated) plate surface as measured by Alizarin Red..... | 91 |
| Figure 20. The mineral concentration of mesenchymal stem cells (MSCs) grown on osteogenic (bone matrix- coated) plate surface as measured by Alizarin Red. | 92 |
| Figure 21. Immunoblot analysis shows the expression level of four osteogenic markers; alkaline phosphatase (ALP), collagen-1 (Col-1), osteopontin (OPN), and osteocalcin (OCN) at day 14..... | 94 |
| Figure 22. Alkaline phosphatase activity of mesenchymal stem cells (MSCs) in monolayer culture in osteogenic plate at days 7, 14, and 21. | 96 |
| Figure 23. Time course of mesenchymal stem cell (MSC) growth and development in alginate beads..... | 98 |
| Figure 24. Time course of alginate bead degradation over a period of 21 days in cell culture... | 99 |
| Figure 25. Mineralisation by released cells from alginate beads in osteogenic plate at day 21 in monolayer culture..... | 100 |
| Figure 26. von Kossa staining results of mesenchymal stem cells (MSCs) released from alginate beads on normal (non-bone-matrix-coated) plate surface. | 101 |
| Figure 27. von Kossa staining results of mesenchymal stem cells (MSCs) released from alginate beads on osteogenic plate surface. | 102 |
| Figure 28. Macroscopic observation of beads implanted in Balb/c mice for 35 days. | 104 |
| Figure 29. Micro-CT images of alginate bead implants..... | 106 |
| Figure 30. Quantitative micro-CT measurements..... | 107 |
| Figure 31. Haematoxylin and eosin (H & E) staining for different groups. | 110 |
| Figure 32. Haematoxylin and eosin (H & E) staining for different groups. | 111 |
| Figure 33. Haematoxylin and eosin (H & E) staining for muscle surrounding the implant site for four different groups..... | 112 |
| Figure 34. The Haematoxylin and eosin (H & E) staining for fat tissue surrounding the implant site for four different groups. | 112 |

| | |
|--|-----|
| Figure 35. Alcian blue staining for the four different groups. | 113 |
| Figure 36. Immunostaining of alginate bead implant paraffin sections for bone marker osteocalcin (OCN) in the four different groups..... | 115 |
| Figure 37. Immunostaining of alginate bead implant paraffin sections for bone marker osteopontin (OPN) in the four different groups. | 116 |
| Figure 38. Immunostaining of alginate bead implant paraffin sections for bone marker alkaline phosphatase (ALP) in the four different groups. | 117 |
| Figure 39. Immunostaining of alginate bead implant paraffin sections for bone marker collagen- I (Col-I) in the four different groups..... | 118 |
| Figure 40. Immunostaining of alginate bead implant paraffin sections for bone matrix marker pro- collagen-I (pro-col-I) in four different groups. | 120 |
| Figure 41. Immunostaining of alginate bead implant paraffin sections for bone matrix marker heat shock protein 47 (HSP47) in four different groups..... | 121 |
| Figure 42. Immunostaining of alginate bead implant paraffin sections for bone matrix marker membrane-type matrix metalloproteinase (MT1-MMP) in the four different groups. | 122 |
| Figure 43. Immunostaining of alginate bead implant paraffin sections for bone matrix marker matrix metalloproteinase 2 (MMP-2) in the four different groups..... | 123 |

List of Tables

| | |
|---|----|
| Table 1. Summary of scaffold features and their effect on bone regeneration. | 40 |
| Table 2. Different treatments used in <i>in vitro</i> studies | 63 |

Chapter One

1. Literature review

1.1. Stem cells

1.1.1. Stem cell definition

Stem cells are usually defined as clonogenic, immature, and undifferentiated cells that are capable of keeping their stemness state during cell division [1]. These cells have two unique features that are critical for tissue homeostasis; firstly, the self-renewal property and secondly, the ability to undergo multi-lineage differentiation [2]. The activity of stem cells is at its peak during embryonic development and can generate all three embryonic germ layers - ectoderm, endoderm, and mesoderm in the developing embryo. The first successful attempt at isolation of embryonic stem cells (ESCs) from mice embryos was in 1981 [3, 4], though the first human ESCs were isolated in 1998 [5]. Adult stem cells are responsible for homeostasis of the tissues in which they reside. These cells can be found in most tissues throughout the body such as the brain, bone marrow, liver, and retina in a particular area of the tissue called the stem cell niche. The stem cell niche is a microenvironment that contains all the cellular and molecular factors that regulate and support stem cells. In spite of the unique properties of stem cells (self-renewal and differentiation), adult stem cells can stay dormant through most of their lifetime and are activated by specific environmental factors under certain circumstances such as injuries and diseases [6, 7]. Stem cells need to be held within the niche and this happens *via* adhesion between stem cells and the underlying basement membrane or support cells. Generally, three main functions are

ascribed to stem cell niches: 1) perpetuation of quiescence, 2) elevation of cell numbers, and 3) direction of cell fate and differentiation [8]. Upon division, if a cell is placed outside the niche, it commits to differentiation depending on the different microenvironmental stimuli and signalling it encounters in its new environment [6].

1.1.1.1. Stem cell division

Asymmetric cell division (ACD) is the way in which stem cells can maintain their self-renewal ability and give rise to progeny in other lineages at the same time [9]. *Drosophila* has been the model for studying ACD [10-13], which revealed two separate mechanisms-extrinsic and intrinsic- involved in ACD. In the extrinsic mechanism, cell division takes place in a way that one of the daughter cells maintains access to the stem cell niche and replaces the divided parent cell, which results in maintaining the stem cell pool while the other daughter cell is isolated from the stem cell niche. Losing contact with the signalling molecules within the niche will initiate differentiation pathways. However, in the intrinsic mechanism, asymmetric inheritance of specific proteins such as protein partitioning-defective protein (PAR) in *Caenorhabditis elegans* [14] and cyclin D2 - a cell cycle regulator in cells- (specifically in mammalian brain cells) can give differential fate to one of the daughter cells just after cell division [15]. A similar mechanism also applies to the *Drosophila* neuroblast [16] **(Figure 1)**.

In bone marrow, there are two known cell populations: the haematopoietic stem cells (HSC) that can give rise to various blood cells, that is, myeloid and lymphoid, and a rare population of non-haematopoietic adult stem cells that resides in the bone marrow as well as most connective tissues of the body. The latter cells have the potential to differentiate into a variety of mesenchymal tissues such as bone, cartilage, adipose, and muscle. By placing whole bone marrow in plastic culture dishes, and removing nonadherent cells after four hours, it was demonstrated for the first time that bone marrow contains a heterogeneous population of cells [17]. The first adherent cells resulting from that experiment formed round-shaped colonies containing fibroblastoids, called a Colony Forming Unit – fibroblast (CFU-f). It was also observed that these adherent cells became more homogeneous in appearance after being passaged several times, and could differentiate into other mesenchymal cells such as bone and adipose cells [17, 18]. Further studies investigated the proliferative ability of these cells as well as their multipotency and differentiation capacity, not only into the three mesenchymal lineage cell types but also into other cell types such as neurons and muscles (**Figure 2**) [19-22]. The term mesenchymal stem cells (MSCs) was suggested for these cells in 1991 [23], considering the multilineage differentiation ability of these cells. However, the misconception that using MSCs as a general term for true stem cells or expanded multipotent progeny has led to the phrase “multipotent mesenchymal stromal cells (MSCs)” from The International Society for Cellular Therapy (ISCT) [23, 24]. Furthermore, the ISCT also defined some criteria for the isolated cells in order for them

to be defined as stem cells: 1) the shape and plastic-adherence capability, 2) the expression/lack of expression of surface antigen - cluster of differentiation (CD) markers, and 3) the ability to selectively differentiate into chondrogenic or osteogenic lineages in response to environmental stimuli [25].

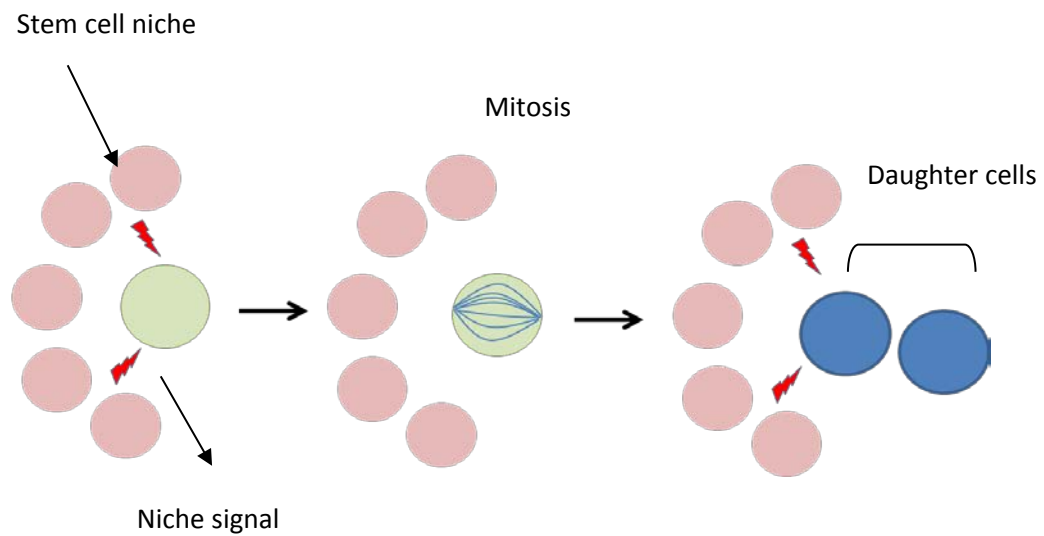


Figure 1. Asymmetric cell division (ACD)

In extrinsic ACD after cell division, one of the cells that remain in the stem cell niche will maintain the stem cell pool whereas the other cell that loses contact with the niche will go through differentiation pathways.

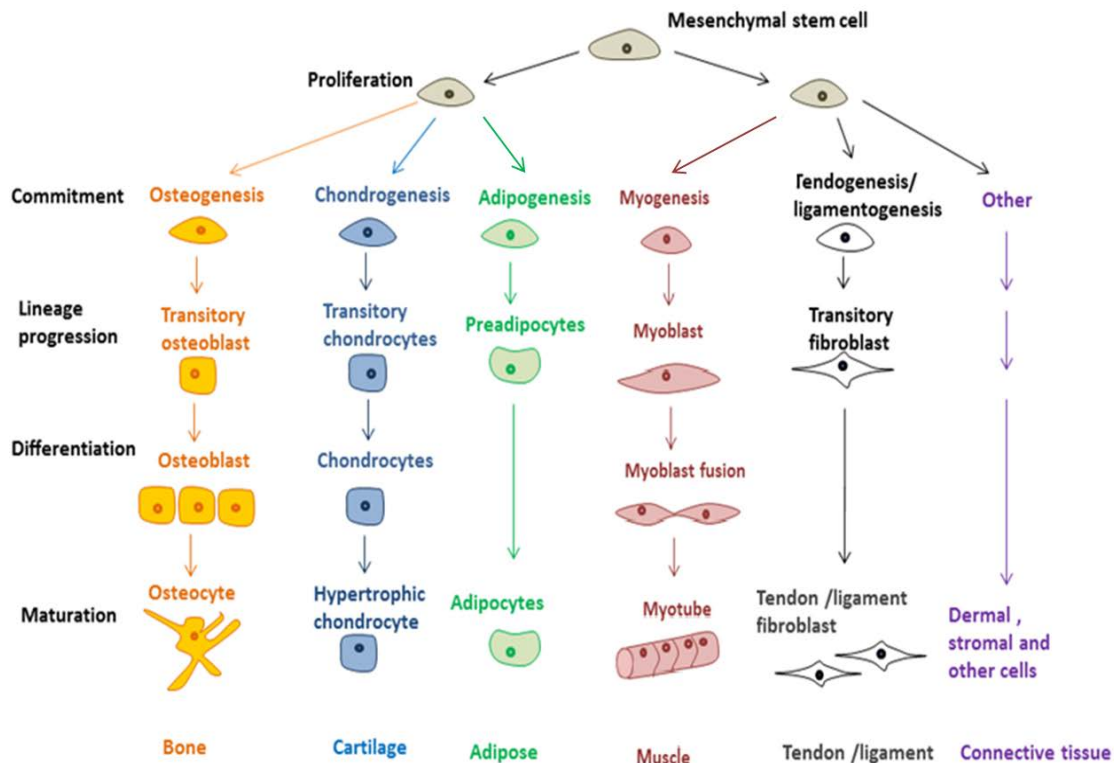


Figure 2. Differentiation capacity of mesenchymal stem cells into mesenchymal lineage. adapted from Caplan *et.al* [21]

1.1.2. Murine bone marrow-derived stem cells

The mouse has been considered the model of choice for various types of scientific research. Nevertheless, difficulties in mouse bone marrow stem cell isolation present some challenges in investigating the principals of stem cell biology and their therapeutic applications [26, 27]. MSCs have been isolated from several species such as human, mouse, rat, dog, baboon, pig, sheep, goat, and rabbit [28]. Although there are a number of protocols for isolation and expansion of human bone marrow derived-MSCs,

isolation and expansion of MSCs in the mouse is far more difficult. During isolation, these cells are usually contaminated with haematopoietic cells, which results in a heterogeneous cell population. Furthermore, expansion of a heterogeneous cell population can occur. This issue has been addressed in the human [20, 29] and other species [30, 31] by serial passaging of adherent cells or co-culture with other cells such as endothelial cells [32, 33]; though this approach has not been very helpful when it comes to mouse bone marrow-derived MSC isolation as the long term expansion of mouse MSCs during culture involves challenges due to the tendency of these cells to lose their proliferative potential or result in highly proliferative MSC populations [34, 35]. However, with certain methods and culture conditions, it is possible to establish a proliferative and homogeneous population of MSCs with the capacity of tri-lineage differentiation [36-38]. These MSCs would be a very useful tool toward understanding and interpreting MSC-based therapies and data for future clinical applications such as tissue engineering.

1.2. Bone tissue engineering

1.2.1. Bone structure and function

Bones provide mechanical support for muscles and promote movement, as well as protecting internal organs. The mechanical support and properties that bone provides are based on its structure and orientation. Flat bones and the outer part of long bones

are comprised of compact (or cortical) bone, which contains ~ 80 – 90 % mineralised tissue providing the mechanical strength. The ends of long bones are made up primarily of trabecular (or cancellous) bone. In contrast, only 15 – 25 % of the trabecular bone is mineralised. Thus, while trabecular bone contributes to the mechanical strength, its initial function is metabolic, as this bone functions as a supply of calcium and phosphate ions. Other than the mentioned functions for bone, recently its role in metabolism came into light. These includes existence of a novel endocrine regulatory loop in which insulin signalling in the osteoblast controls postnatal bone development and simultaneously regulates insulin sensitivity and pancreatic insulin secretion to regulate glucose homeostasis. [39, 40]

In addition, in the adult organism, many bones contain cavities filled with the bone marrow, and represent the anatomical site for blood cell and platelet production (haematopoiesis) [41].

Bones are mainly comprised of three different cell types: osteoblasts, osteocytes, and osteoclasts. Osteoblasts, which derive from MSCs, are cuboidal, post-proliferative cells with high synthetic activity and are responsible for bone extracellular matrix deposition and mineralisation. Osteocytes are star-shaped mature osteoblasts and are smaller in size, and are embedded in a mineralised matrix and are the most abundant cell type in mature bone. Osteoclasts are multinucleated cells of haematopoietic origin with osteolytic properties, and are responsible for bone resorption. The coordinated action

of osteoblasts and osteoclasts secure bone homeostasis during development and remodelling throughout a lifetime (**Figure 3**) [42, 43].

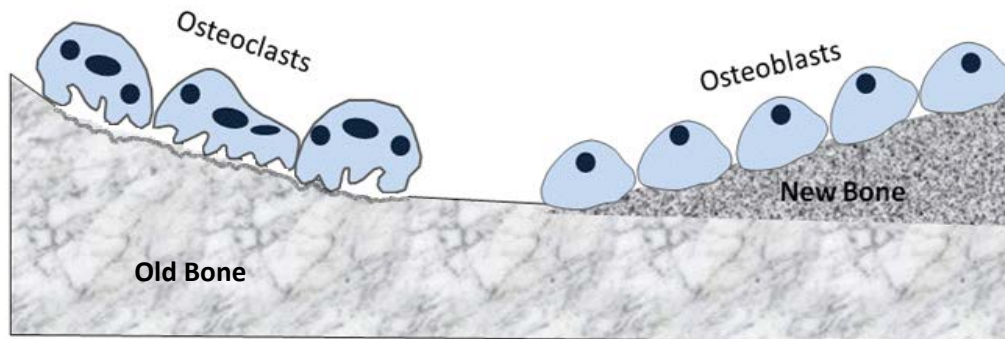


Figure 3.The remodelling of compact bone

Osteoclasts acting together in small group excavate a tunnel through the old bone. Osteoblasts enter the tunnel behind them, line its walls, and begin to form new bone.

1.2.2. Bone extracellular matrix (ECM)

Bone extracellular matrix (ECM) is composed of two main components. The organic part, which makes 30-40 percent of the tissue, mostly consists of type I collagen fibrils in a bed of proteoglycan aggregates (mainly biglycan and decorin) and glycoproteins. Glycoproteins represent the largest proportion of non-collagenous proteins (NCPs) and include thrombospondin [44], bone sialoprotein [45], alkaline phosphatase [46], osteonectin [47], osteopontin, and osteocalcin [48], as well as amino acids with high affinity for calcium, such as aspartic and glutamic acid residues. The inorganic or

mineral part of the bone is mainly made of calcium phosphate crystals in the form of hydroxyapatite (HA), which constitutes 60-70 percent of the bone tissue. In addition to HA, other minerals such as bicarbonate, citrate, magnesium, potassium, and sodium are also found [49].

1.2.3. Healing, a natural process

Bone is a highly vascularised tissue and, as mentioned before, the balance between the activities of osteoclasts (bone-resorbing cells) and osteoblasts (bone-forming cells) leads to a continuous remodelling of the bone, which makes it adaptable to mechanical stress and helps the tissue to maintain its health and repair potential. Bone homeostasis occurs *via* basic multicellular units (BMUs) [50]. Each unit includes a “cutting cone” of osteoclastic bone reabsorption followed by osteoblasts laying down new bone in the trail of osteoclasts, and the end result is an osteon [51]. Proper cell proliferation, differentiation, migration, and remodelling of the extracellular matrix will lead to the development and regeneration of bone tissue. Cellular condensation initiates bone formation, where mesenchymal cells spread out, migrate, proliferate, and stick together *via* adhesion molecules.

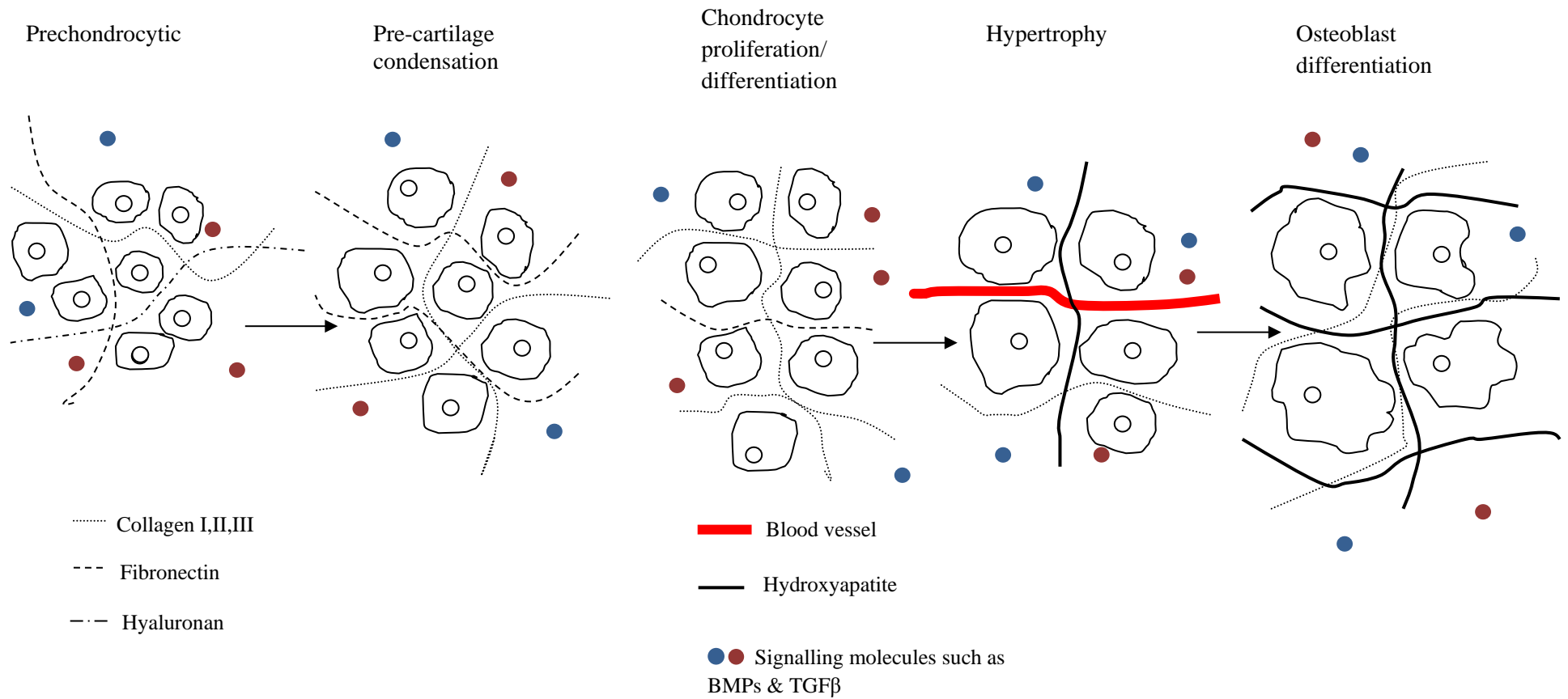


Figure 4. Matrix changes during endochondral ossification.

As an *in vivo* example of the critical role of the extracellular matrix (ECM) during tissue development, the figure illustrates ECM changes during endochondral ossification. The ECM evolves at each stage of ossification.

There are two mechanisms responsible for bone development: bones can directly develop from MSCs into osteoblasts, called *intramembranous ossification*, or at an early stage where a cartilage template can form, which, after a while, can be replaced by bone, called *endochondral ossification*.

Intramembranous ossification occurs during development of flat bones and is peripheral to the site of the fracture during bone healing. During intramembranous ossification, cells of the mesenchymal lineage, which are embedded in a membrane of connective tissue, directly undergo osteogenic differentiation and synthesize the osteoid (non-mineralised matrix), which eventually mineralise. Stem cell specification toward the osteogenic lineage is basically regulated by the combined action of three transcription factors, such as RUNX2, OSX and nuclear β -catenin. Several experimental studies suggest that RUNX2 directs osteogenesis in the early phases of stem cell differentiation, while OSX and nuclear β -catenin act downstream consolidating the transition toward the osteoblastic phenotype [52, 53].

The latter (endochondral ossification) takes place during the development of short and long bones, the growth of the length of long bones (growth plate), and during the natural healing of bone fractures. [54, 55]. During this process the mesenchymal progenitor cells first aggregate into a cartilage template and are then replaced by bone [55, 56]. Prior to endochondral ossification, migration of pre-chondrocytic mesenchymal cells occurs (**Figure 4**). Migration of pre-chondrocytic mesenchymal cells to the bone-forming region leads to ECM formation, which is mostly made of

hyaluronan and collagen type-I. These mesenchymal cells produce condensed nodules following the chondrogenic phase [55, 57].

During the condensation stage, lots of changes occur during cell-matrix interactions. These changes are mediated by specific molecules including N-cadherin, fibronectin, syndecans, tenascin, thrombospondins, neural cell adhesion molecule, focal adhesion kinase, paxillin, and matrix metalloproteinases (MMPs) [57]. The extracellular space becomes limited due to increased activity of hyaluronidase and more compact dispersion of collagen types I and III and fibronectin. Afterwards, pre-chondrocytic cells proliferate and differentiate to osteocytes to provide both mechanical support and scaffold for the hard osteoid tissue that will form later [58]. Chondrocyte differentiation is defined by cartilage-supporting matrix synthesis, which includes a variety of collagens such as collagen-II, collagen-IX, and collagen-XI, and various proteoglycans such as aggrecan. The process of chondrocyte maturation continues by hypertrophy as the cells secrete hydroxyapatite into the ECM for mineralisation [59, 60]. During hypertrophy, chondrocytes secrete collagen type-X and matrix metalloproteinase-13 (MMP13), and these events lead to changes in ECM protein composition. Degradation of the ECM facilitates vascular invasion and recruitment of chondroclasts, which results in the removal of apoptotic chondrocytes and migration of new MSCs which later differentiate into osteoblasts that exude bone matrix [60]. Woven bone gradually substitutes cartilaginous tissue. This remodelling process is highly dependent on the function of MMP molecules, especially matrix

metalloprotease-14 (MMP14), which is also known as membrane type 1 matrix metalloprotease (MT1-MMP) as collagen I, II, and III are substrates for MMP14 protease function [61-63]. To do so, MMP14 uses matrix metalloprotease-2 (MMP2) as a substrate and activates it by cleaving its pro-domain, which leads to bone formation stage [64, 65]. Furthermore a large number of small signalling molecules like cytokines and growth factors (IL-4, BMPs, TGF- β and VEGF) further influences bone cell activity. These factors are produced by hypertrophic chondrocytes during the hypertrophy stage and thus are part of mechanisms by which bone cells can influence each other's behaviour. Some are incorporated into the bone matrix and are released again when bone matrix is resorbed. This can locally alter behaviour of bone cells. An important regulatory mechanism is the RANK-RANKL pathway. Osteoblasts produce RANKL that attaches to receptors on the surface of pre-osteoclasts and signals these cells to differentiate into mature osteoclasts. In this stage, bone matrix is made of mineralised and proteinaceous ECM and is called the primary bone formation stage. As the process continues to its final stage, the secondary bone formation stage, the ECM becomes more solid and reconstructs itself to weight-tolerable cortical or trabecular bone [66].

Inflammation is the key difference in developmental skeletogenesis versus regenerative skeletogenesis. During regenerative skeletogenesis, inflammatory cells secrete necessary growth factors and cytokines to recruit MSCs and initiate bone formation. However, developmental skeletogenesis is regulated by non-inflammation-associated differentiation and growth factors [67, 68].

Usually, bone has the ability to heal small lesions due to its ability to undergo spontaneous regeneration, so no invasive procedure such as surgery is required and conventional therapy like casting would be sufficient. However, spontaneous healing does not apply in cases like non-union or critical-size bone defect (CSD). Non-union is defined as “a fracture that is over nine months old and has not shown radiographic signs of progression toward healing for three consecutive months” [69]. In the case of continuous poor or no healing, the final stage of aseptic non-union would be pseudoarthrosis. One approach toward management of pseudoarthrosis is grafting, which sometimes involves not only complete removal of the fracture site but also tissue around the non-union site [51]. Critical-size bone defect is “the smallest size intraosseous wound in a particular bone that will not heal spontaneously during the lifetime of the animal”, and the plan for therapeutic management of CSD is bone grafting and transplants [51].

1.2.4. Bone grafts

In order to have a successful bone graft, there are certain criteria which have to be considered. During bone regeneration after the bone graft, three crucial processes have to take place in order to generate new bone formation: osteogenesis, osteoinduction, and/or osteoconduction.

Osteogenesis is the act of bone formation as a result of osteoid expression by osteoblasts followed by mineral deposition. Osteoinduction however, is the induction of differentiation of undifferentiated cells such as stem cells and other osteoprogenitor cells toward the osteoblast lineage. Osteoconduction is the ability of the graft to promote and enhance migration and attachment of osteoprogenitor cells and osteoblasts as well as vessel formation in order to support the new tissue formation. To have a clinically and physiologically functional bone graft, the graft has to exhibit the above features.

1.2.4.1. Autografts

Autogenous cancellous bone or autograft is believed to be the ideal graft material as it is harvested from and implanted into the same individual [70]. These grafts are usually taken from the iliac crest, rib, fibula, or tibia of the patient. These segments of bone are highly vascularised and possess osteogenic potential due to the presence of viable osteoprogenitor cells as well as osteoconduction/induction capacity. Furthermore, as this graft is from the same patient, it will not transmit disease to the recipient and the risk of immunoreactions is low. However, cancellous bone taken from the patient is not readily available in unlimited quantities. The process of harvesting the bone imposes potential complications and pain to the patient as well as possible complications that may occur after surgery including inflammation, infection, and donor site morbidity [71, 72].

1.2.4.2. Allografts

Allografts are harvested from a human donor other than the patient, the prerequisite of harvesting being genetic compatibility. The graft specimen has to go through some processes to eliminate and reduce the risk of immunoreactions and disease transfer such as freeze-drying, washing, demineralisation, and gamma-irradiation or ethylene oxide sterilization. However, although these procedures reduce the risk of disease transmission and immunoreactions, they also lessen the osteogenic potential of these grafts [73, 74].

1.2.4.3. Xenograft

Unlike autografts and allografts, xenografts are obtained from a non-human donor. Xenografts are not commonly accepted or used in clinical applications due to ethical issues and disease transfer. These grafts are usually used as *bone void filler* to fill burr hole and craniotomy defects and in smoothing facial skeletal contour abnormalities. Examples of these grafts include: BioOss [75] an inorganic matrix from cows [76], porcine organic bone matrix [77], equine [78], and bio coral grafts [79, 80], and Norian CRS Bone Cement [81].

1.2.4.4. Prosthesis

The use of a large prosthesis is a common solution to overcome the above-mentioned complications. Nonetheless, as there is no biological interaction between the prosthesis and tissue, the prosthesis may simply give in and the revision surgery may be required in order to fix or replace it [82, 83]. This becomes particularly problematic in growing recipients [84]. Other concerns such as risk of allergy and toxicity [85] raise the new idea of using alternative materials, and consequently, open a new horizon of tissue engineering.

1.2.4.5. Alternative solution: tissue engineering

The search for alternative approaches toward bone repair and replacement of the conventional methods has resulted in the new field of tissue engineering. This field has evolved rapidly over the last 15 years. Scaffolds with designed microstructures give sound structural support and adequate mass transport of nutrients and oxygen to facilitate tissue regeneration. There are numerous reports on various tissues grown *in vitro* including bone [74], cartilage [86], main bronchus [87], and blood vessels [88]. The achievements in the area of tissue engineering in various disciplines are due to the rapid advancement in knowledge of stem cell biology and increased understanding of their response to environmental cues [89]. The unique ability of MSCs to sense and react to secreted molecules and cytokines in the case of injury, and migrate to the lesion site

makes them an excellent candidate for use in tissue engineering. However, one cannot disregard the need of a suitable vehicle for stem cell delivery. Hence, lots of effort has been put into fabrication of an optimal scaffold with the necessary characteristics for stem cell delivery [66].

1.2.5. Scaffolds

Similar to scaffolds in the field of construction, the scaffold for tissue engineering and regenerative medicine needs to be strong, reliable, and able to endure the environmental conditions for the specific period of time. Moreover, the scaffold should be removable without damaging or affecting the newly formed or repaired structure [90]. In tissue regeneration, the scaffold is a three-dimensional (3D) construct that acts as a template for cell adhesion, proliferation, differentiation, and extracellular matrix formation to provide a suitable environment for the newly regenerated tissue.

1.2.5.1. Scaffold requirements

For successful bone tissue engineering, a suitable environment in which osteogenic cells are able to migrate, differentiate, and proliferate is necessary. The scaffold, as a three-dimensional structure, can accommodate stem cells in this context and promote new bone formation as well as provide mechanical support during bone regeneration [91]. To design and manufacture an ideal scaffold for stem cells to survive and be able

to proliferate and differentiate, a few considerations need to be taken into account **(Table 1)**. The biocompatibility of the material that the scaffold is being made of is important to avoid an adverse immunological reaction it may cause in the body. Biodegradability is another important characteristic of the scaffold, which means that the scaffold should be able to be degraded inside the body naturally at an appropriate time and controllable rate. In addition, the degradation products should not be toxic and must be metabolised naturally in the body [92]. Furthermore, porosity and permeability of the scaffold is essential for high yield of cell seeding (*in vitro*) and proper infiltration (*in vivo*), nutrient transport, tissue ingrowth, and vascularisation [93]. The mechanical stability of the scaffold is another important, desirable feature [92]. The construct should mimic the native bone environment and structure to make the scaffold ideally osteoconductive, osteoinductive, and osseointegrative of stem cells to native bone [91, 94].

Table 1. Summary of scaffold features and their effect on bone regeneration.

| Scaffold characterisation | Biological effect |
|----------------------------------|---|
| Biomaterial and biocompatibility | <ul style="list-style-type: none"> - Cell proliferation and differentiation - Appropriate for <i>in vivo</i> implantation |
| Geometry and architecture | <ul style="list-style-type: none"> - Encourage three dimensional growth of the cell - Controlling the growing tissue morphology - Support cell proliferation |
| Porosity | <ul style="list-style-type: none"> - Encouraging cell differentiation, recruitment, aggregation, and vascularisation |
| Mechanical properties | <ul style="list-style-type: none"> - Support mechanical loading |
| Degradation rate | <ul style="list-style-type: none"> - Make space for new tissue ingrowth - Allow the extracellular matrix to remodel |
| Biochemical stimuli | <ul style="list-style-type: none"> - Embody proper growth factors and cytokines for cell function enhancement |

1. 2.5.2. Scaffold materials

A variety of materials including metals, ceramics, polymers (natural and synthetic), and their blends have been used for the replacement and repair of damaged bone tissues. Metals and ceramics have two major disadvantages for tissue engineering applications: they are non-biodegradable, and their processability is limited [95]. Synthetic and natural polymer scaffold applications have been comprehensively examined in the lab and clinic in order to replace bone tissue [96-99]. The polymer materials are more applicable in the case of scaffold fabrication and the fabrication technique due to their

desirable properties such as biocompatibility and degradation, mechanical properties, and microstructure [100, 101].

1. 2.5.2.1. Synthetic polymers

Synthetic polymers, both organic and inorganic materials, are used in a wide variety of biomedical applications. The family of saturated aliphatic polymers including polylactic acid (PLA), polyglycolic acid (PGA), poly (lactic-co-glycolide) (PLG), and their blends, are the conventional materials that have been used in bone tissue engineering. These polymers have a high molecular weight and are usually polymerised *via* a condensation reaction. The other method of polymerisation is ring-opening polymerisation (ROP), which has been used in the polylactic group. The main core of all aliphatic polymers is the same, the only difference being the substituent group that accounts for a variation in molecular weight and degradation rate [14, 15].

There are other biodegradable synthetic polymers that are being investigated in the field of tissue engineering. These polymers include polycaprolactone (PCL), polyanhydrides, polyphosphazenes, and bioactive glass. The ability to attach to bone and soft tissue makes these materials good candidates for bone graft material. These polymers are able to form a layer of hydroxyapatite in the margin of bone and allow the graft material to integrate the implant to live tissue [92, 102]. Synthetic non-degradable polymers include alloplastic, polymethylmethacrylate (PMMA), polytetrafluoroethylene (PTFE), and polyhydroxyethylmethacrylate (PHEMA) [103,

104]. To overcome the undesirable feature of non-degradability in these useful materials, and induce controlled degradation and improve biocompatibility, one can combine them with degradable and natural polymers.

1.2.5.2.2. Natural polymers

The first biomaterials with biodegradability features that had been considered for use in bone tissue engineering clinically were natural polymers. Collagen [105-107], fibrin [108-111], silk [112-114], hyaluronic acid [115, 116], chitosan [117, 118], and alginate [91, 106, 109, 119-122] are used in bone and cartilage tissue engineering applications. These materials are able to enhance cell attachment and proliferation in biological systems due to their better interactions with cells compared to other polymers such as synthetic ones. Natural polymers have a highly organised structure and also possess extracellular ligands that may bind to cell receptors. However, limited supply and low weight-bearing capacity, high cost, and difficulty in processing them for clinical applications are some disadvantages of natural polymers [71, 118].

1.2.5.2.3. Composites

Composite materials consist of two or more separate materials which can benefit from all the positive feature of each to provide a scaffold with better features. The polymer/ceramic composite scaffold serves as an imitation of natural bone, which is

made of hyaluronic acid and organic collagen. HA belongs to the mineral part of the living bone, and is required for better osteoconductivity. In polymer/ceramic composites, HA can be used as the ceramic part while collagen, gelatin, chitosan, chitin, elastin, poly methymethacrylate, polypropylene fumarate, polyphosphazenes, and poly hydroxybutyrate, PCL, PLA, PLG, poly anhydride, and polyorthoester, each can serve as the polymer component of the composite. In such constructs, the living bone matrix can spontaneously integrate into the HA layer. The degradation pattern of the polymer may be affected by the bioactive phase in the polymer composite. Changes in degradation kinetics are related to a pH-buffering effect at the surface of the polymer due to rapid proton exchange for alkali in the ceramic, which changes the rate of polymer degradation in pH-dependent cases (acidic degradation) [123-125]. In composite constructs, degradation rates may change due to ceramic accessibility in the composite structure, which leads to water absorption and hydrophilicity of the hydrophobic polymer structure [125]. An improved environment for cell seeding, survival, growth, differentiation, load-bearing, and other mechanical properties are some of the beneficial features of composite material for tissue engineering [126].

1.2.5.2.4. Blends

A blend is a category of polymeric material which is manufactured by a combination of synthetic–natural, natural–natural, and synthetic–synthetic polymers. The purpose of blending these materials is to benefit from idiosyncratic advantages of each material, features which include mechanical characteristics, ease of processing and low

production cost of synthetic material, biocompatibility, and controlled biodegradability of the natural polymers to match the cell growth rate [127]. PLA, PLG, and PCL as synthetic polymers and gelatin, elastin, chitosan, starch and alginate as natural polymers have been widely used in manufacturing blend materials [128, 129].

1.2.6. Natural polymers: alginates

Due to certain interesting chemical and physical properties of alginates, they have been used in a broad range of applications in different fields. In the food and beverage industry, alginates are used as thickeners and stabilisers. They also are used for yeast encapsulation in the ethanol production industry. Alginates are also applicable in other industries such as paper and paint production, ceramic shaping, sewage water treatment and purification [130-133]. Alginates have also been used in the healthcare and pharmaceutical industries as matrices for cell encapsulation and transplantation since 1980 when the first successful encapsulation of islet cells was achieved [134].

1.2.6.1. Structure and sources

Alginate refers to a family of polyanionic copolymers of 1-4 linear linkages of β -D-mannuronic acid (M) and α -L-gluronic acid (G). The various compositions of these isomers results in at least three distinctive conformations of the hexopyranose ring [132]. The M/G content of the alginates directly affects the stiffness of the gel and will

subsequently affect the behaviour of the encapsulated cells. For example, a high G content leads to more stable gel compared to the high M content, which can affect the final purpose of encapsulation (cell proliferation and growth, or metabolism and secretory activity) [135, 136]. These polysaccharides were initially isolated from brown algae, namely *Laminaria hyperborea*, *Ascophyllum nodosum*, and *Macrocystis pyrifera* and bacteria such as *Azotobacter* and *Pseudomonas*. However, isolation from bacteria is not cost-effective, so the material is sourced from brown algae [132]. **(Figure 5)**

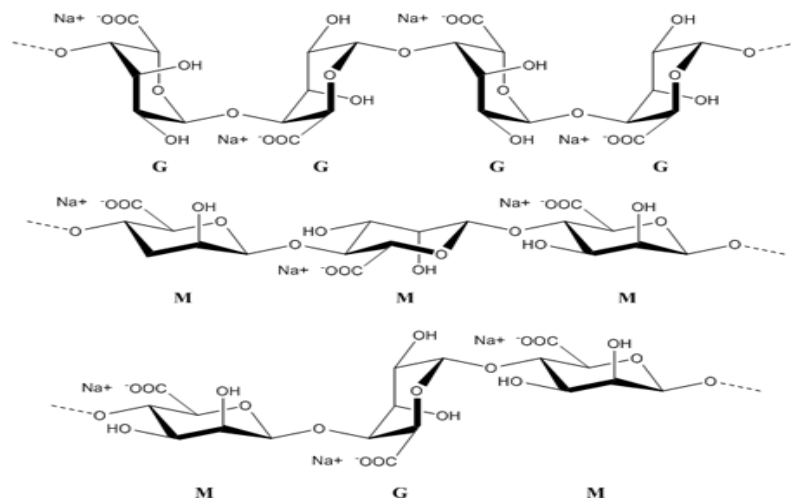


Figure 5. Alginate structure.

1-4 linear linkages of α -L-guronic acid (G) and β -D-mannuronic acid (M) [126].

1.2.6.2. Cell encapsulation and interaction

Sodium alginate is soluble in an aqueous solution, which is called a hydrogel. Ionic interaction with certain divalent cations such as calcium (Ca^{2+}), strontium (Sr^{2+}), and barium (Ba^{2+}) at room temperature results in the gelation of sodium alginate and consequent formation of a three dimensional structure. Mechanical properties including mechanical stability, viscosity, and elastic modulus of alginates are the key factors that affect the interaction of cell-gel during cell encapsulation [137, 138]. As there are no receptors for alginate polymers in mammalian cells, this polymer acts as a practically inert environment and, consequently, the adhesion and proliferation of cells within alginate is not affected by it [139]. To improve the cell-gel interaction, some adhesion molecules such as laminin [140], collagen [141], gelatin [91], and fibrin [109] have been supplemented into alginate during cell encapsulation. However, coupling using such materials is challenging to control and may lead to non-specific cell interactions. Hence, coupling of short chain amino acids was introduced to improve the cell-gel interaction. The fibronectin-derived adhesion peptide arginine-glycine-aspartic acid (RGD) and its subtypes are commonly used to improve the cell adhesion properties of alginate; considering that RGD-receptors have been identified and well characterized in mammalian cells [142]. Furthermore, the manipulation of alginate composition with the above-mentioned elements could affect and improve the degradation rate and make alginate more suitable for tissue engineering.

The mechanism that is responsible for nutrition supply and waste removal from encapsulated cells is simple diffusion because of the absence of a vasculature system. As a result, the size of the sphere is an important limiting factor in mass transport in encapsulated cells [143]. Encapsulation can be achieved by using simple methods such as a syringe or pipette [133, 144] or more precise methods including atomisation and emulsification. However, the resultant spheres obtained from the different methods would vary in size, which eventually will affect the survival and proliferation of encapsulated cells. It has been shown that spheres with a diameter of 0.9-1 mm displayed a cell layer approximately 0.2 mm thick at the periphery, while cells in the centre of the microcapsules were dead, which indicates insufficient nutrition transport to the centre. However, this problem can be resolved by reducing the size of the spheres [143, 145].

1.2.6.3. Stem cell encapsulation in alginate for bone regeneration

Encapsulation of bone marrow-derived stem cells in alginate for the purpose of bone tissue formation has been examined extensively and has shown promising results as an alternative solution for bone healing. However, to use alginate encapsulation clinically, a few strategies have been introduced. One approach is to encapsulate the osteoprogenitor cells [146, 147] and another strategy is to co-encapsulate these cells

with osteogenic supplements in order to initiate and support osteogenic differentiation [148-150].

1.2.7. Growth factors as osteogenic supplement

In recent years, growth factors such as bone morphogenetic proteins (BMPs) have been used extensively in bone tissue engineering. These are the main signalling molecules for growth, proliferation, and differentiation of bone progenitor cells, and deliver certain advantages that make them effective and suitable for use in pre-clinical and clinical settings [151].

1.2.7.1. Bone morphogenetic proteins (BMPs)

Bone morphogenetic proteins belong to the superfamily of transforming growth factor-beta (TGF- β) and are structurally related. To date more than twenty BMPs have been identified. Several BMPs such as -2, -4, -6, -7, and -9 have shown direct effects on bone formation through bone morphogenic cascades, which result in proliferation and differentiation of osteoprogenitor cells and MSCs, and final bone formation [151, 152]. Furthermore, two BMPs are available commercially for use in clinical treatment - recombinant human (rh) BMP-2 (Infuse™) [153] and rhBMP-7 (OP-1™) [154]. These BMPs are being used widely as substitutes for autografts or in combination with grafts to increase their efficacy.

The use of BMPs as an alternative for grafts has several advantages such as reducing morbidity- and surgery-related complications and also overcoming the limitation of supply as BMPs can be made using recombinant DNA technology [155]. However, the application of BMPs also has certain limitations. As BMPs works in a dose-dependent manner, the concentration of BMPs needs to reach a threshold level in order to initiate bone formation. Additionally, there is a rapid systemic clearance half-life for rh-BMP-2 (7-16 minutes) and 10-15 hours for rhBMP-7, which necessitates the need to use supraphysiological doses in order to rectify the rapid wash-out in order to achieve a satisfying response [148]. Moreover, other limitations such as insufficient responsiveness of cells, possible inhibitory effect of high doses of BMPs on other tissues, and possible side-effects have come to light [156]. Furthermore, recent contradicting reports have been published about no positive effect of BMP-2 on fracture healing, as well as increasing debate with regards to its side effects such as osteolysis, implant reposition, loss of alignment, urogenital, bladder retention, and bone overgrowth into the spinal canal, which are the most common complications that have reported when rhBMP-2 is used compared with other graft methods [157-172]. The production cost of recombinant protein is another reason to search for other growth factors with bone regenerative potential.

1.2.7.2. Platelet-rich plasma (PRP)

The concentration of platelet in plasma is almost 1×10^6 platelets in 5 ml of plasma, which contains a 3- to 5-fold increase in growth factor concentration. The main role of platelets is in wound healing. The first reaction after wounding and bleeding is activation of platelets by contact with collagen and subsequent release of the growth factors to initiate the healing process [173]. The known cytokines in platelet are mostly involved in cell proliferation, chemotaxis, cell differentiation, and angiogenesis, which make it a good candidate to be used in bone repair [174, 175]. The majority of the growth factors that have been considered to be used as a supplement for osteogenic differentiation are somehow derivatives of PRP such as: platelet-derived growth factor (PDGF) [176], vascular endothelial growth factor (VEGF) [177], and fibroblast growth factor (FGF) [178]. While it has been shown that using PRP and its derivatives can support bone formation in different animal models [179-183], not all the studies are supportive of using PRP as a reliable and efficient clinical therapy in bone complications [184-186].

1.2.8. PEDF

Pigment epithelium-derived factor (PEDF) is a glycoprotein that belongs to the superfamily of serpin protease inhibitor proteins without inhibitory function, encoded by the gene *SERPINF1* located on chromosome 17p13, which is well-conserved in

evolution [187]. It is a protein of 418 amino acids, with a size of 50kDa and is widely expressed in most bodily tissues [188]. The highest amount of expression has been observed in the eye, foetal and adult liver, adult testis, ovaries, placenta, and the pancreas. [189]. A significant reduction in the expression of PEDF is found in senescent (aging) cells [190]. PEDF was originally isolated from the conditioned medium of cultured human foetal retinal pigment epithelium cells [189]. It is an extracellular protein which shows the typical secondary and tertiary structure of a serpin and binds to collagen-1 and heparin. The α -sheet is the dominant feature of the secondary structure and comprises the core structural domain of the protein, being closely involved in dynamic movements that are part of serpin function [191]. The existence of a reactive centre loop (RCL) is another feature of serpins, and it is a proteinase recognition site and a critical component of the function of serpins [189]. PEDF contains an RCL structure but the function of this is still unknown [189].

While PEDF is increasingly becoming known for its anti-cancer properties, it is a pluripotent molecule with neurotrophic qualities, as well as having anti-angiogenic, anti-proliferative, pro-differentiation, neuroprotective, and anti-inflammatory roles [192-194]. Recent studies have demonstrated that PEDF supports the survival and proliferation of neural, retinal, and embryonic stem cell populations [195]. PEDF is also detected in areas of endochondral ossification and active bone remodelling [196]. As mentioned before, endochondral ossification is one of the main processes that MSCs go through for bone tissue formation [56].

1.2.8.1. PEDF and mesenchymal stem cells (MSCs)

PEDF is one of the most abundant proteins identified in murine MSC (mMSC)-conditioned medium [197]. Immunofluorescent staining has shown a high level of PEDF in the rough endoplasmic reticulum/Golgi areas [197]. PEDF is also found to be located near the plasma membrane and in the extracellular space, giving PEDF the ability to bind to collagen and proteoglycans in the extracellular matrix.

During differentiation of MSCs to osteoblasts, the expression of several genes begins or is elevated and this includes PEDF. It has been shown that a high level of PEDF is expressed in osteoblasts during the early stages of bone development, and to a lesser extent in osteoclasts [198, 199]. Osteoblasts and possibly osteoclasts are able to synthesise and release PEDF, and this protein has a critical role in normal and abnormal bone angiogenesis [198, 200]. In developing bones, blood vessel growth is localised and MSCs may play a role as pericytes in support of newly formed blood vessels, which is a very active process during endochondral ossification [201, 202]. In locations such as the long bone growth plate, blood vessels selectively invade the region between hypertrophic chondrocytes and newly formed bone matrix. These newly-formed vessels allow migration of osteoblasts, which leads to new bone matrix deposition and bone elongation. PEDF is expressed in the epiphyseal cartilage and in the areas of active bone remodelling in the primary spongiosa and periosteum of metaphyseal bone [196]. There is a gradual decrease in the intensity of PEDF expression as chondrocytes differentiate toward bone at the base of the growth plate. The expression pattern of

PEDF varies in bone (**Figure 6**); a high level of expression was observed in the germinal zone, followed by a decrease in expression in the proliferation, maturation, and final hypertrophic zones [196, 198].

1.3. Aims and Objectives

The hypothesis of the current study is that PEDF is intrinsically involved in osteoblast differentiation and bone formation.

The main objective of this thesis was to investigate the effect of PEDF as an osteogenic supplement for MSCs in an alginate bead scaffold for bone tissue formation *in vitro* and *in vivo*.

In order to examine the hypothesis, a series of *in vitro* experiments were carried out. The stemness of the isolated cells from mouse bone marrow first examined using specific surface markers and other necessary assays such as tri-lineage differentiation. The osteogenic potential of PEDF then examined in normal and osteogenic plates in mono layer and capsulated in alginate and confirmed *via* several qualitative and quantitative methods including immunofluorescent, immunoblotting, von kossa , alizarin Red staining and enzyme activity assay. The study further taken to animal model to test the hypothesis in normal physiological environment.

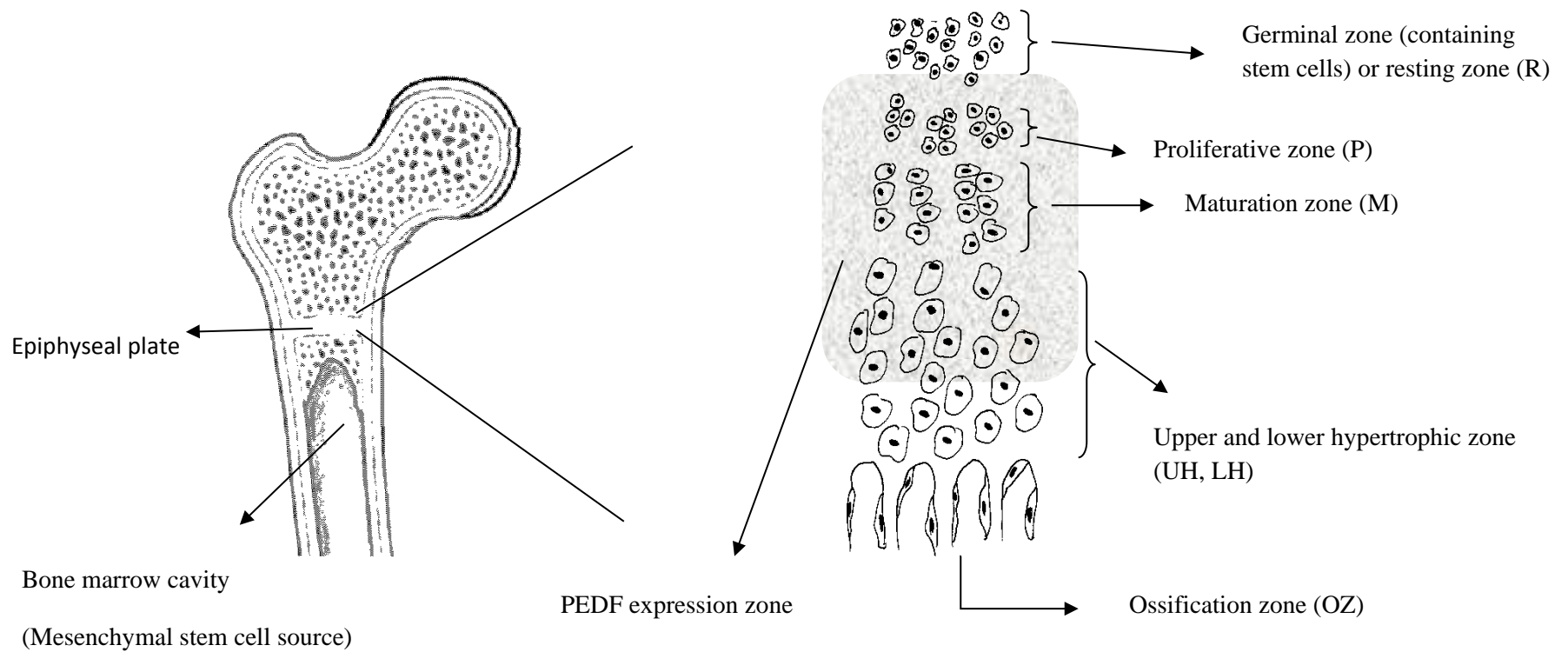


Figure 6. PEDF is expressed in the epiphyseal cartilage (growth plate) and in the areas of active bone remodelling.
 The highest level of expression is observed in the proliferative zone, maturation zone, and upper hypertrophic zone respectively.

Chapter Two

2. Material and Methods

2.1. *In vitro* study

2.1.1. Cell culture

All the cell culture and *in vitro* assays were carried out in Greiner culture flasks or plates (96-well, 23-well, 12-well and 6-well) at 37°C and 5% CO₂ unless otherwise specified.

All cell culture reagents and chemicals were purchased from Sigma-Aldrich (St Louis, MO, USA) unless otherwise stated. Dulbecco's modified Eagle medium (DMEM), with low glucose, supplemented with 1% penicillin/streptomycin and 10% heat-inactivated foetal bovine serum (FBS) is referred to as complete media. Each experiment was repeated twice and carried out with 4 replicates ($n=4$) unless otherwise stated.

2.1.2. Stem cell isolation and expansion

Wild-type 6 weeks Balb/c mice were sourced from the Monash Animal Research Platform, Clayton- VIC, Australia. Animal ethics approval was granted prior to commencing the study from the Victoria University Animal Experimentation Ethics Committee (AEEC 16/10).

Mesenchymal stem cells were isolated from the marrow resident in mice long bones according to an established protocol with some modifications [38]. Animals were killed

by cervical dislocation and the hind limbs were removed and kept on ice in complete media, while removing all the muscles and connective tissue from bone by scraping and also during cell collection. After removing the growth plates, bone marrow was flushed out with complete media using a 27 gauge syringe. The cell suspension was then filtered through a 100 mm mesh filter (Millipore) to remove any bone or muscle tissue and then cultured in a 150 cm culture flask in 20 ml of complete medium. Every 8 hours, the nonadherent cells were washed then removed with phosphate buffered saline (PBS) and fresh media added for the next 72 hours. The adherent cells were then washed with PBS and the fresh media added every 3 days for the next 3-4 weeks until cells became 80-90% confluent. Cells were split and passaged every 10-14 days following media removal and washed with 10 ml PBS. Cells were detached following incubation with 2 ml of 0.25% trypsin/1 mM ethylenediaminetetraacetic acid (EDTA) for 2 minutes at room temperature and grown until passage 4 for the derivation of a pure stem cell population and to increase the cell number. All experiments were performed within 10 passages. As mentioned before, the culture media contained 10% FBS which contains PEDF. Unsupplemented medium, that is one without FBS would lead to senescence and inhibits cell proliferation and ultimately leads to apoptosis. However, considering that all the cells were treated with the same basic media the effect of this PEDF in medium can be ignored.

2.1.3. Immunocytochemistry

Stemness of the isolated cells is indicated by the expression of CD73 and CD105 as well as a lack of expression of hematopoietic markers, CD34 and CD19 [25, 69, 203]. Immunocytochemical analysis was performed to characterise the surface antigen expression of CD34, CD19, CD73, and CD105 of the isolated cells according to a previously described protocol, with some modifications [204]. Cells were blocked after permeabilisation using 0.3% saponin following by a peroxidase block (Dako, Melbourne, Australia) for 5 min, with 2% serum (Dako, Melbourne, Australia) corresponding to the appropriate antibodies for 30 minutes. Cells were then incubated overnight with anti-CD34, -CD19, -CD73, and -CD105 (Santa Cruz) in 1:500 dilution, and were subsequently probed with a biotinylated secondary antibody (Dako, Melbourne, Australia) at a 1:2000 dilution followed by Vectastain ABC kit (Vector Laboratories, Burlingame, CA, USA) according to the manufacturer's instructions and 3,3'-diaminobenzidine (DAB) staining. Haematoxylin staining was used to visualise the nucleus. Microscopic imaging was performed using a Zeiss Axioplan 2 microscope (Zeiss-Australia).

2.1.4. Flow cytometry analysis

The expression of surface markers was also evaluated using an Attune[®] acoustic focusing cytometer (Thermofisher Scientific, NY, USA). Cells were detached with trypsin/EDTA and a single cell suspension in 5% PBS and FBS was prepared. The cells

were incubated on ice with anti-CD34, -CD19, -CD73, and -CD105 for one hour (1:50 dilution). After centrifuging at 14000 *g* for 3 minutes, the cells were washed with PBS twice, resuspended in 5% PBS/BSA, and labelled with the corresponding fluorescent secondary antibody (1:100 dilution) on ice for 1 hour. Instrument settings were calibrated using unstained cells along with stained cells for fluorescein isothiocyanate (FITC) and tetramethylrhodamine (TRITC). Cells were gated for FSC-H versus FSC-A to eliminate cell doublets and larger clumps, then analysed using dot plots measuring forward versus side scatter and red fluorescence versus FITC (green) fluorescence, as well as histogram plots measuring events with TRITC (red) fluorescence and green fluorescence. Data analysis was performed using Flowjo software (Miltenyi Biotec, Bergisch Gladbach, Germany).

2.1.5. Tri-lineage differentiation

In order to investigate the capability of stem cells to differentiate into different mesenchymal lineages, they were induced to differentiate into adipocytes, chondrocytes, and osteocytes as follows:

2.1.5.1. Adipogenic differentiation

Cells were seeded onto 6-well plates at a seeding density of 10^4 cells/well. After 24 hours, adipogenic media (STEMPRO®-Gibco) was added and the media changed every 3 days for 21 days. Adipogenic differentiation was confirmed using Oil Red O staining. In

brief, after 21 days, cells were rinsed once with PBS and then fixed with 10 % formalin for 30 minutes; cells were then washed with 60% isopropanol for 5 minutes after rinsing off the formalin with milli Q water. The cells were incubated in 0.3% Oil red O solution for 30 minutes. Wells were washed with milli Q water twice and then nuclei were stained with haematoxylin and imaged using a microscope [205]. Oil droplets within the cells represent differentiation towards the adipose lineage.

2.1.5.2. Chondrogenic differentiation

Cells were seeded onto a low adherent surface 96-well plate using a seeding density of 10^5 cells/well. The plates were centrifuged at 400g for 3 minutes, and without disturbing the pellet, chondrogenic medium (STEMPRO®-Gibco) was added. Every 3 days for 21 days the chondrogenic medium was added carefully to avoid disturbing the formed spheres. Chondrogenic differentiation was confirmed using Alcian Blue staining. In brief, after 21 days, media were removed and spheres were rinsed once with PBS, and fixed with 10% formalin for 30 minutes. After fixation, spheres were washed with PBS and then stained with 1% Alcian blue solution for 30 minutes. Afterwards, spheres were washed with 0.1 N HCl, followed by three washes with distilled water, and then visualised using a microscope. Blue staining indicated the presence of proteoglycans synthesised by chondrocytes.

2.1.5.3. Osteogenic differentiation

Cells were seeded on a 6-well plate with a seeding density of 10^4 cells/well. After 24 hours, osteogenic media (R & D system) was added and the media changed every 3 days for 21 days. Osteogenic differentiation was confirmed using von Kossa staining. In brief, after 21 days, media was removed and cells were rinsed once with PBS, and fixed with 10% formalin for 30 minutes. Then, cells were stained with 5% silver nitrate and the plate placed under light for 30 minutes for colour to develop. Wells were rinsed once with distilled water, treated with 5% sodium thiosulphate solution for 5 minutes, and then washed with water once more. The extent of mineralisation was visualised under a light microscope.

2.1.6. Fabrication of alginate beads with MSC encapsulation

A 1.5 % (w/v) medium viscosity sodium alginate solution was prepared by dissolving alginate in double-distilled water. MSCs were added to the alginate solution at a density of 1×10^6 cells/ml of alginate and mixed to homogeneity with gentle pipetting and manual shaking. PEDF protein (BioProducts MD, Bethesda-Washington DC, USA) was added to the cells-in-alginate suspension to a final concentration of 100 nM. The resultant suspension was added dropwise by means of a 27 gauge syringe into 0.1 M calcium chloride while stirring. The final calcium/alginate beads had an approximate diameter of 1.5 ± 0.3 mm [206].

2.1.7. Viability of MSCs (PEDF and beads)

In each well of a 24-well plate, alginate beads containing 2.5×10^5 cells were dispensed (n = 4). Five different timepoints - days 1, 2, 3, 5, and 7 – were assessed. To assess metabolic activity, 10% Cell Titer Blue (Promega, Melbourne, Australia) was added to each well at each timepoint according to manufacturer's instructions. Alginate beads with encapsulated cells were incubated in this solution at 37°C for 2-4 hours (until the colour began to change to purple from blue). Media (0.1 mL) from each well was transferred to a 96-well black, clear-bottom plate and fluorescence measured (570nm_{Ex}- 600 nm_{Em}) using a Fluostar, (BMG Labtech, Melbourne, Australia) plate reader.

2.1.8. Osteogenic differentiation of MSCs

To examine the pro-differentiation potential of PEDF, PEDF was added to a final concentration of 100 nM to MSCs in both conditions – growing as a monolayer culture and encapsulated within the alginate bead matrix in normal and osteogenic plates (Corning® Osteo Assay Surface), which had been coated with inorganic crystalline calcium phosphate. To assess the possible effect of other components within the medium, such as β -glycerophosphate (β -GP) and calcium chloride (CaCl_2), a set of controls was also tested to assess the effect of different factors and to rule out the false positive effect of factors such as β -GP and CaCl_2 [207] (Table 2). Each of these added factors has a role in osteogenic differentiation. Dexamethasone with 10nM

concentration, similar to the physiological level of glucocorticoids (10 nM) is the optimal concentration for mineralised nodule formation and can induce osteoblast differentiation by activating Runx2 transcription factor. The role of ascorbic acid in osteogenic differentiation is mainly attributed to the secretion of Col1 into the extracellular matrix. β -glycerophosphate facilitates osteogenic differentiation by being the source of phosphate for hydroxyapatite. Calcium chloride served as source of calcium for later stage of mineralised nodule formation [208].

Table 2. Different treatments used in *in vitro* studies

| Treatment | Component |
|------------------|---|
| A | Complete media + 100 nM PEDF+ 10 mM β -GP + 1.4 mM CaCl ₂ |
| B | Complete media + 100 nM PEDF |
| C* | Complete media + 10 mM β -GP + 1.4 mM CaCl ₂ |
| D* | Complete media |
| E | Complete media + 10 mM β -GP + 1.4 mM CaCl ₂ + 10 mM dexamethasone + 50 μ g/ml ascorbic acid |
| F | Commercial (R&D system) osteogenic media |

*Controls for treatments A and B respectively

2.1.9. Fluorescence immunocytochemistry

To observe the osteogenic differentiation of BMSCs treated with 100 nM PEDF, at seeding densities of 10000, 5000, and 1000 cells/well at day 7, 14, and 21 respectively (n = 4), four different osteogenic markers [118, 209-211] - alkaline phosphatase,

osteopontin, osteocalcin, and collagen-1 (Santa Cruz Biotechnologies, CA, USA) – were evaluated *via* immunocytochemistry [212] . Each of these markers represents different stages of osteoblastic differentiation. For example, ALP and OPN are early and mid-late differentiation markers while OCN is a late-osteogenic marker. In brief, cells were blocked with 2% serum after permeabilisation using 0.2% saponin and 0.5% bovine serum albumin (BSA), (Dako, Melbourne, Australia) corresponding to the appropriate antibodies (Santa Cruz Biotechnologies, CA, USA) for 30 minutes. Cells were then incubated overnight with primary antibody for osteogenic markers (OCN, OPN, collagen-I, and ALP in 1:250 dilution), after which cells were treated with the appropriate secondary fluorescent antibody (Santa Cruz Biotechnologies, CA, USA) at a 1:2000 dilution for 30 minutes and subsequently with 1:1000 4', 6-diamidino-2-phenylindole dihydrochloride (DAPI). Microscopic imaging was performed using a Nikon Eclipse Ti inverted microscope.

2.1.10. Alizarin red staining (ARS)

The monolayer culture was evaluated to quantify the formation of calcium deposits at days 7, 14, and 21 by staining with 4% Alizarin red solution. For each timepoint, cells were seeded in 48-well plates at three different cell densities. The seeding densities were 10000, 5000, and 1000 cells/well for day 7, 14, and 21 respectively. The cells were treated as outlined in **Table 2**. At

appropriate timepoints, cells were stained with 4% AR after fixation with 4% paraformaldehyde for 15 minutes. After washing the cells three times for five minutes each, 400µl of 10% acetic acid was added to each well for 30 minutes with gentle shaking. Cells were then scraped and removed to a 1 mL microfuge tube and heated to 85°C followed by centrifugation at 14000g for 5 minutes. Supernatants were removed and the pH adjusted to 4-4.5 by adding 10% ammonium hydroxide for each sample, then transferred to a 96-well plate and read at OD₄₀₅. A standard curve was prepared using Alizarin red standards [213].

2.1.11. von Kossa staining

The cells in monolayers and cells released from beads at different timepoints of culture (with seeding density of 10000, 5000, and 1000 cells/well for day 7, 14, and 21 respectively) were stained to visualise the mineral phosphate deposition. In the case of the monolayer culture in both normal and osteogenic plates, after fixing the cells with 4% paraformaldehyde for 15 minutes, mineralised nodules were stained with 5% silver nitrate and the plate placed under light for 30 minutes. Wells were rinsed once with distilled water, treated with 5% sodium thiosulphate solution for 5 min, and then washed with water once more [214]. Mineralisation of released cells from beads also was detected using von Kossa staining. Each well was rinsed with distilled water after

carefully removing beads from each well and staining was performed in the same manner as for the monolayer cultures.

2.1.12. Immunoblotting

Immunoblotting was performed on the MSCs cultured under conditions described previously (Table 2, A-F). Cells were grown to 85-90% confluency in 75 cm² flasks, harvested by scraping, and total cellular proteins extracted using ice-cold RIPA lysis buffer (20mM Tris-HCl, 150mM NaCl, 1mM EDTA, 1mM EGTA, 1% NP40, 2.5mM pyrophosphate, 1mM β -glycerophosphate, and 1mM sodium vanadate) containing complete protease inhibitors. Lysates were electrophoresed through a 4–20% gradient NuPAGE gel (Invitrogen, Melbourne, Australia) and electrotransferred to a polyvinylidene difluoride (PVDF; Invitrogen) membrane. Membranes then were blocked with 5% skim milk for 1 hour. Primary antibodies (Santa Cruz Biotechnologies, CA, USA) for osteogenic markers (OCN, OPN, collagen-I, and ALP) were applied and then incubated overnight at 4°C while shaking gently in a 1.5% skim milk solution. Secondary-HRP antibodies were incubated with the membranes in a 1.5% skim milk solution for one hour and were visualised using the ECL-Plus chemiluminescence system (Amersham Biosciences, Sydney, Australia) [215].

2.1.13. Alkaline phosphatase activity

The alkaline phosphatase (ALP) activity was determined using a fluorescence detection kit according to the manufacturer's protocol. In brief, cells were seeded in 48-well plates at three different cell densities using osteogenic plates. The seeding densities were 10000, 5000, and 1000 cells/well for day 7, 14, and 21 respectively. At each timepoint, cell lysates were collected using CellLytic lysis buffer. Samples were incubated for 15-30 minutes at 65°C and cooled on ice for 2 minutes. A mixture of dilution buffer and fluorescent buffer in 1:8 ratio was then added to 20 µl of sample in a 96 well plate. Finally, 1 µl of substrate was added to each well and the fluorescence measured (360 nm_{Ex}- 440 nm_{Em}) every 15 minutes for 5 hours. A standard curve was prepared using ALP standards.

2.1.14. Statistical analysis

Each datum point represents the mean of four experiments and the error bars represent the standard deviation from the mean. Statistical significance was determined using one way or two-way ANOVA and Student's *t*-test for paired and unpaired data. Differences were considered significant if the *p*-value was less than or equal to 0.05.

2.2. *In vivo* study

2.2.1. Animals

Wild type 5 weeks Balb/c mice were obtained from the Animal Resources Centre (Perth, Australia). Animal ethics approval was granted from the Curtin University Animal Ethics Committee prior to experimentation (AEC-2013-21). All the animals used in this study were both age, gender and weight matched with the animals that the stem cell were isolated from.

2.2.2. Procedure

Animals were randomly divided into four groups upon arrival ($n = 8$ mice/group) and kept and monitored for five days prior to the experiment. On the day of surgery, alginate beads in 4 different conditions, which consisted of alginate beads (negative control), alginate beads with 100 nM PEDF, alginate beads with MSCs without PEDF, and alginate beads containing 100nM PEDF and MSCs, were fabricated 3 hours before surgery.

Mice were anaesthetised with isoflurane and both lateral thigh furs clipped. Aseptically, a lateral skin incision along each thigh was made and a muscle pocket created using a pair of blunt scissors. Alginate beads were carefully implanted into a gastrocnemius muscle pocket ($n = 8$ mice/group, 10 beads/leg \sim 50,000 MSCs per implant site). Muscle and skin layers were sutured and animals monitored closely after surgery until full recovery. Metacam 1.5mg/kg was injected subcutaneously (SC)

immediately after surgery, and Buprenorphine (0.075mg/kg) was also injected SC to manage pain in animals every 12 hours for 72 hours post-surgery. Mice had unrestricted access to food and water, and were on a 12 hours light/dark cycle. Five weeks after beads insertion (end of the study), mice were euthanased by isoflurane inhalation, followed by cervical dislocation, and the implant and surrounding tissue harvested. Left limb of each animal were used for micro CT and right limb were used for histology experiments. Micro-CT was performed on implant sites to determine whether bone tissue had been produced. Implants and surrounding muscle and fat pad tissues were processed histologically post-fixation in 10% buffered formalin, then embedded in paraffin, and sectioned at 5 μ m.

2.2.3. Microcomputed tomography (μ -CT) and bone volume analysis

Mouse hind limbs were placed supine in the bed of a Skyscan 1076 *in vivo* X-ray microcomputed tomography machine. Two-dimensional (2-D) projections were obtained using an X-ray source setting of 70 kV and 139 μ A, with beam filtration through a 1.0 mm aluminium filter. Data were collected every 0.5° rotation step through 180°. The scanning width was 35 mm, and the height was 17 mm. Reconstruction was performed employing a modified Feldkamp back projection algorithm. The resulting raw image data were Gaussian filtered and globally thresholded at the fixed range of 0.0–0.0752 cross-section to image conversion to extract the mineral phase. Using transverse image slices, trabecular bone was

segmented from the cortical bone using vendor-supplied analysis software (CT-Analyser, Skyscan, BE), with semi-automated contouring. Bridging of the metaphyseal growth plate was used as the anatomical landmark for the proximal origin of trabecular bone. The selected region of interest spanned approximately 50 slices, and was analysed using morphometric software to determine trabecular bone volume ratio (Bone Volume/Tissue Volume [BV/TV]), and volumetric cortical Bone Mineral Density (BMD, g/cm³), after calibration with standard hydroxyapatite “phantoms”.

2.2.4. Immunohistochemistry and histological staining

2.2.4.1. Immunohistochemistry

Prior to any tissue staining, 5 µm sections on SuperFrost (Thermo Fisher Scientific, Melbourne, Australia) slides were deparaffinised with 100% xylene and rehydrated with a series of concentrations of ethanol (100%, 70% and 30%). Antigen retrieval was carried out with a high pH buffer consisting of 10mM Tris and 1mM EDTA (pH 9.0) for 12 min at high temperature (~90°C). Endogenous peroxidase activity was blocked with 3% hydrogen peroxide in phosphate buffered saline (PBS, pH 7.4). Blocking was achieved with BSA for 30 minutes and tissues were subsequently incubated overnight at 4°C with primary antibody (Santa Cruz Biotechnology) for OCN, OPN, ALP, pro-collagen I, MT1-MMP, HSP47, collagen I, and MMP-2. Tissue sections then were treated with a biotinylated link (DAKO), followed by streptavidin-HRP (DAKO). Staining was

achieved with DAB after incubating the sections with biotinylated secondary antibody for one hour. Counterstaining was subsequently achieved by dipping the sections 3 times in haematoxylin followed by dipping 3 times in Scott's tap water. Tissues were dehydrated in a series of ethanol washes in increasing concentrations (30%, 70%, and 100%) for 5 minutes each prior to a five minute xylene rinse. Mounting was achieved using Depex solution. Imaging was performed with an Olympus BX51 microscope and CellSens software (Olympus, Perth, Australia)

2.2.4.2. Alcian Blue staining

Sections were deparaffinised in 100% xylene and followed by rehydration with a series of concentrations of ethanol (100%, 70%, and 30%). After staining the slides with Alcian blue stain (pH~ 2.5) for 30 minutes and washing 2 times, sections were counterstained with 0.1% Nuclear Fast Red stain for one minute. Sections then were dehydrated in a series of ethanol washes in increasing concentrations (30%, 70%, and 100%) for 5 minutes each prior to a five minute xylene rinse. Mounting was achieved using a Depex solution.

2.2.4.3. Haematoxylin and eosin staining (H & E staining)

Sections were deparaffinised in 100% xylene, followed by rehydration with a series of concentrations of ethanol (100%, 70%, and 30%). After staining the slides with haematoxylin for four minutes, sections were differentiated with 0.3% acid alcohol, and stained with eosin for 2 minutes.

Chapter Three

3. Results

3.1. *In vitro* studies

3.1.1. Stem cell isolation, identification, culture, and viability

To isolate the stem cell population from mouse bone marrow, the cultured cells were treated regularly with trypsin to reduce the number of haematopoietic cells. Before cells became fully confluent, the morphology of the cells was observed to see if it fitted the described criteria of MSC. **Figure 6** is a bright field microscopic image of the isolated stem cells. As pointed *via* arrows, the cells were spindle-shaped and showed several morphological shapes from very slender and elongated to more cuboidal with less cytoplasm and shorter pseudopodia.

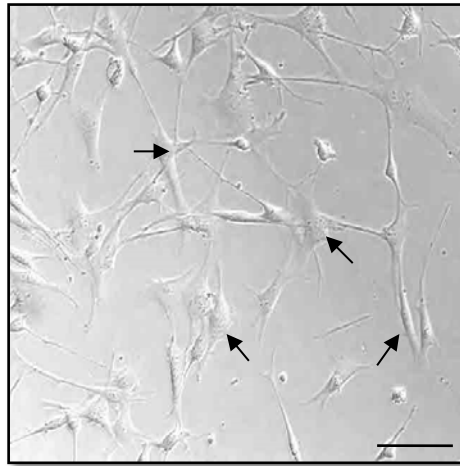


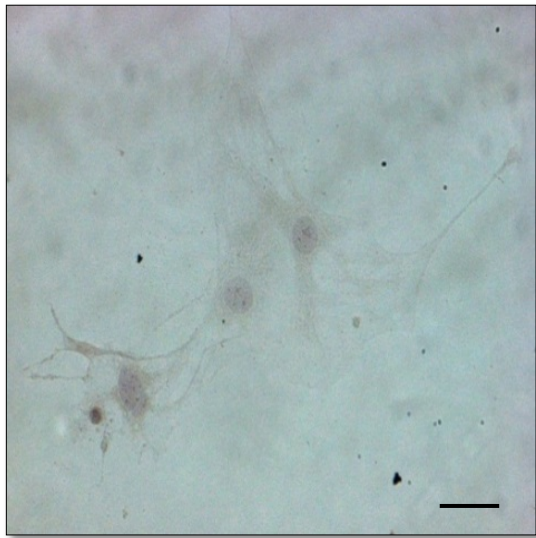
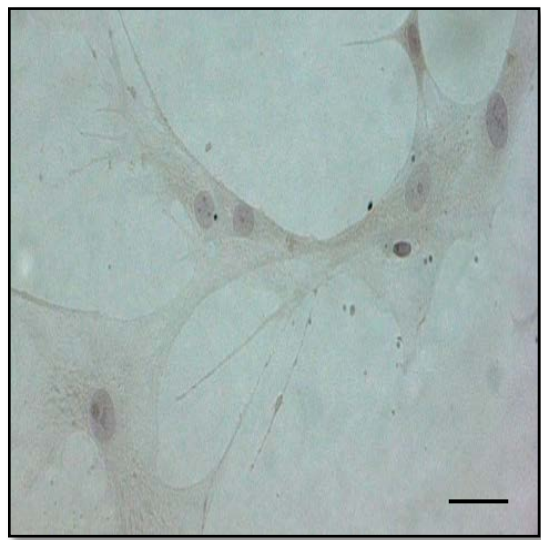
Figure 7. Morphological features of the isolated mesenchymal stem cells (MSCs)
Spindle-shaped morphology of MSCs that appear at day 1(black arrows). *Scale bar* =20 μ m.

3.1.1.1. Immunocytochemistry, FACS analysis and trilineage differentiation

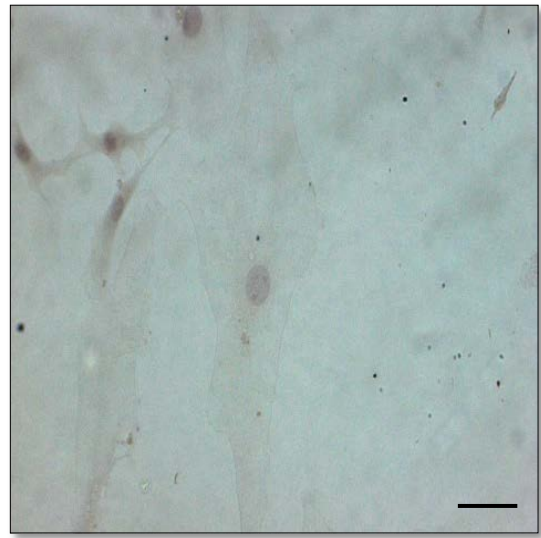
When cells reached the desired confluency (around 85-90 %), they were examined *via* a panel of four specific surface markers (CD 34, CD 19, CD 105, and CD 73) which are critical for confirming the stemness of the cells [25]. Two markers (CD 34 and CD 19) out of the panel of four were not expressed by the cells (**Figure 7a-b**), while there was positive staining for the other two (CD105, CD 73), which indicated the expression of these surface markers by the cells (**Figure 7c-d**). FACS analysis (**Figure 8**), also confirmed lack of expression of CD34 and CD19 and the presence of CD105 and CD73, which indicated that the MSCs were not contaminated by haematopoietic cells. The trilineage differentiation potential of stem cells was also tested. The isolated cells had the capacity to differentiate to adipogenic, chondrogenic, and osteogenic lineages, which was visualised using oil red O, alcian blue, and von Kossa staining respectively. As shown in **Figure 9-a**, the blue staining represents the glycosaminoglycan presence in cells differentiated to chondrocytes. In **Figure 9-b**, cells accumulated oil droplets, as demonstrated by oil red O staining, and represented adipogenic differentiation. Osteogenic differentiation of the stem cells was confirmed by von Kossa staining, which showed organic phosphate deposits made by differentiated cells (**Figure 9-c**).

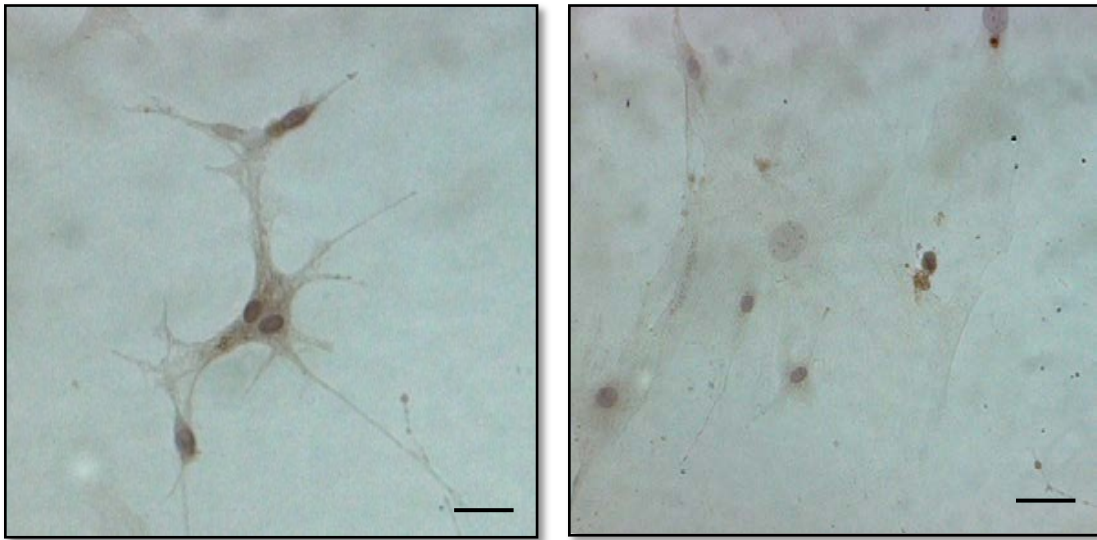


a

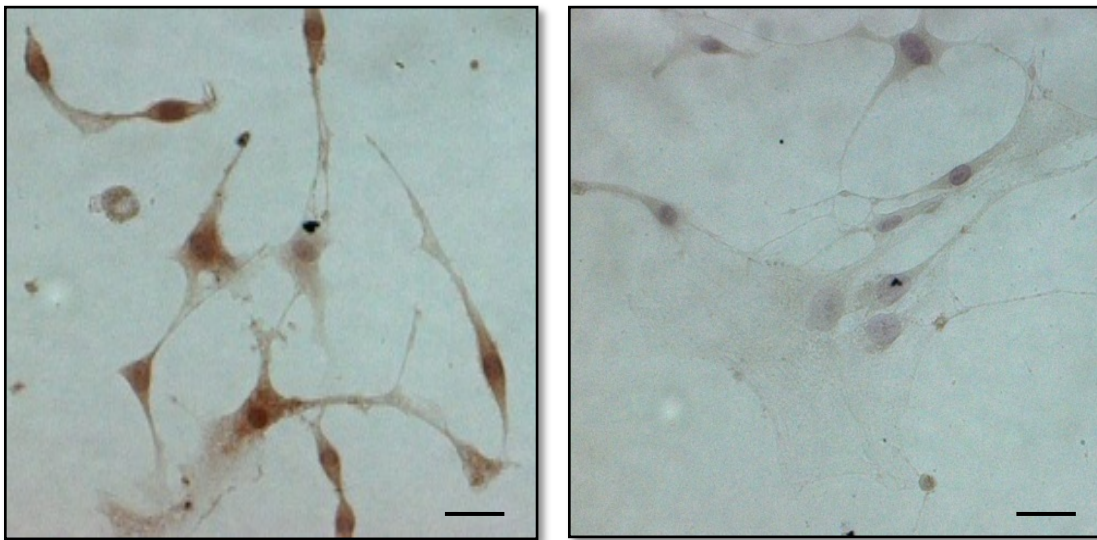


b





c



d

Figure 8. Immunocytochemical identification of harvested mesenchymal stem cells (MSCs) by light microscopy.

MSCs at passage 5 post-harvest were analysed under the light microscope post-immunocytochemistry. (a) Lack of expression of surface marker CD34. (b) Lack of expression of surface marker CD19. (c) Left, expression of surface marker CD105. Right, negative control (d) Left, expression of surface marker CD73. Right, negative control Scale bar = 20 μ m.

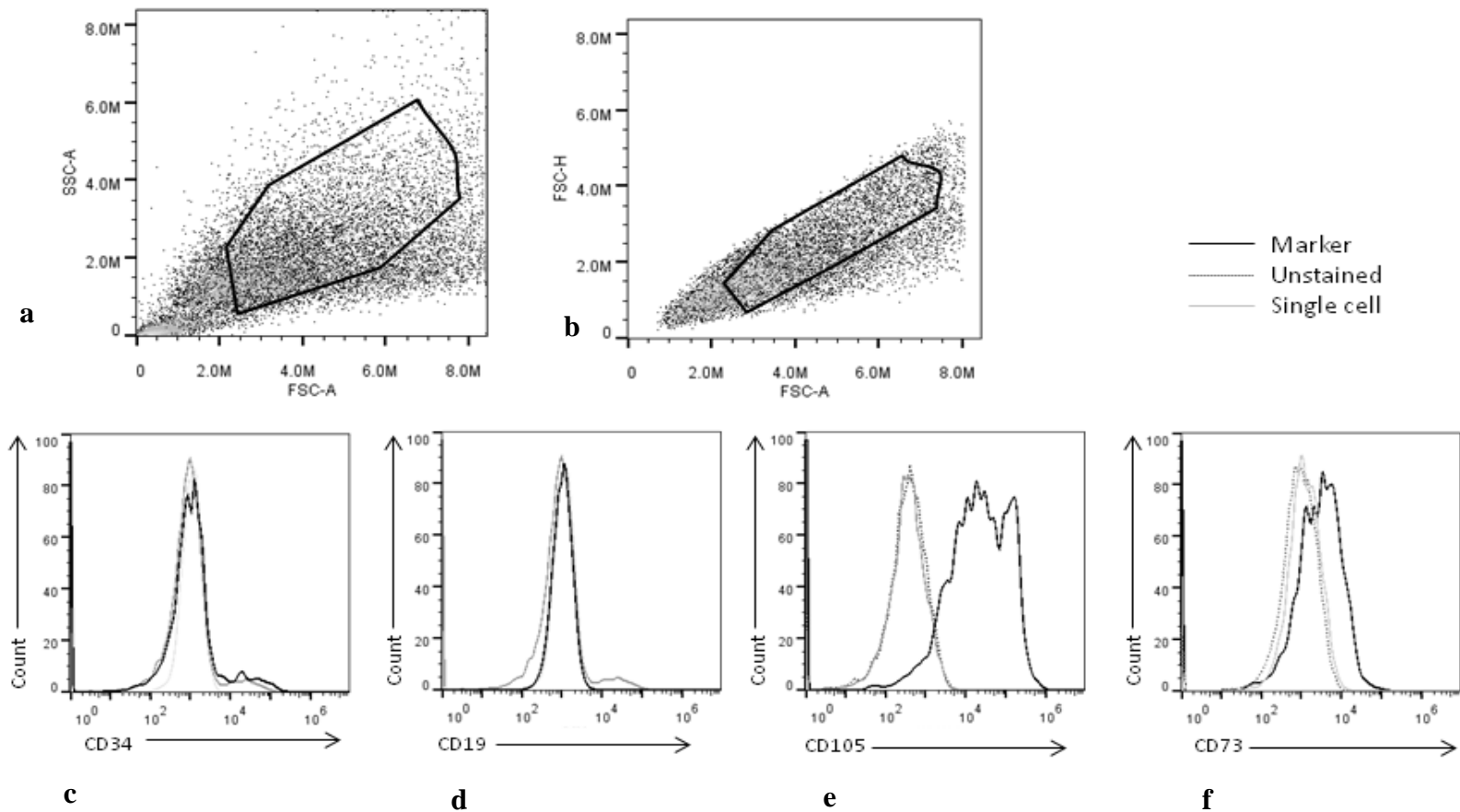


Figure 9. Flow cytometric identification of harvested mesenchymal stem cells (MSCs).

MSCs at passage 5 post-harvest were analysed *via* flow cytometry. Histogram analysis of cell surface markers showed that MSCs were not contaminated by haematopoietic cell lineages. (a) Cells were gated for stem cell population. (b) Stem cell population gated for single cells. (c) Lack of expression for CD 34. (d) Lack of expression for CD 19. (e) Expression of CD 105. (f) Expression of CD 73.

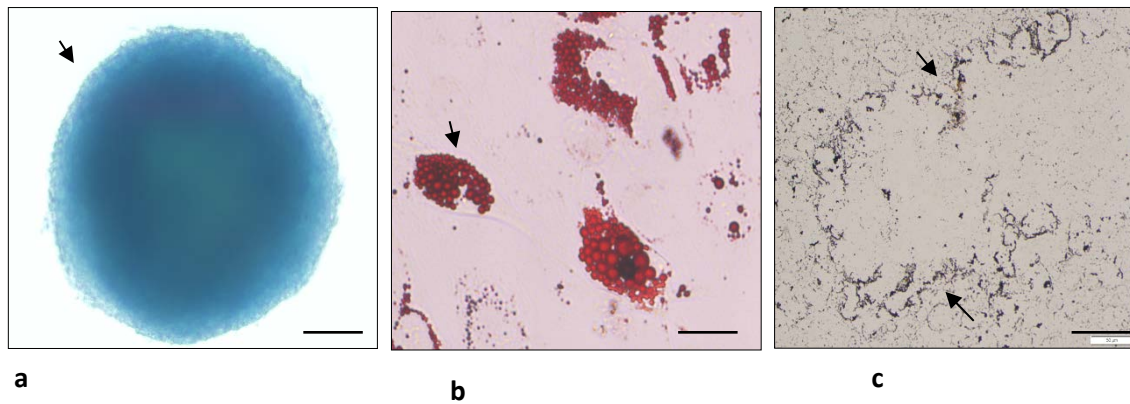


Figure 10. Differentiation capacity of mesenchymal stem cell.

(a) Chondrogenic differentiation visualised by alcian blue, (b) Adipogenic differentiation visualised by oil red O, and (c) Osteogenic differentiation visualised by von Kossa staining. Scale bar = 50 μ m.

3.1.1.2. Stem cell viability

To test the effect of PEDF and alginate on cell viability, cells in monolayers and encapsulated in alginate beads were examined for seven days at five timepoints - days 1, 2, 3, 5, and day 7. The CT-Blue assay was carried out to assess the viability of the cells. In monolayer culture, cells were treated with 100 nM PEDF [192, 216] along with cells grown in complete DMEM. With the cells in monolayers, the CT-Blue assay showed no significant difference between cells treated with PEDF and negative control at the first three timepoints. However, on day 5 of the experiment, cells treated with 100 nM PEDF appeared to have an increase in viability compared to controls (not statistically significant) (**Figure 10**). Furthermore, there was a statistically significant difference between viability of the cells treated with PEDF and untreated control at day 7 ($p \leq 0.01$). The encapsulated cells in alginate beads in both conditions (without and

with PEDF) showed no significant difference at any timepoint. However, PEDF treatment in day 3 raised the cell viability percentage, although it was not statistically significant. Overall, there was no particular trend and there was no significant difference between PEDF-treated and untreated cells (**Figure 11**).

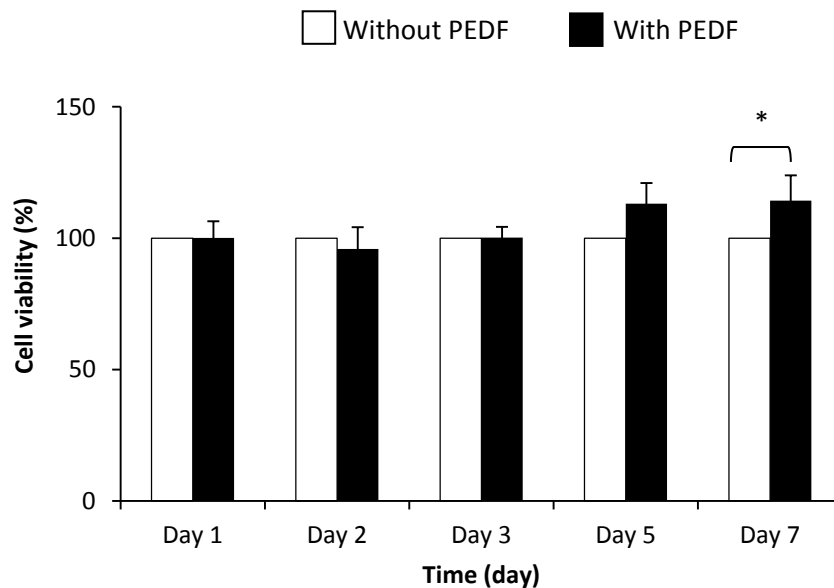


Figure 11. Viability of mesenchymal stem cells (MSCs) in the presence of pigment epithelium-derived factor (PEDF).

Viability of MSCs under control condition and PEDF treatment in monolayers over 7 days. $n = 8$. * $p < 0.01$.

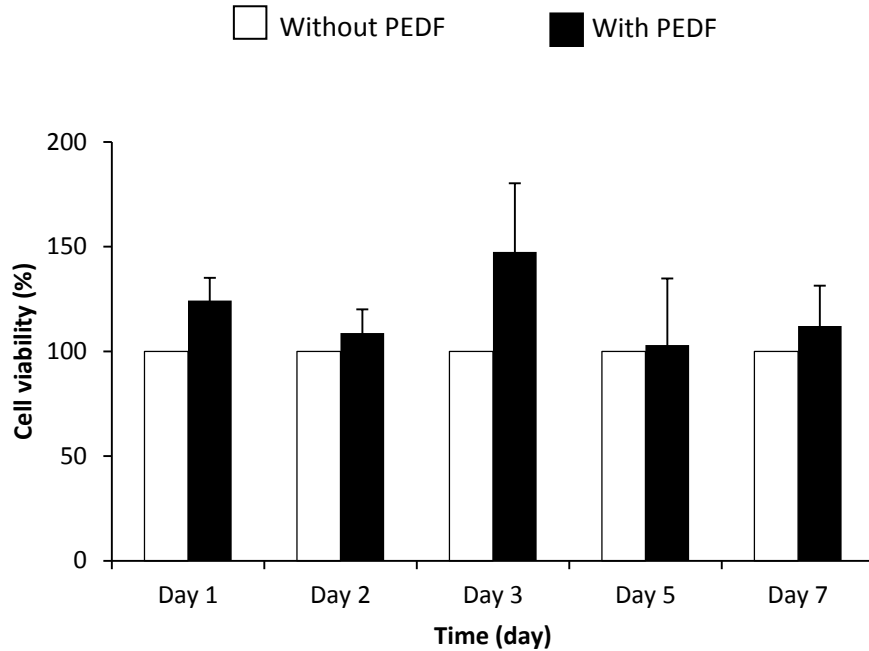


Figure 12. Viability of mesenchymal stem cells (MSCs) in the presence of pigment epithelium-derived factor (PEDF).

Viability of MSCs encapsulated in alginate beads under control condition and PEDF treatment over 7 days. $n = 4$.

3.1.2. Osteogenic differentiation of MSCs in monolayer culture

3.1.2.1. Fluorescence immunocytochemistry

To explore the potential osteogenic effect of PEDF, stem cells were seeded in 24-well plates for the duration of 21 days with 3 timepoints (day 7, 14, and day 21). Four osteogenic markers, osteopontin (OPN), osteocalcin (OCN), collagen I (Col-I), and alkaline phosphatase (ALP) were selected in order to evaluate the expression of osteoblast-specific protein in different stages of osteogenic differentiation. Cells were treated with 100 nM PEDF [216] and other control media as described previously (**Table 2 in 2.1.8**). The expression of OPN, OCN, Col-I, and ALP increased gradually from

day seven till day 14 in treatments A, B, E, and F respectively (**Figures 12, 13, 14, and 15**). However, the expression of ALP was decreased after day 14, and the fluorescence intensity was less at day 21 for treatments A, B, E, and F. No staining was observed for treatments C and D (DMEM + β -GP +CaCl₂ and DMEM respectively) for the above mentioned osteogenic markers.

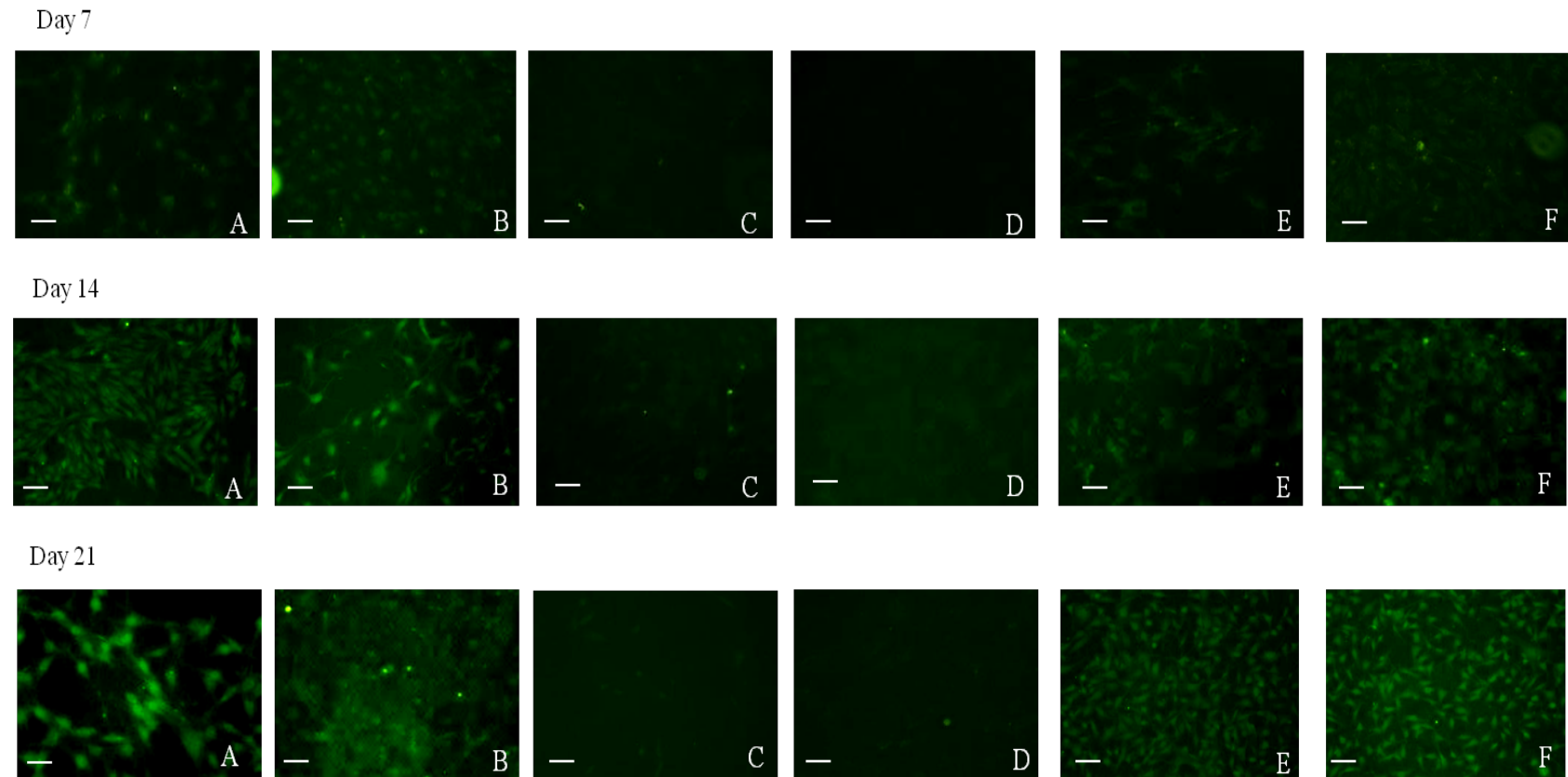


Figure 13. Immunocytochemistry of osteopontin (OPN) marker in monolayer culture of differentiated mesenchymal stem cells (MSCs) under conditions A – F (key below) at days 7, 14, and 21.

Key: A, complete media + 100 nM PEDF + 10 mM β -glycerophosphate (β -GP) + 1.4 mM calcium chloride (CaCl_2), B, complete media + 100 nM PEDF, C, complete media + 10 mM β -GP+ 1.4 mM CaCl_2 , D, complete media, E, complete media + 10 mM β -GP + 1.4 mM CaCl_2 + 10 mM dexamethasone + 50 μ g/ml ascorbic acid, F, commercial osteogenic media. $n = 4$. Scale bar =100 μ m.

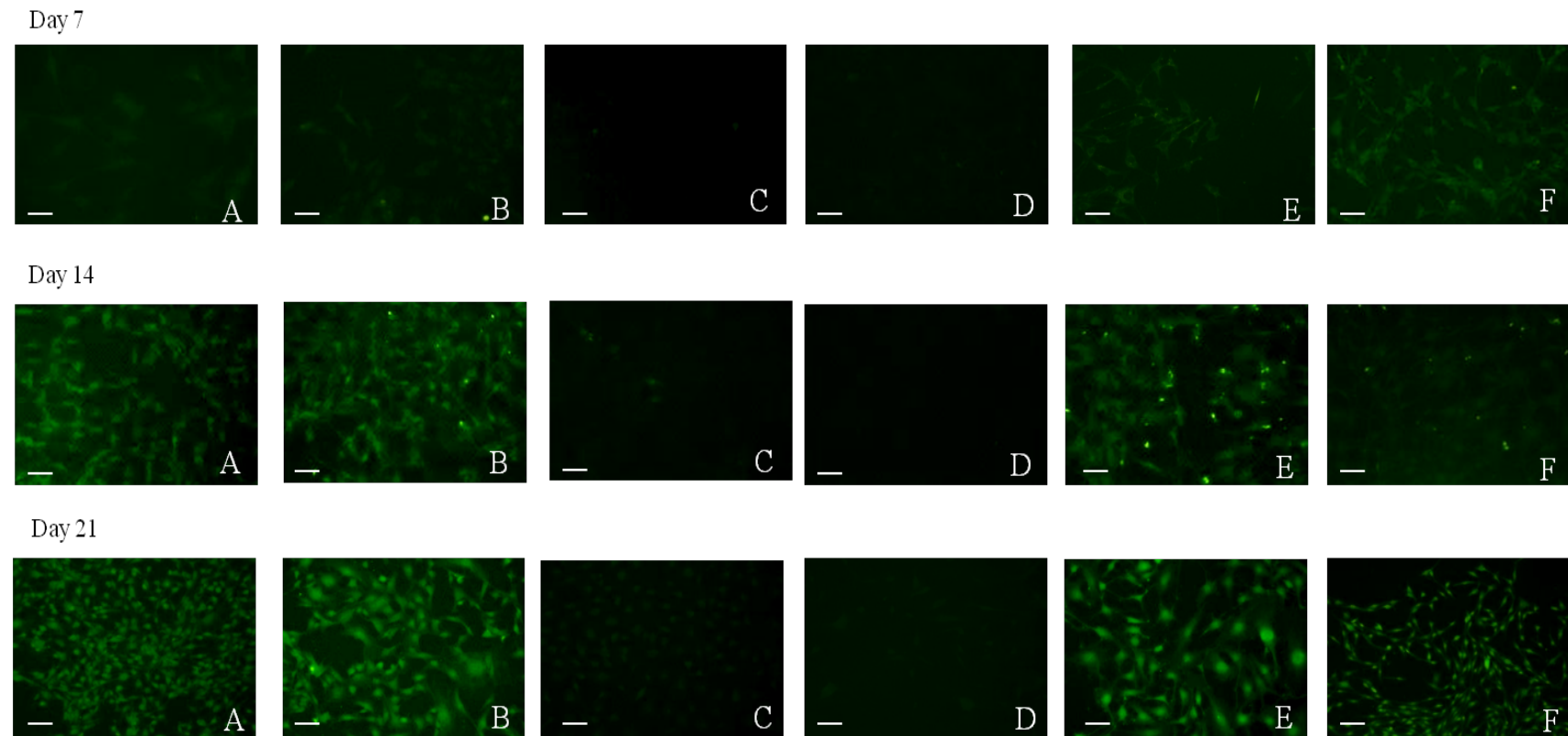
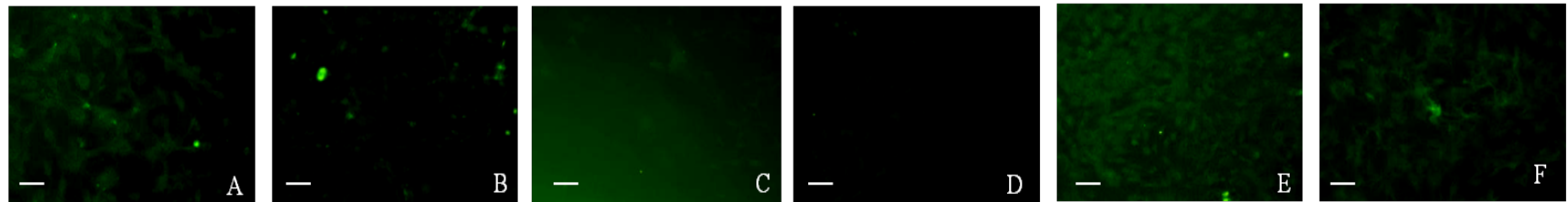


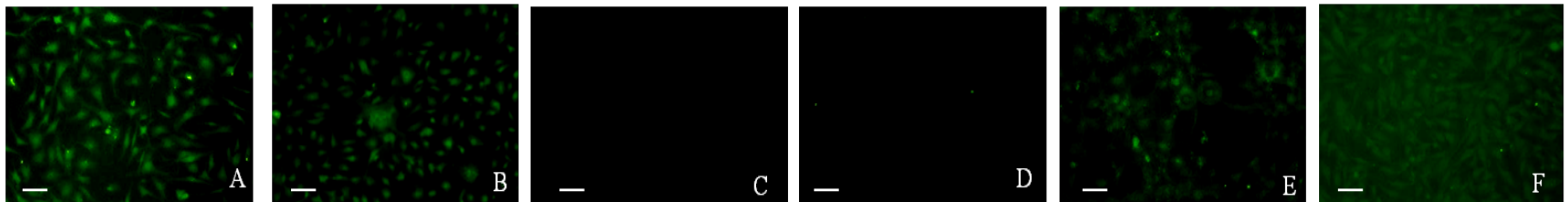
Figure 14. Immunocytochemistry of osteocalcin (OCN) marker in monolayer culture of differentiated mesenchymal stem cells (MSCs) under conditions A – F (key below) at days 7, 14, and 21.

Key: A, complete media + 100 nM PEDF + 10 mM β -glycerophosphate (β -GP) + 1.4 mM calcium chloride (CaCl_2), B, complete media + 100 nM PEDF, C, complete media + 10 mM β -GP+ 1.4 mM CaCl_2 , D, complete media, E, complete media + 10 mM β -GP + 1.4 mM CaCl_2 + 10 mM dexamethasone + 50 μ g/ml ascorbic acid, F, commercial osteogenic media. $n = 4$. Scale bar = 100 μ m.

Day 7



Day 14



Day 21

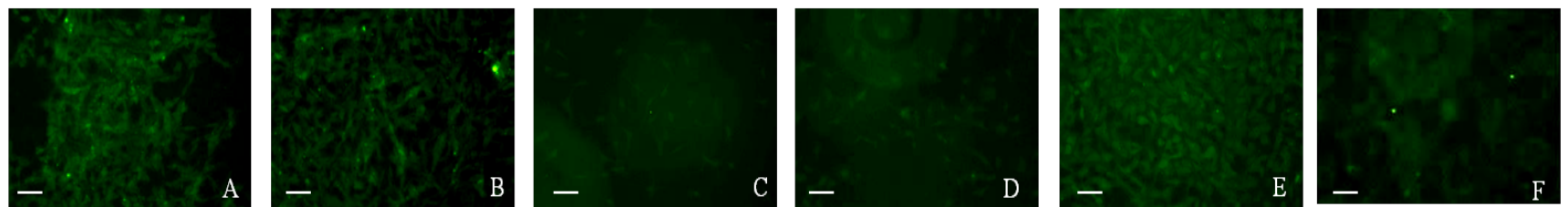
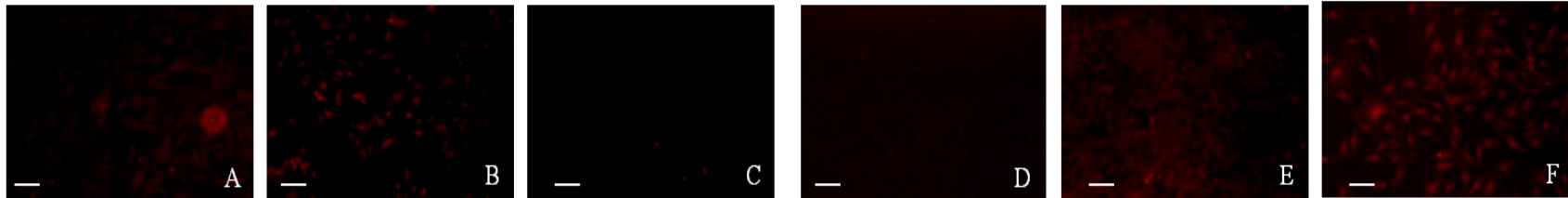


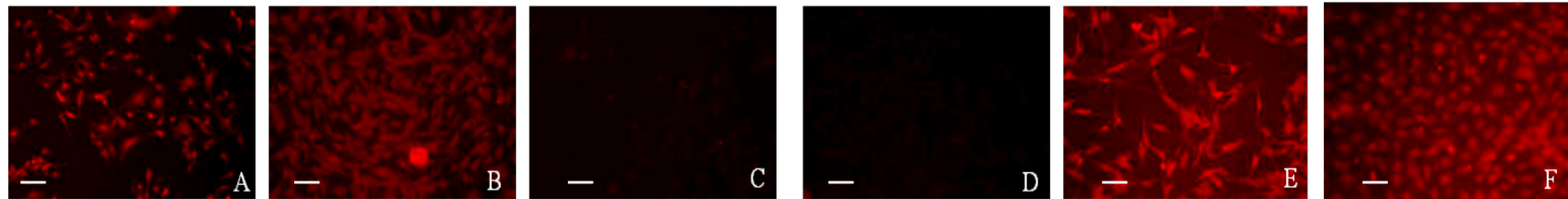
Figure 15. Immunocytochemistry of collagen I (Col I) in monolayer culture of differentiated mesenchymal stem cells (MSCs) under conditions A – F (key below) at days 7, 14, and 21.

Key: A, complete media + 100 nM PEDF + 10 mM β -glycerophosphate (β -GP) + 1.4 mM calcium chloride (CaCl_2), B, complete media + 100 nM PEDF, C, complete media + 10 mM β -GP + 1.4 mM CaCl_2 , D, complete media, E, complete media + 10 mM β -GP + 1.4 mM CaCl_2 + 10 mM dexamethasone + 50 $\mu\text{g}/\text{ml}$ ascorbic acid, F, commercial osteogenic media. $n = 4$. Scale bar = 100 μm .

Day 7



Day 14



Day 21

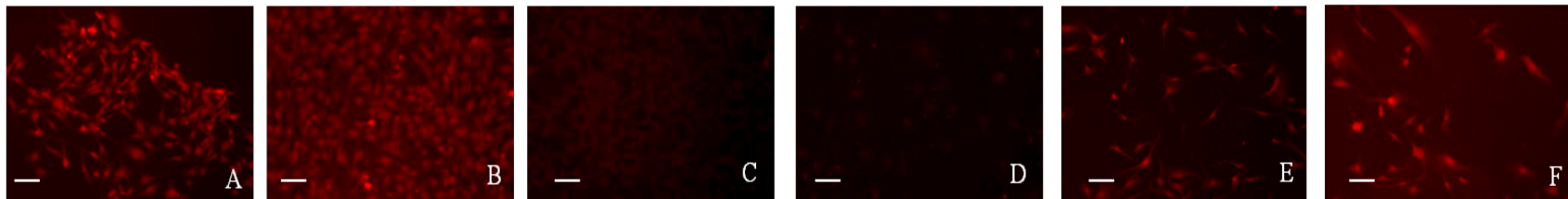


Figure 16. Immunocytochemistry of alkaline phosphatase (ALP) marker in monolayer culture of differentiated mesenchymal stem cells (MSCs) under conditions A – F (key below) at days 7, 14, and 21.

Key: A, complete media + 100 nM PEDF + 10 mM β -glycerophosphate (β -GP) + 1.4 mM calcium chloride (CaCl_2), B, complete media + 100 nM PEDF, C, complete media + 10 mM β -GP+ 1.4 mM CaCl_2 , D, complete media, E, complete media + 10 mM β -GP + 1.4 mM CaCl_2 + 10 mM dexamethasone + 50 μ g/ml ascorbic acid, F, commercial osteogenic media. $n = 4$. Scale bar = 100 μ m

3.1.2.2. von Kossa staining

The mineralisation of cells was observed using von Kossa staining of monolayer cultures in normal (non-coated) plates. The mineralised cell deposit at day 21 is shown in **Figure 16**. Treatment F showed a high amount of mineralisation at day 21, while treatments A, B, and E also showed significant mineral deposition. In treatments C and D, no mineralisation was detected. Only mature osteoblasts carry out mineralisation, hence von Kossa staining is not expected to be positive at the earlier points. The same trend was observed in monolayer cultures of stem cells in osteogenic plates. However, the intensity and amount of staining seemed higher in osteogenic plates. This was as expected as the crystalline calcium phosphate coating in the plate supports osteogenic differentiation and mineral formation (**Figure 17**).

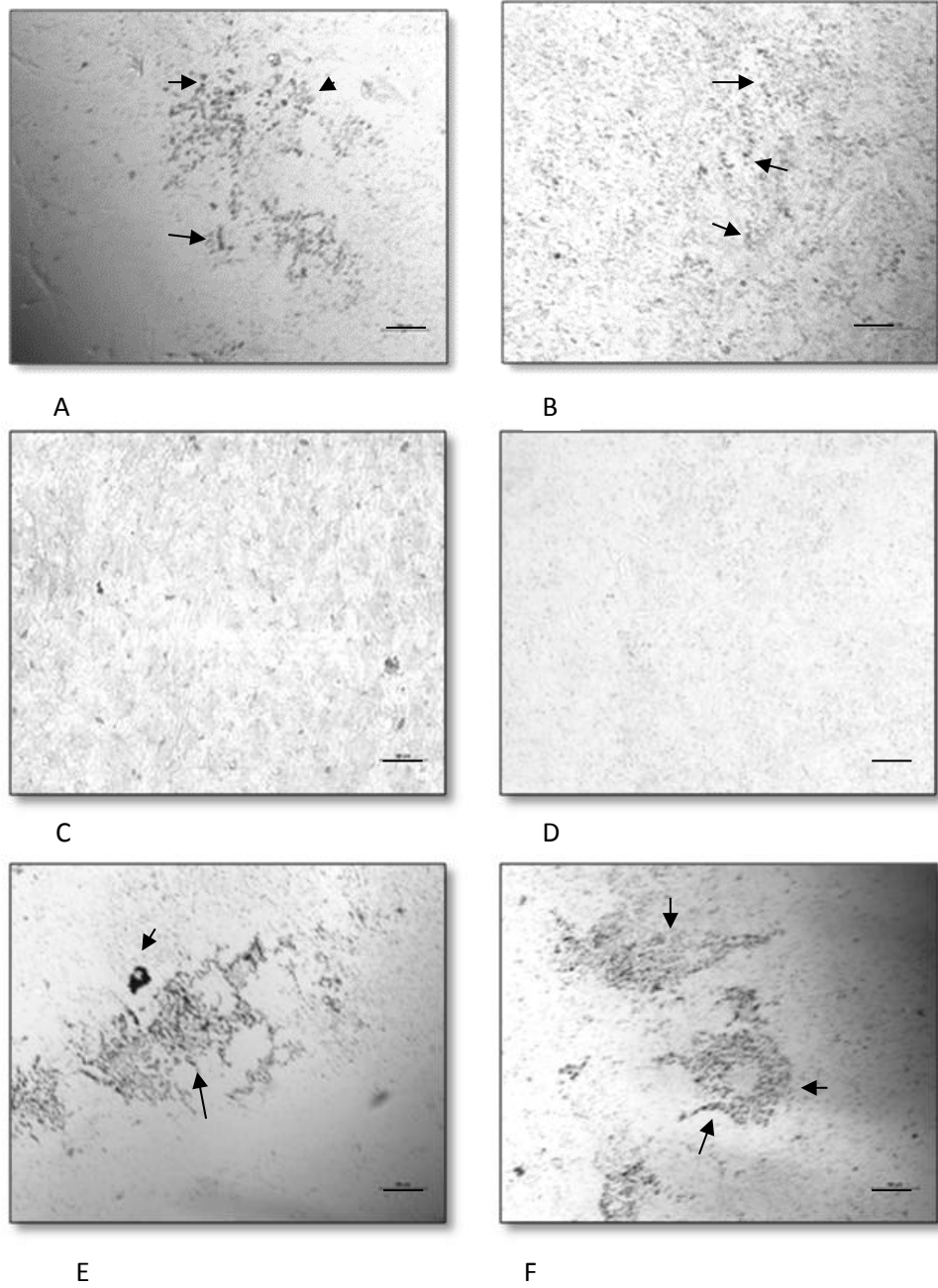


Figure 17. von Kossa staining results of mesenchymal stem cells (MSCs) grown on uncoated plate surface.

Images of stained mineral deposits (arrows) from differentiated MSCs. Key: A, complete media + 100 nM PEDF + 10 mM β -glycerophosphate (β -GP) + 1.4 mM calcium chloride (CaCl_2), B, complete media + 100 nM PEDF, C, complete media + 10 mM β -GP+ 1.4 mM CaCl_2 , D, complete media, E, complete media + 10 mM β -GP + 1.4 mM CaCl_2 + 10 mM dexamethasone + 50 $\mu\text{g}/\text{ml}$ ascorbic acid, F, commercial osteogenic media. $n = 4$. Scale bar = 10 μm

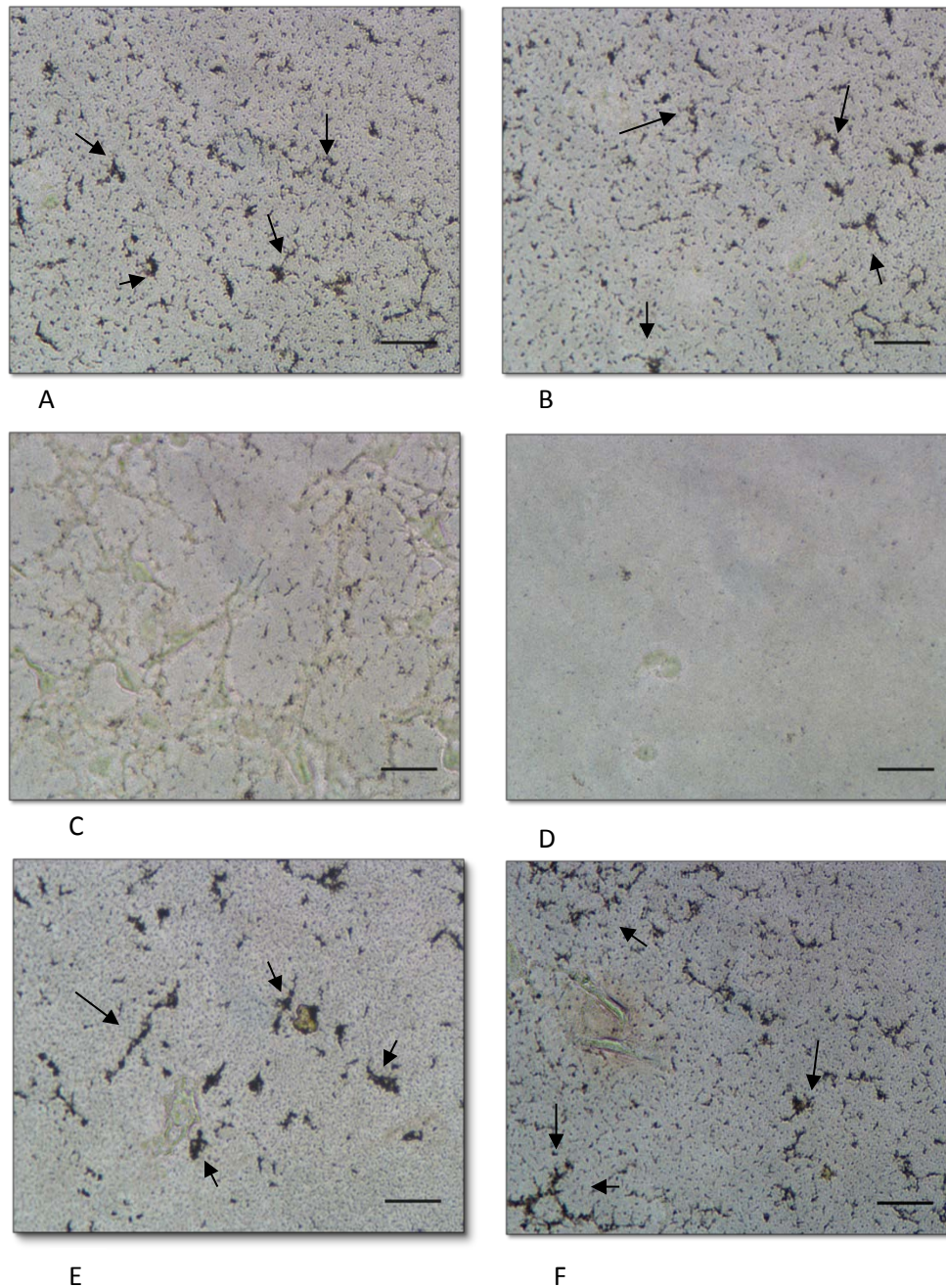


Figure 18. von Kossa staining results of mesenchymal stem cells (MSCs) grown on osteogenic plates.

Images of stained mineral deposits (arrows) from differentiated MSCs. Key: A, complete media + 100 nM PEDF + 10 mM β -glycerophosphate (β -GP) + 1.4 mM calcium chloride (CaCl_2), B, complete media + 100 nM PEDF, C, complete media + 10 mM β -GP + 1.4 mM CaCl_2 , D, complete media, E, complete media + 10 mM β -GP + 1.4 mM CaCl_2 + 10 mM dexamethasone + 50 $\mu\text{g/ml}$ ascorbic acid, F, commercial osteogenic media. $n = 4$. Scale bar = 10 μm .

3.1.2.3. Alizarin red staining (ARS)

The monolayer cultures were evaluated quantitatively for formation of calcium deposits at days 7, 14, 21 by staining with AR solution. An increasing trend was observed in the amount of mineralised calcium in treatments A, B, E, and F during the differentiation period, whereas the negative controls (treatments C and D) showed very little/no mineralisation at the corresponding study periods. As shown in **Figure 18**, there is a significant difference ($p \leq 0.05$) in the amount of mineralisation between treatments A, B and their negative control C, D respectively. Furthermore, there is a significant difference between all treatments (A, B, C, and D) with positive controls (E and F).

The amount of calcium was also evaluated in osteogenic plates at day 21 for the MSC culture under treatments based on Table 2. As shown in **Figure 19**, there is a significant difference ($p \leq 0.01$) in the amount of mineralisation between treatments A, B, E, and F, and treatments C and D. As shown in **Figure 19**, there is no significant difference between the amount of calcium detected in positive controls (E and F) and treatments (A and B). It appears that the crystalline calcium phosphate coating in the plate supports osteogenic differentiation in treatment A and B, which was also shown *via* von Kossa staining for organic phosphate deposition.

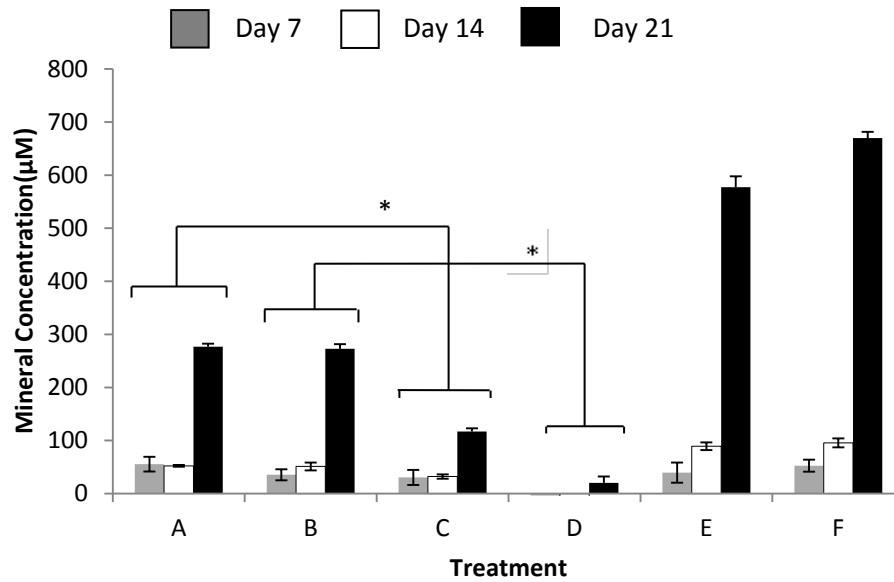


Figure 19. The mineral concentration of mesenchymal stem cells (MSCs) grown on normal (non-bone-matrix-coated) plate surface as measured by Alizarin Red

Key: A, complete media + 100 nM PEDF + 10 mM β -glycerophosphate (β -GP) + 1.4 mM calcium chloride (CaCl_2), B, complete media + 100 nM PEDF, C, complete media + 10 mM β -GP+ 1.4 mM CaCl_2 , D, complete media, E, complete media + 10 mM β -GP + 1.4 mM CaCl_2 + 10 mM dexamethasone + 50 $\mu\text{g}/\text{ml}$ ascorbic acid, F, commercial osteogenic media. n = 4. * $p < 0.05$.

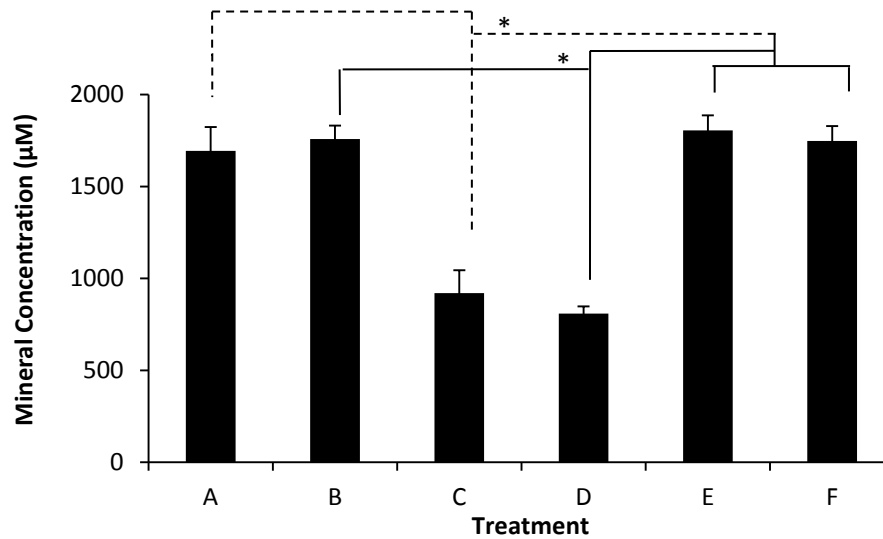
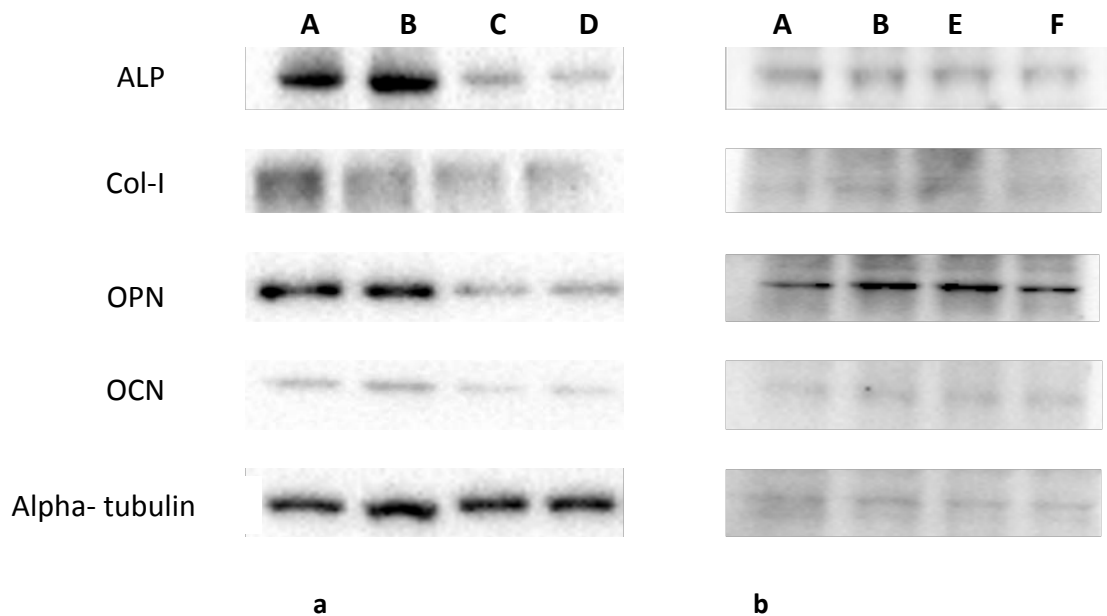


Figure 20. The mineral concentration of mesenchymal stem cells (MSCs) grown on osteogenic (bone matrix- coated) plate surface as measured by Alizarin Red.

Key: A, complete media + 100 nM PEDF + 10 mM β -glycerophosphate (β -GP) + 1.4 mM calcium chloride (CaCl_2), B, complete media + 100 nM PEDF, C, complete media + 10 mM β -GP+ 1.4 mM CaCl_2 , D, complete media, E, complete media + 10 mM β -GP + 1.4 mM CaCl_2 + 10 mM dexamethasone + 50 $\mu\text{g}/\text{ml}$ ascorbic acid, F, commercial osteogenic media. $n = 4$. * $p < 0.01$.

3.1.2.4. Immunoblotting

Figure 20 shows the Immunoblotting of the whole cell lysates of MSCs for all conditions based on **Table 2**. The first panel (Figure 21-a) shows the results of Western blotting for treatments A-D at day 14. The proteins corresponding to osteoblastic differentiation in treatments A and B were observed in contrast to negative controls. The second panel (Figure 21-b) shows the results for the same osteogenic markers for treatments A, B, E, and F at similar timepoints. The nearly two-fold increases in expression of mid osteoblastic markers (OCN and ALP in treatment B) indicate the progression of stem cells toward osteoblasts. Two-fold increase in expression of OPN and a significant drop in expression of ALP in treatment E (positive control) shows the final stage of osteoblastic differentiation of these cells. The consistent intensity, although faint, is in accordance with other findings from fluorescence immunocytochemistry, mineralisation staining, and quantification



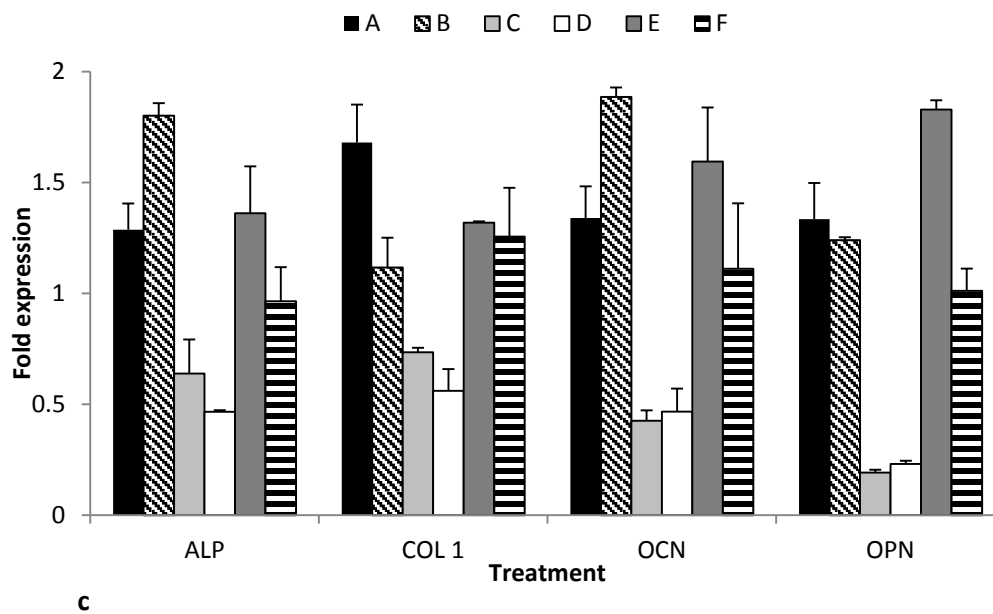


Figure 21. Immunoblot analysis shows the expression level of four osteogenic markers; alkaline phosphatase (ALP), collagen-1 (Col-1), osteopontin (OPN), and osteocalcin (OCN) at day 14.

(a). Comparing PEDF treatments (A and B) with negative controls (C and D). (b). Comparing PEDF treatments (A and B) with positive controls (E and F). *key:* A, complete media + 100 nM PEDF + 10 mM β -glycerophosphate (β -GP) + 1.4 mM calcium chloride (CaCl_2), B, complete media + 100 nM PEDF, C, complete media + 10 mM β -GP+ 1.4 mM CaCl_2 , D, complete media, E, complete media + 10 mM β -GP + 1.4 mM CaCl_2 + 10 mM dexamethasone + 50 $\mu\text{g}/\text{ml}$ ascorbic acid, F, commercial osteogenic media. $n = 3$. (c). Quantitative analysis of immunoblot bands

3.1.2.5. ALP activity

Alkaline phosphatase (ALP) enzyme activity is one of the indicators of osteoblastic differentiation. ALP activity of the MSCs in previously described conditions, cultured on osteogenic plates, was measured on day 7, 14, and 21. As shown in **Figure 21**, the ALP activity of cells in all the treatments was similar except in treatment F, which was nearly twice as much as the other treatments at day 7. As the cells progressed through the differentiation path, the activity of the enzyme increased and reached its peak at day 14 and then decreased as the cells converted to osteoblastic cells. There was a significant difference between enzyme activity in days 7 to 14 and 14 to 21 in treatments A, B, E, and F, which indicates the transformation of MSCs to mature osteoblasts. There was a significant difference ($p \leq 0.05$) in ALP activity in all three recorded timepoints between negative controls (treatment C and D) and the rest of the treatments.

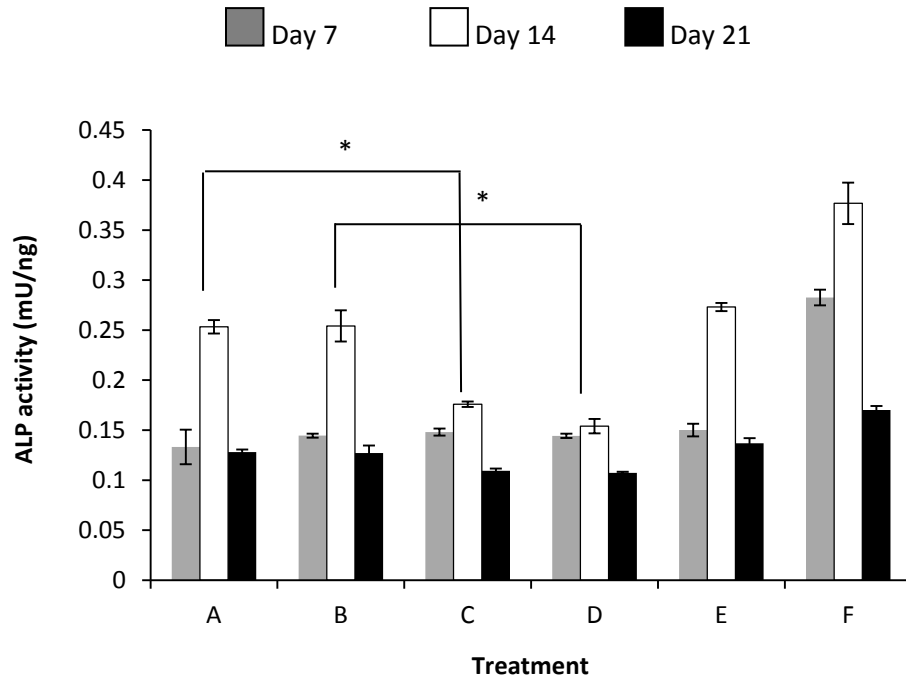


Figure 22. Alkaline phosphatase activity of mesenchymal stem cells (MSCs) in monolayer culture in osteogenic plate at days 7, 14, and 21.

key: A, complete media + 100 nM PEDF + 10 mM β -glycerophosphate (β -GP) + 1.4 mM calcium chloride (CaCl_2), B, complete media + 100 nM PEDF, C, complete media + 10 mM β -GP+ 1.4 mM CaCl_2 , D, complete media, E, complete media + 10 mM β -GP + 1.4 mM CaCl_2 + 10 mM dexamethasone + 50 $\mu\text{g}/\text{ml}$ ascorbic acid, F, commercial osteogenic media. $n = 4$, * $p < 0.05$.

3.1.3. Osteogenic differentiation of MSCs encapsulated in alginate beads

3.1.3.1. Alginate bead degradation and cell release

Microphotographs of MSCs encapsulated in alginate beads under six previously described treatments (Table 1) are shown in a weekly timeline until day 21 in **Figure 22**. At day 7, beads in treatments B, E, and F started to break up or “crack” and release the stem cells. Bead degradation in treatment A started after day 14, while for beads in treatments B, E, and F, the degradation process started within the first 7 days; and almost 80 % of the beads in treatment F, 44 % and 41 % of beads in treatments E and B, respectively, were degraded and released the encapsulated cells within 14 days. On day 21, all of the alginate beads in treatments E and F and more than 60 % of the alginate beads in treatment B released the encapsulated cells, while 33 % from treatment D and 18 and 11 % of alginate beads in treatments A and C respectively were degraded and released the cells (**Figure 23**). There is a significant difference between percentages of degradation in treatments B, E, and F, and treatment A, C, and D ($p \leq 0.05$).

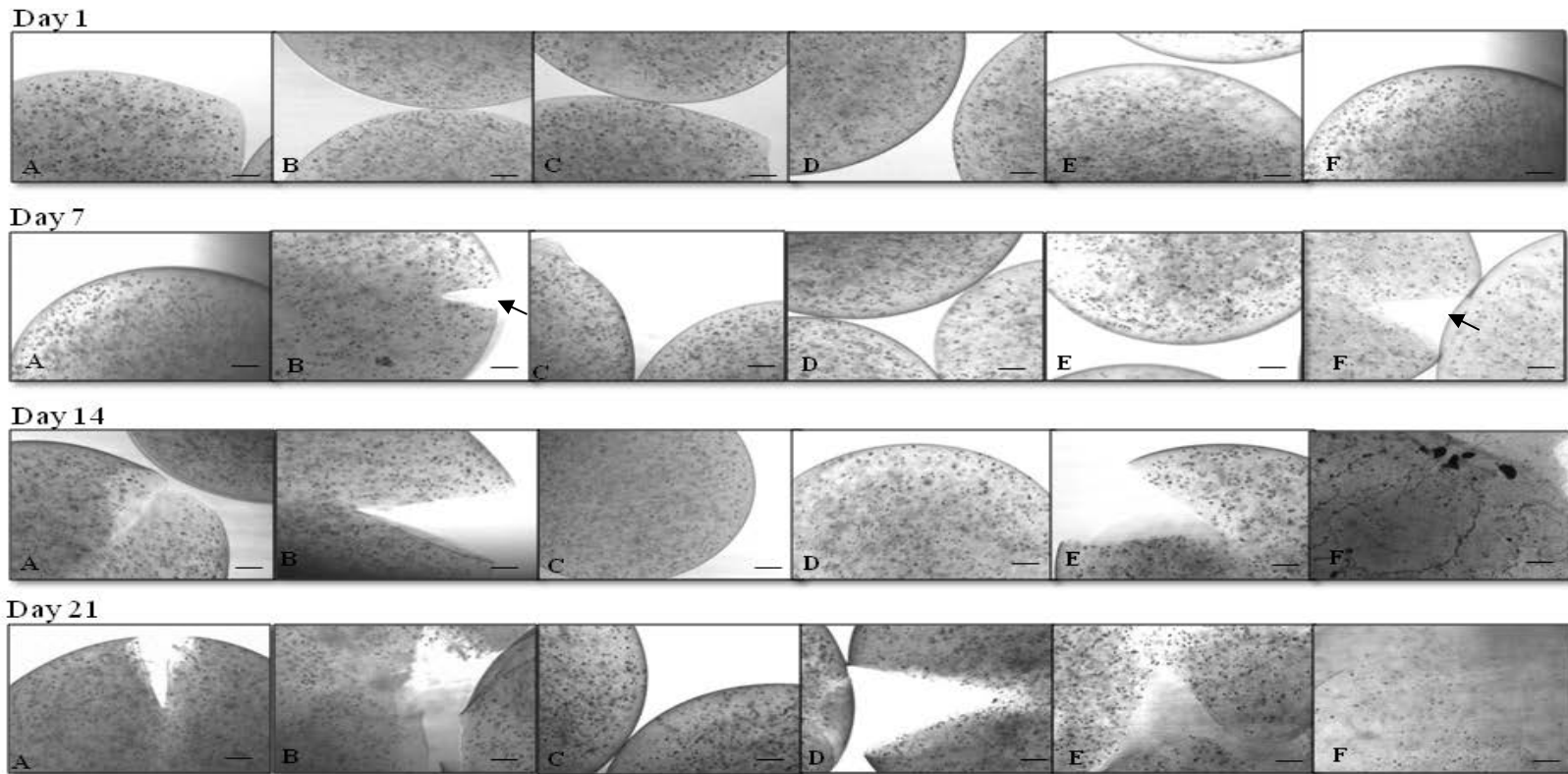


Figure 23. Time-course of mesenchymal stem cell (MSC) growth and development in alginate beads.

Alginate beads at days 7, 14 and 21 post-MSC-encapsulation in cell culture. Beads are beginning to 'crack' as early as day 7 under some conditions (*arrow*). *key*: A, complete media + 100 nM PEDF + 10 mM β -glycerophosphate (β -GP) + 1.4 mM calcium chloride (CaCl_2), B, complete media + 100 nM PEDF, C, complete media + 10 mM β -GP+ 1.4 mM CaCl_2 , D, complete media, E, complete media + 10 mM β -GP + 1.4 mM CaCl_2 + 10 mM dexamethasone + 50 $\mu\text{g/ml}$ ascorbic acid, F, commercial osteogenic media. $n = 4$, *scale bar* = 50 μm .

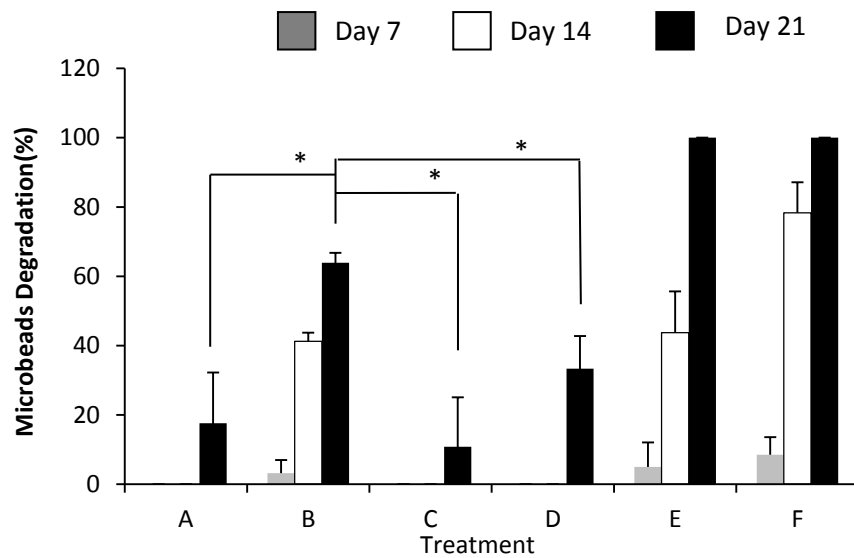


Figure 24. Time-course of alginate bead degradation over a period of 21 days in cell culture. Key: A, complete media + 100 nM PEDF + 10 mM β -glycerophosphate (β -GP) + 1.4 mM calcium chloride (CaCl_2), B, complete media + 100 nM PEDF, C, complete media + 10 mM β -GP+ 1.4 mM CaCl_2 , D, complete media, E, complete media + 10 mM β -GP + 1.4 mM CaCl_2 + 10 mM dexamethasone + 50 $\mu\text{g}/\text{ml}$ ascorbic acid, F, commercial osteogenic media. $n = 4$, * $p < 0.05$

3.1.3.2. Alizarin red staining

The quantitative evaluation of calcium deposits from released cells from alginate beads at day 21 in osteogenic plates is shown in **Figure 24**. There is a significant difference between the amounts of mineralisation in treatments A, B, E, and F with treatments C and D ($p \leq 0.05$). The crystalline calcium phosphate coating in the osteogenic plate supports osteogenic differentiation of the released cells.

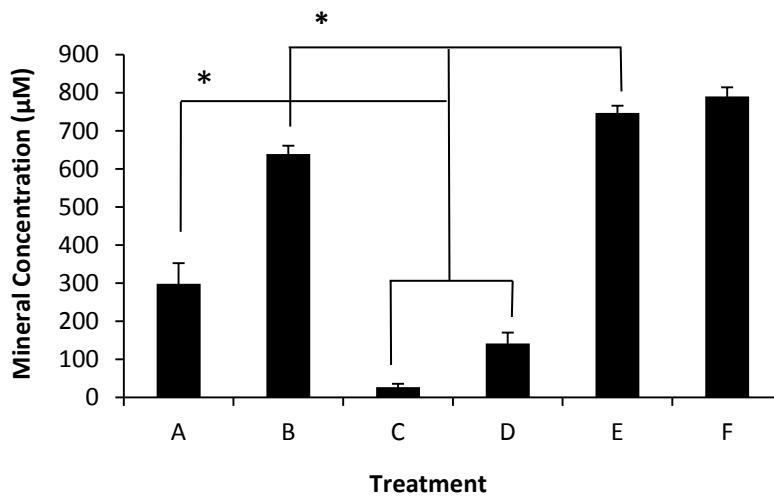


Figure 25. Mineralisation by released cells from alginate beads in osteogenic plate at day 21 in monolayer culture.

The mineral concentration was measured by Alizarin Red assay. Key: A, Complete media + 100 nM PEDF + 10 mM β -GP + 1.4 mM CaCl_2 , B, Complete media + 100 nM PEDF, C, Complete media + 10 mM β -GP + 1.4 mM CaCl_2 , D, Complete media, E, Complete media + 10 mM β -GP + 1.4 mM CaCl_2 + 10 mM dexamethasone + 50 $\mu\text{g/ml}$ ascorbic acid, F, Commercial osteogenic media. $n=4$, * $p<0.05$

3.1.3.3. von Kossa staining

Figure 25 shows the mineralisation of the cells released from alginate beads in normal plates as well as osteogenic plates (**Figure 26**) at day 21. In normal plates, the staining for mineralisation in treatments A and B is similar in amount and no mineralisation was observed in treatments C and D; however, the staining for mineralised nodules in osteogenic plates in treatment B is comparable with treatments E and F, while treatment A along with treatments C and D show no staining and indicate the absence of mineralisation.

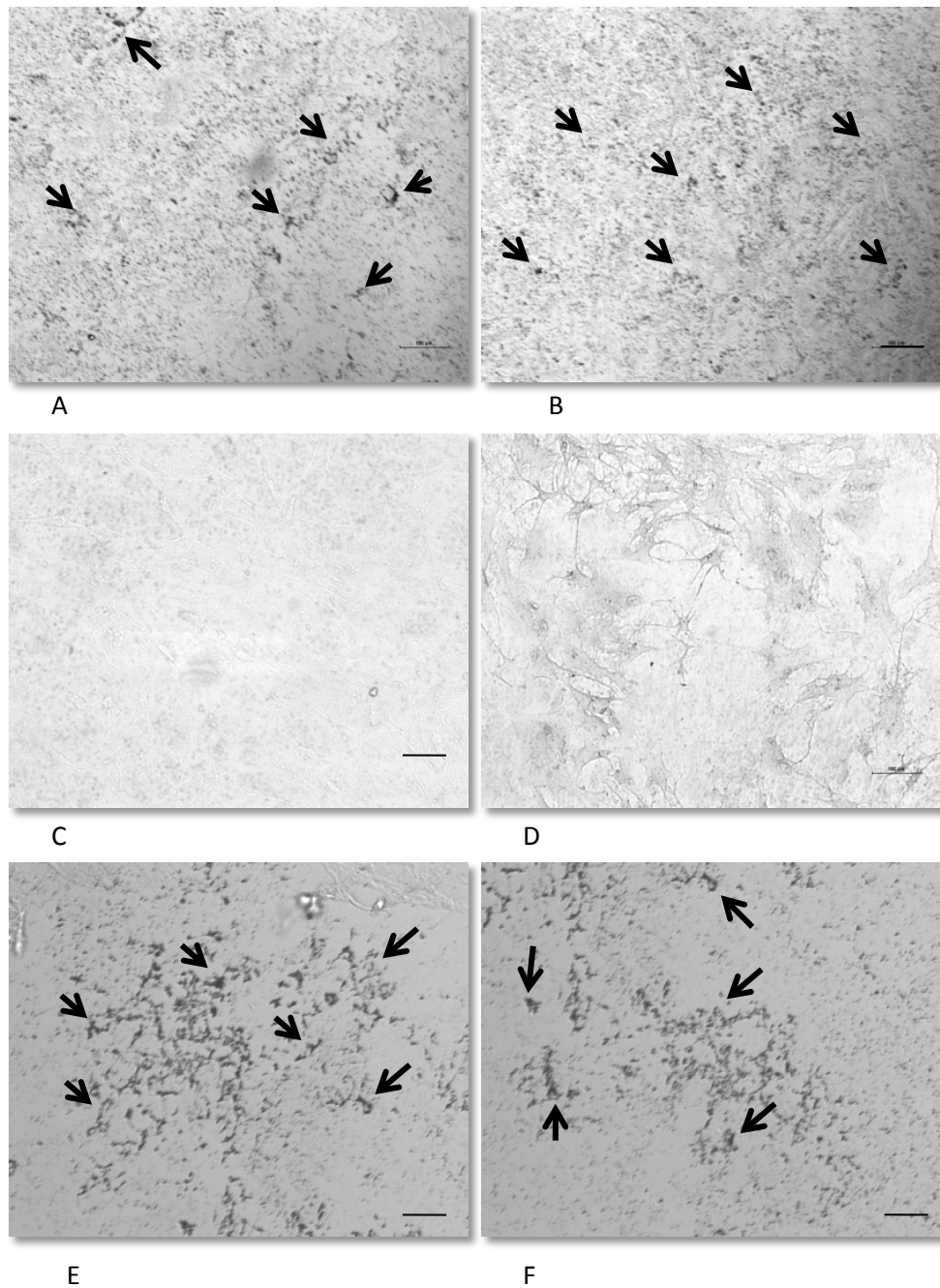


Figure 26. von Kossa staining results of mesenchymal stem cells (MSCs) released from alginate beads on normal (non-bone-matrix-coated) plate surface.

Images of stained mineral deposits (arrows) from differentiated MSCs. Key: A, complete media + 100 nM PEDF + 10 mM β -glycerophosphate (β -GP) + 1.4 mM calcium chloride (CaCl_2), B, complete media + 100 nM PEDF, C, complete media + 10 mM β -GP + 1.4 mM CaCl_2 , D, complete media, E, complete media + 10 mM β -GP + 1.4 mM CaCl_2 + 10 mM dexamethasone + 50 $\mu\text{g}/\text{ml}$ ascorbic acid, F, commercial osteogenic media. $n = 4$. Scale bar = 10 μm .

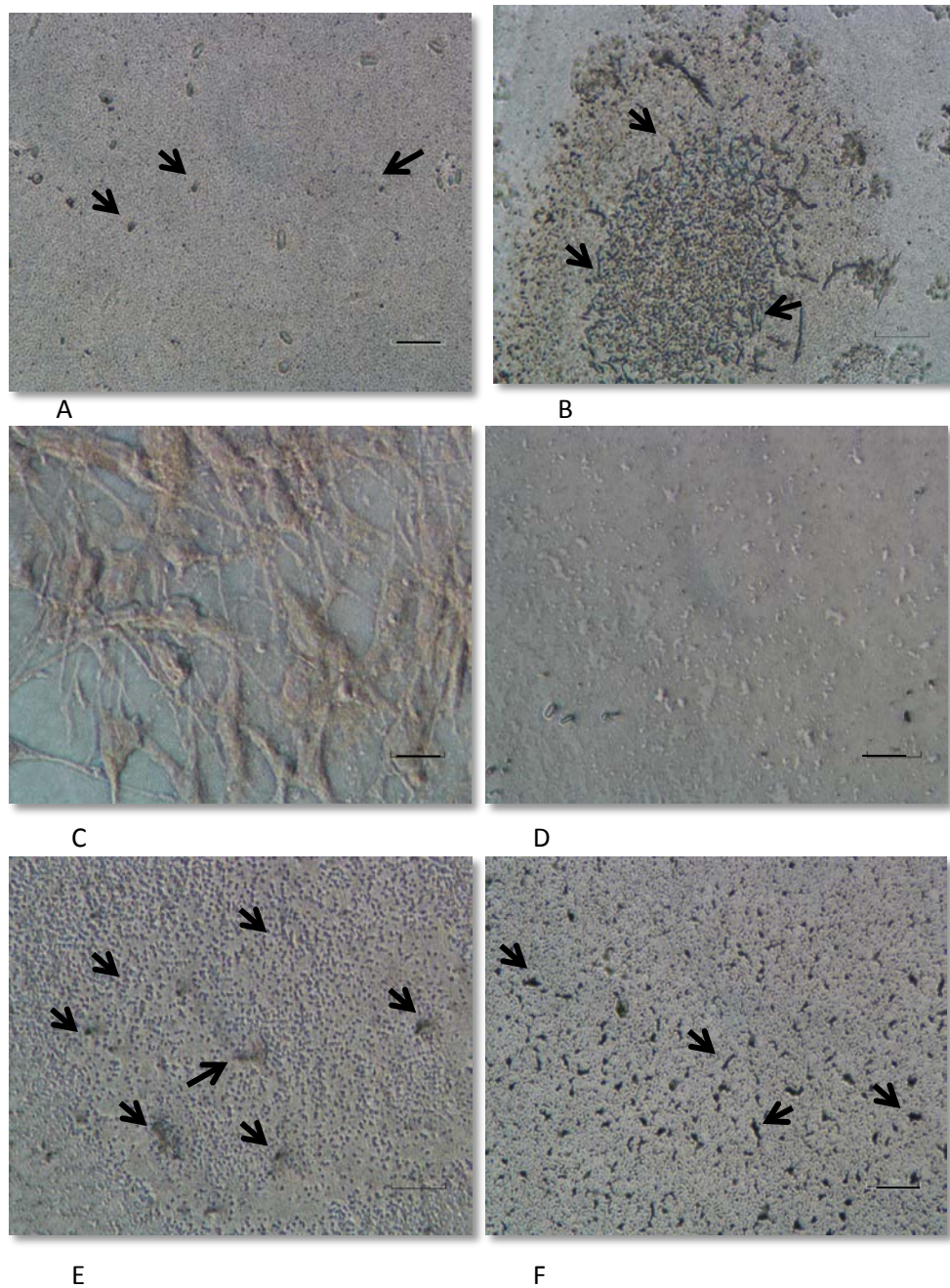


Figure 27. von Kossa staining results of mesenchymal stem cells (MSCs) released from alginate beads on osteogenic plate surface.

Images of stained mineral deposits (arrows) from differentiated MSCs. *Key:* A, complete media + 100 nM PEDF + 10 mM β -GP + 1.4 mM calcium chloride (CaCl_2), B, complete media + 100 nM PEDF, C, complete media + 10 mM β -GP + 1.4 mM CaCl_2 , D, complete media, E, complete media + 10 mM β -GP + 1.4 mM CaCl_2 + 10 mM dexamethasone + 50 $\mu\text{g}/\text{ml}$ ascorbic acid, F, commercial osteogenic media. $n = 4$. Scale bar = 10 μm

3.2. *In vivo* study

3.2.1. Macroscopic findings

An intramuscular pocket was created for alginate bead implantation. PEDF in alginate beads, MSCs in alginate beads, PEDF + MSCs in alginate beads, and empty alginate beads were carefully inserted into the muscle pocket, and after 35 days all of the implants in the first three groups resulted in implants that had blood vessels clearly visible and with yellowish-white morphology to the implants (**Figure 27.a-c**), which indicated the cellular occupancy of the implants as opposed to the 'milky-white' hue observed in the empty bead cohort (**Figure 27.d**). Macroscopically, in the empty bead group, beads with acellular matrix were noted as well as the beads having a brittle texture. Furthermore, alginate beads were intact and kept their spherical shapes, and no enzymatic/cellular degradation/interaction was visible. In contrast with these findings, in the other three groups, the implants had an elastic-feel texture and the alginate beads had lost their integrity and fused together as a result of enzymatic/cellular degradation/interaction and formed a yellow mass surrounded with blood vessels. They also exhibit layer-looked especially in PEDF in alginate beads and MSCs with PEDF in alginate beads group. The vasculature around the implants of alginate and PEDF, and alginate with PEDF and MSCs, were more prominent compared to the vessels around alginate with MSC implants. This is an interesting finding considering that PEDF is usually known for its anti-angiogenic properties.

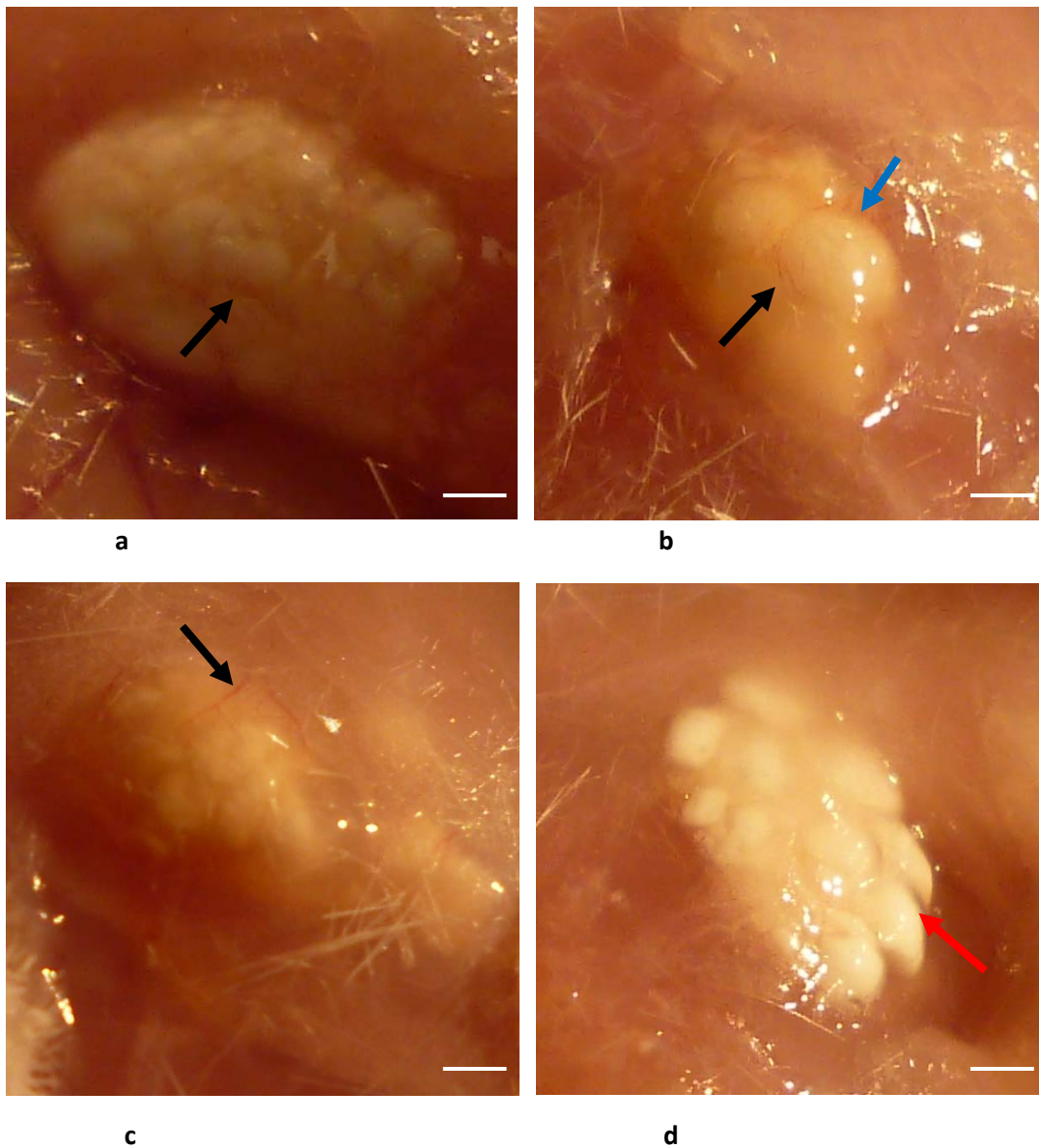


Figure 28. Macroscopic observation of beads implanted in Balb/c mice for 35 days.

(a) Alginate beads with pigment epithelium-derived factor (PEDF). (b) Alginate beads with mesenchymal stem cells (MSCs) (c) Alginate beads with MSCs and PEDF. (d) Empty alginate beads with a milky-white hue and acellular texture (*red arrow*). Blood vessels (*black arrow*) and yellowish hue (*blue arrow*) were noted. *Scale bar* = 1mm.

3.2.2. Micro-CT

Micro-CT imaging revealed the formation of osteoid tissue in the implant site (**Figure 28**). In the alginate with PEDF group (**Figure 28-a**), the formation of considerable osteoid tissue in the implant area is visible as well as in the alginate and MSC group but in a much lesser extent (**Figure 28-b**). Interestingly, micro-CT images of the alginate with PEDF and MSC group (**Figure 28-c**) showed a significant amount of osteoid tissue. Micro-CT imaging also picked up some mass formation in the empty alginate bead group. The structure of the latter was in complete contrast with the images from other groups. As pointed out by the blue arrows in **Figure 28 a-c**, the mass formed in the first three groups is more likely an osteoid tissue (woven bone) with crinkled edges and a wrinkled/rippled surface, whereas in the alginate alone group (yellow arrow), complete round edges with a smooth surface are visible. Quantitative micro-CT was also carried out for a few important bone parameters (**Figure 29 a-c**). The bone volume in three different groups was quantified *via* micro-CT imaging. There is a significant difference in bone volume in MSCs with PEDF in alginate beads compared to PEDF in alginate beads, and MSCs in alginate beads (**Figure 29-a**). The same significant difference was also observed for the structural thickness of the formed tissue (**Figure 29-b**). However, the comparison of tissue mineral density of the same three groups showed no significant difference (**Figure 29-c**). Overall, the order of *de novo* bone formation in increasing order was: MSCs in beads < PEDF in beads < MSCs + PEDF in beads.

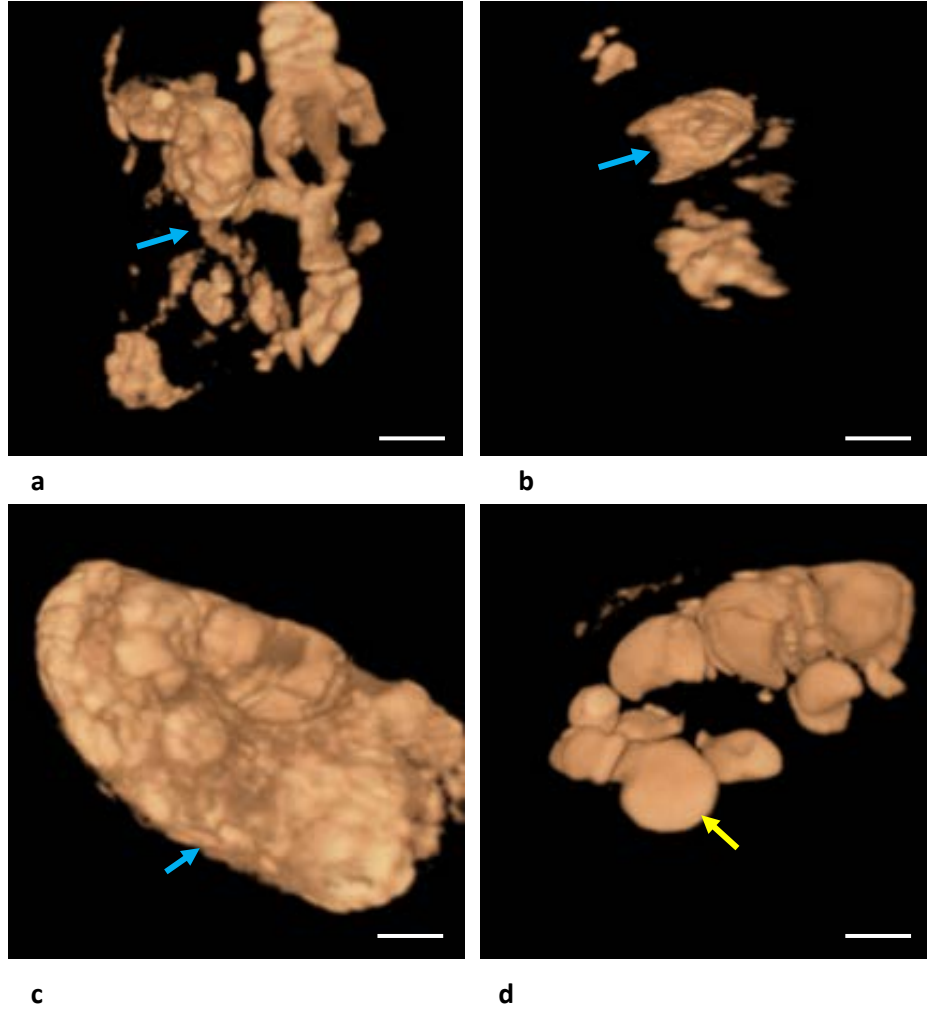


Figure 29. Micro-CT images of alginate bead implants.

(a) Alginate beads with pigment epithelium-derived factor (PEDF) (b) alginate beads with mesenchymal stem cells (MSCs) and PEDF (c) alginate beads with MSCs (d) empty alginate beads. *Arrow: yellow, smooth exterior of alginate bead implants; blue, rough exterior of alginate bead implants. Scale bar = 1mm*

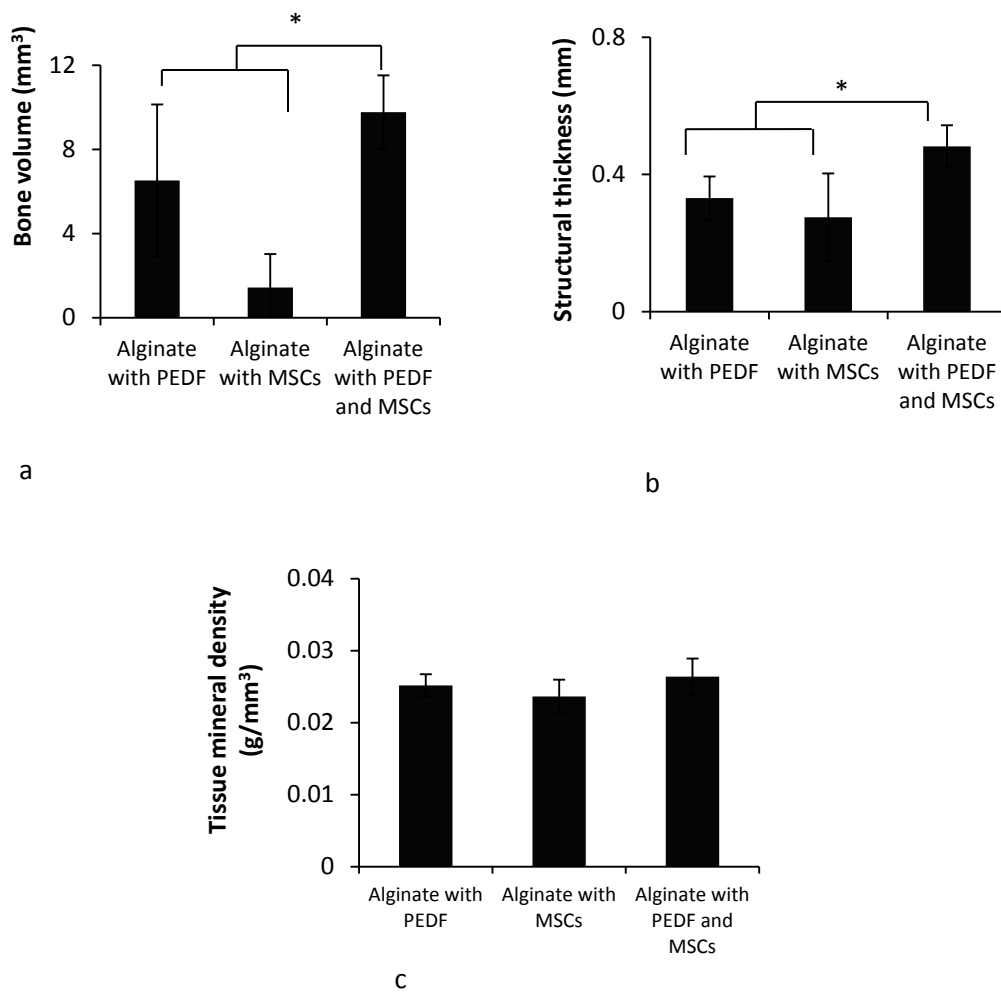


Figure 30. Quantitative micro-CT measurements.

Measurements of (a) bone volume (mm³) determined in three different groups, (b) structural thickness (mm), and (c) tissue mineral density (g/mm³). $n = 6$, $* p < 0.05$.

3.2.3. Haematoxylin and eosin (H & E staining)

Two sets of figures are presented as a panel of four images to compare the morphology and degradation state of the implants with different magnification *via* haematoxylin and eosin (H&E) staining.

Figure 30 shows a low magnification image of the alginate beads implant in four different groups. Figure 30 a-c shows PEDF in alginate beads, MSCs in alginate beads, and MSCs with PEDF in alginate beads respectively. In all of these three groups, alginate beads show degradation and loss of integrity and shape, which were greatest in the group of MSCs with PEDF in alginate beads. In this group, the beads fused together and formed a mass of cells with an alginate residue in between. A lesser level of degradation was observed in the other two groups (PEDF in alginate beads and MSCs in alginate beads). **Figure 30-d** shows the alginate bead alone group. In this group, beads kept their spherical shape and stayed intact with no sign of degradation. Higher magnification images of beads from the different groups are shown in **Figure 31**. In the first image (**Figure 31-a**), it seems that PEDF caused cell migration [217, 218] (believed to be mainly stem cells) toward the alginate beads from available sources such as adipose tissue near the implant site. Considering the formation of osteoid tissue in this group, based on micro-CT results, it can be postulated that PEDF can attract stem cells from nearby tissues such as adipose tissue and muscle and modulate their differentiation toward an osteoblastic phenotype. Black arrow shows the osteoblasts. **Figure 31-b** shows the MSCs in alginate beads group. Some light purple nuclei (nuclear

ghosts) were visible in this group, suggesting that some of the cells died during the course of the study (red arrow). However, a significant number of the cells survived and partially differentiated toward an osteoblastic phenotype. **Figure 31-c** shows the MSCs with PEDF in alginate beads group. The cellular organization within these beads was homogeneous and differentiation of stem cells to osteoblasts is visible throughout the section (black arrow). An alginate bead is shown in **Figure 31-d**. Intact alginate with some of the surrounding cells showed no significant change in morphology, size, and degradation.

The H & E staining for fat (**Figure 32**) and muscle (**Figure 33**) surrounding the implant site shows that both muscle and fatpad tissue morphology were not altered by PEDF.

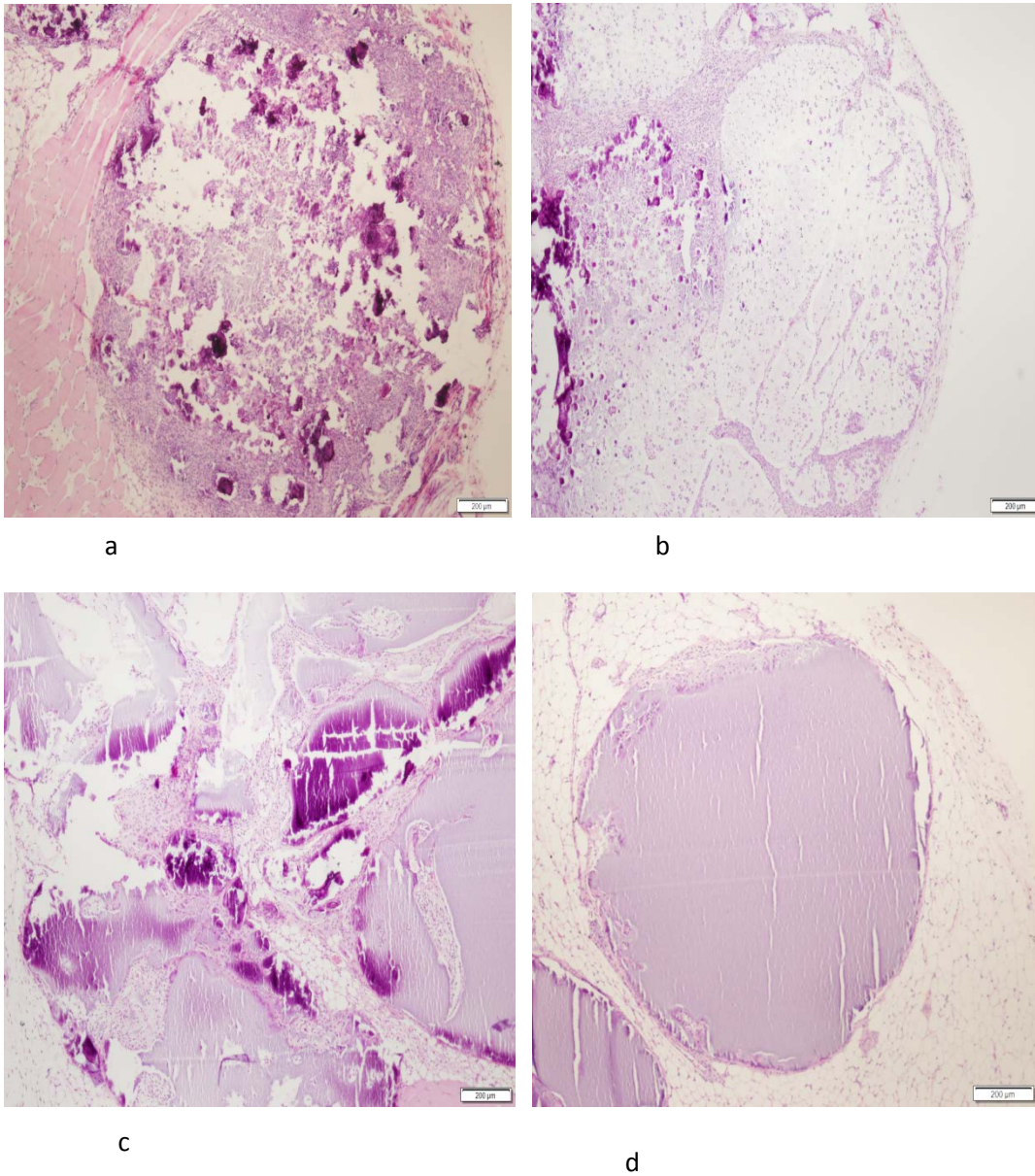


Figure 31. Haematoxylin and eosin (H & E) staining for different groups.

View of alginate bead degradation in four different groups, a) alginate bead with pigment epithelium-derived factor (PEDF) b) alginate bead with mesenchymal stem cells (MSCs), c) alginate bead with MSCs and PEDF d) alginate bead. *Scale bar=200 μm.*

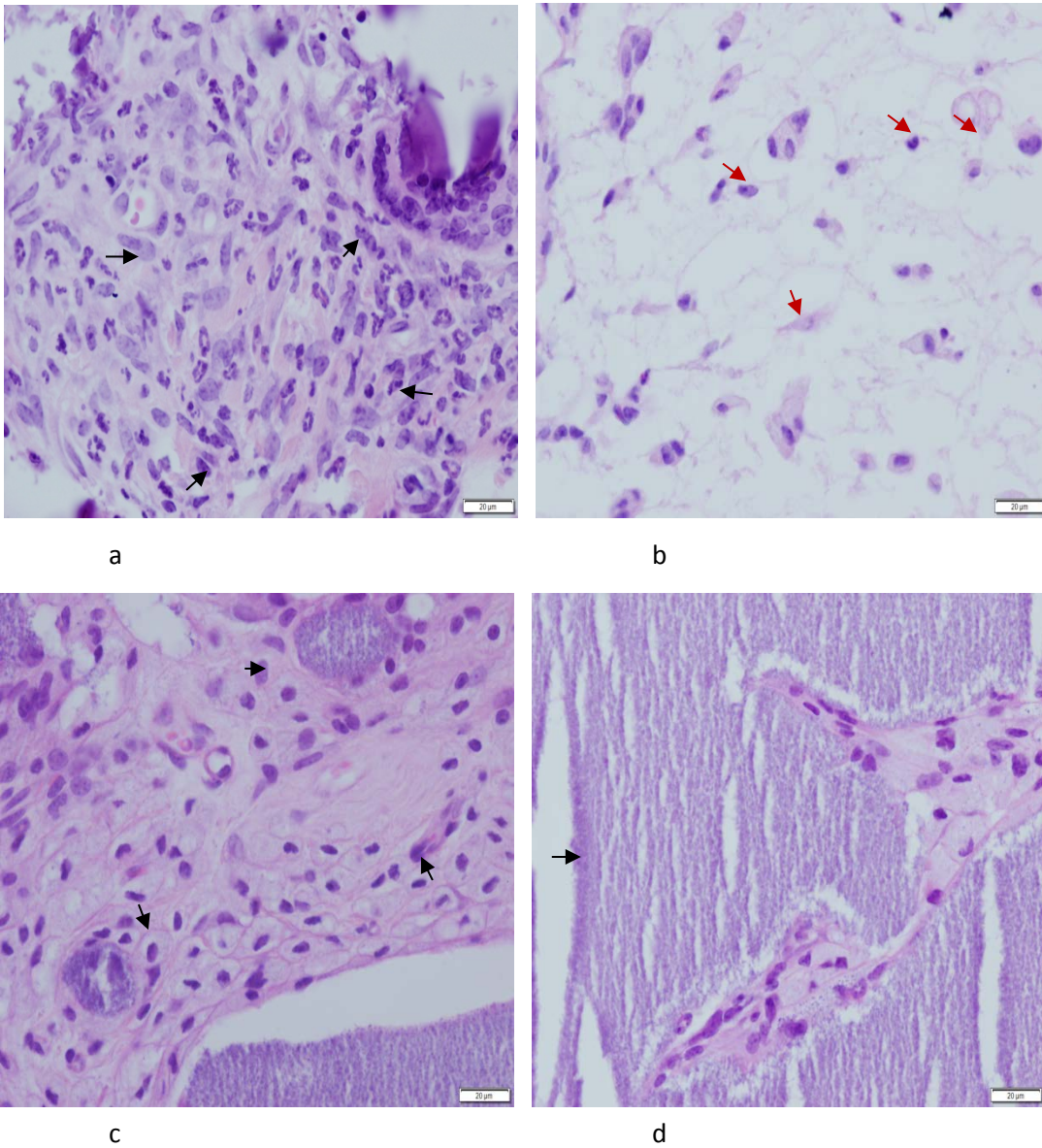


Figure 32. Haematoxylin and eosin (H & E) staining for different groups.

High magnification of alginate bead degradation in four different groups, key: a) alginate bead with pigment epithelium-derived factor (PEDF) b) alginate bead with mesenchymal stem cells (MSCs), c) alginate bead with MSCs and PEDF d) alginate bead. Arrow: *black*, osteoblasts, *red*, dead cells. Scale bar=20 µm.

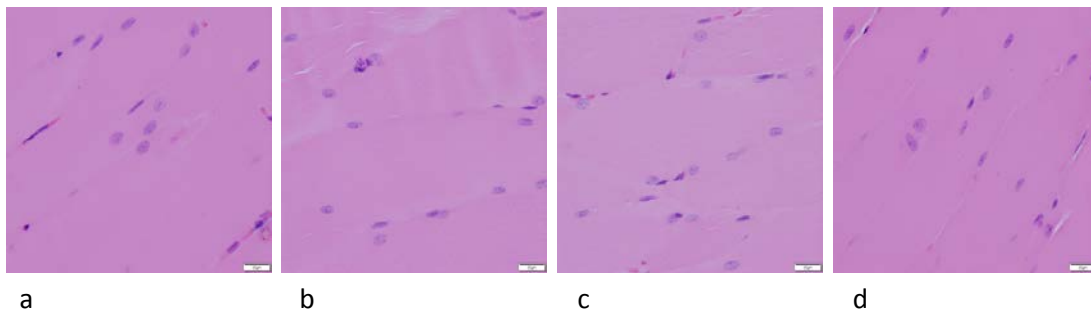


Figure 33. Haematoxylin and eosin (H & E) staining for muscle surrounding the implant site for four different groups.

Key: a) alginate bead with pigment epithelium-derived factor (PEDF), b) alginate bead with mesenchymal stem cells (MSCs), c) alginate bead with MSCs and PEDF, d) alginate bead. *Scale bar = 20 μ m.*

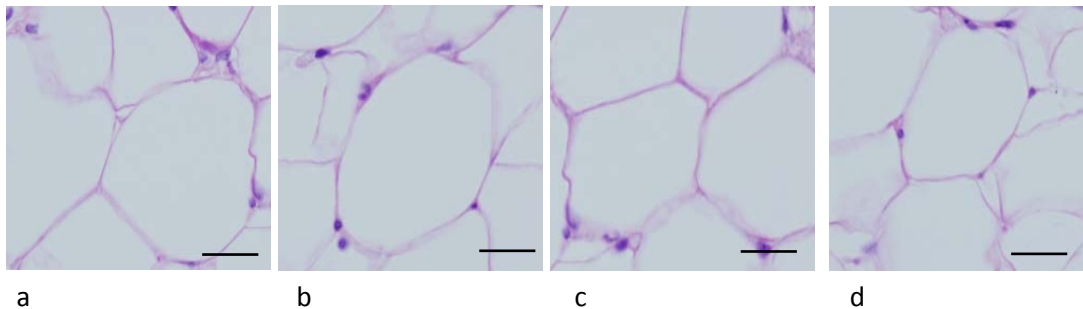


Figure 34. The Haematoxylin and eosin (H & E) staining for fat tissue surrounding the implant site for four different groups.

Key: a) alginate bead with pigment epithelium-derived factor (PEDF), b) alginate bead with mesenchymal stem cells (MSCs), c) alginate bead with MSCs and PEDF, d) alginate bead. *Scale bar = 50 μ m.*

3.2.4. Alcian blue staining

Alcian blue staining for PEDF in the alginate bead group (**Figure 34-a**) and MSCs in alginate group (**Figure 34-b**), did not show the blue hue attributed to the glycosaminoglycan-rich matrix (black arrows), which is seen in the PEDF + MSCs in alginate beads group (**Figure 34-c**). The low level of glycosaminoglycan production in the implant site indicated that cells were less likely to be of the chondrogenic lineage. In the alginate alone group, no staining was observed (**Figure 34-d**).

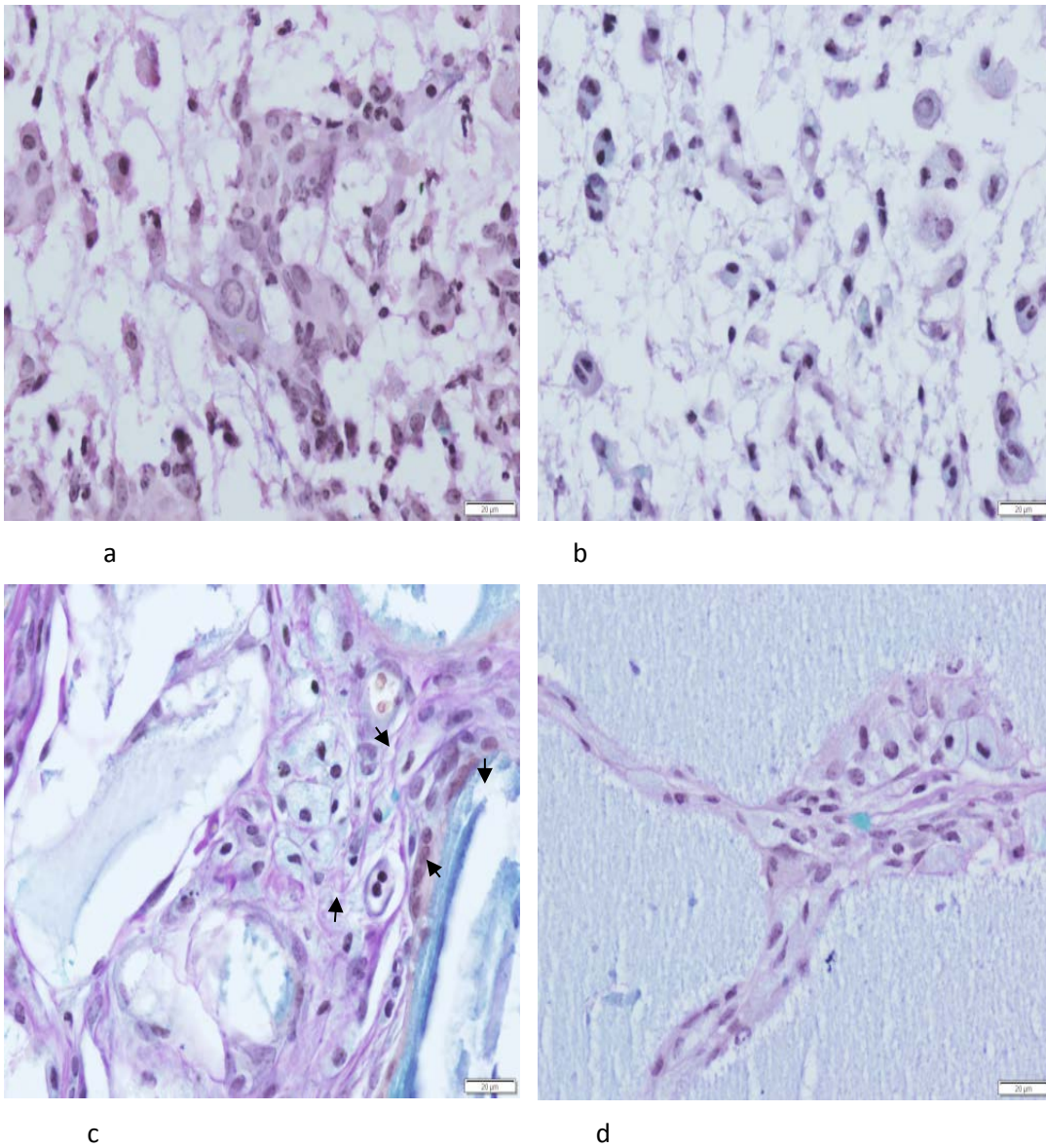


Figure 35. Alcian blue staining for the four different groups.

Key: a) alginate bead with pigment epithelium-derived factor (PEDF), b) alginate bead with mesenchymal stem cells (MSCs), c) alginate bead with MSCs and PEDF, d) alginate bead. The blue hue indicating the presence of a glycosaminoglycan-rich matrix in group c (*black arrow*)
 Scale bar= 20μm.

3.2.5. Immunohistochemistry

The immunohistochemistry of bone markers OCN, OPN, ALP, and col-I, and markers related to bone matrix formation such as pro-col-I, HSP47, MT1-MMP, and MMP-2 was explored.

High intensity staining (yellow arrows) for OCN for the MSCs with PEDF in alginate bead **(Figure 35-c)** group was observed. Furthermore, a notable amount of staining as also seen for the alginate beads with PEDF group **(Figure 35-a)**. The alginate beads with MSCs **(Figure 35-b)** group showed no positive staining for this marker. The acellular structure of the alginate alone group **(Figure 35-d)** showed a yellow-light brown background due to DAB staining (black arrow). Interestingly, the intensity of staining for OPN (yellow arrows) was higher in the alginate beads with PEDF group **(Figure 36-a)** compared to the MSCs with PEDF in alginate beads group **(Figure 36-c)**. Some cells in the MSCs in alginate bead group **(Figure 36-b)** also showed positive staining for this marker; however, no staining was observed in the alginate alone group **(Figure 36-d)** other than the yellow-light brown background.

No expression for ALP was observed in the alginate beads with PEDF group **(Figure 37-a)**, MSCs with PEDF in alginate beads group **(Figure 37-c)**, and alginate alone group **(Figure 37-d)**, while a considerable amount of staining was observed in the MSCs in alginate beads group **(Figure 37-b)**. The distribution of col-I was greater but more localised in the PEDF + alginate **(Figure 38 a)** and MSCs in alginate beads groups **(Figure 38 b)**. A more homogenous and even distribution of col-I was observed in the MSCs

with PEDF in alginate beads group (**Figure 38 c**) but no staining was observed in the alginate alone group (**Figure 38-d**) other than a yellow-light brown background.

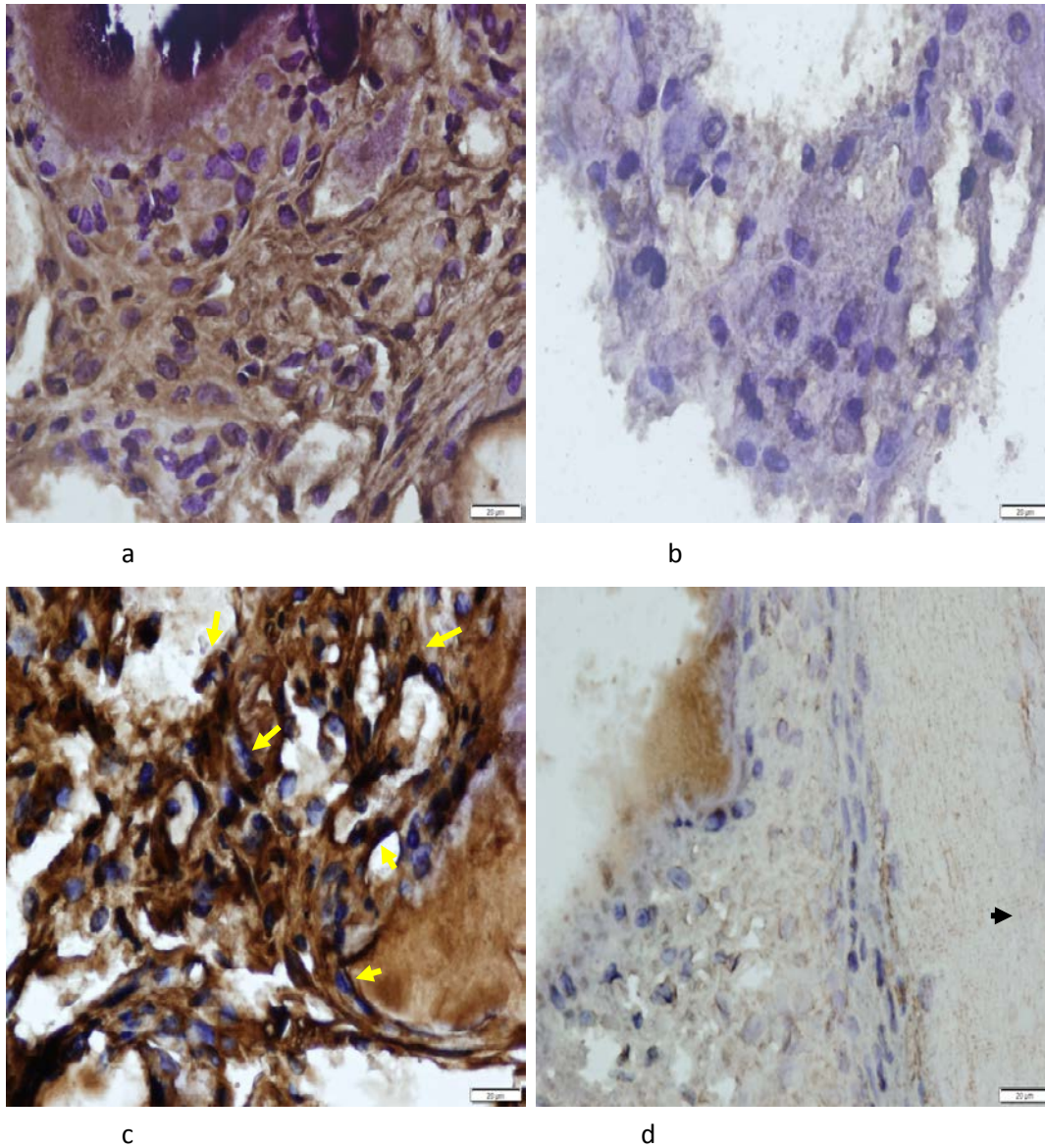


Figure 36. Immunostaining of alginate bead implant paraffin sections for bone marker osteocalcin (OCN) in the four different groups.

Key: a) alginate beads with pigment epithelium-derived factor (PEDF), b) alginate beads with mesenchymal stem cells (MSCs), c) alginate beads with MSCs and PEDF, d) alginate beads. *Arrows:* black, acellular alginate bead matrix; yellow, positive staining. *Scale bar* = 20µm.

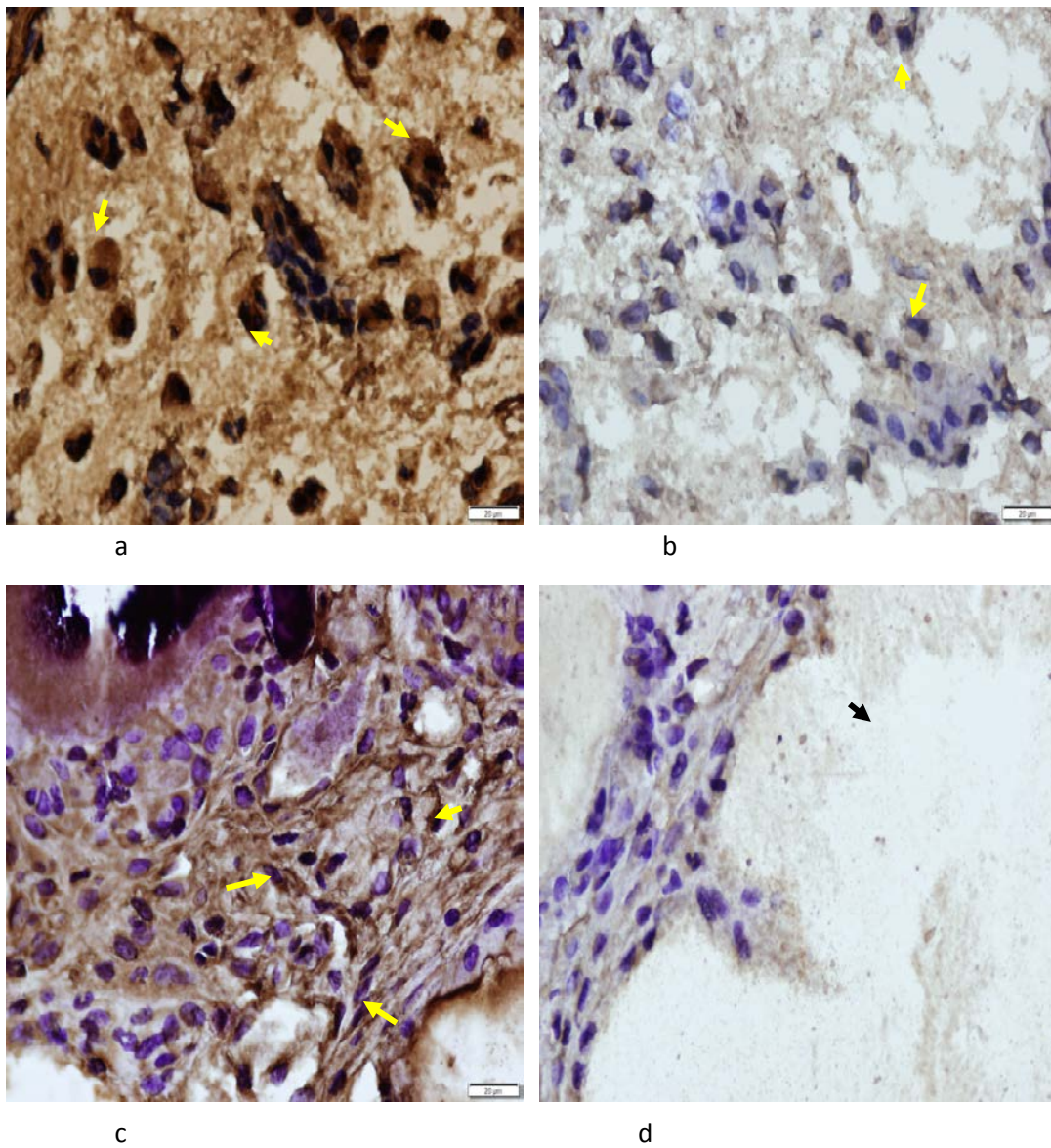


Figure 37. Immunostaining of alginate bead implant paraffin sections for bone marker osteopontin (OPN) in the four different groups.

Key: a) alginate beads with pigment epithelium-derived factor (PEDF), b) alginate beads with mesenchymal stem cells (MSCs), c) alginate beads with MSCs and PEDF, d) alginate beads. *Arrows:* black, acellular alginate bead matrix; yellow, positive staining. *Scale bar* = 20µm.

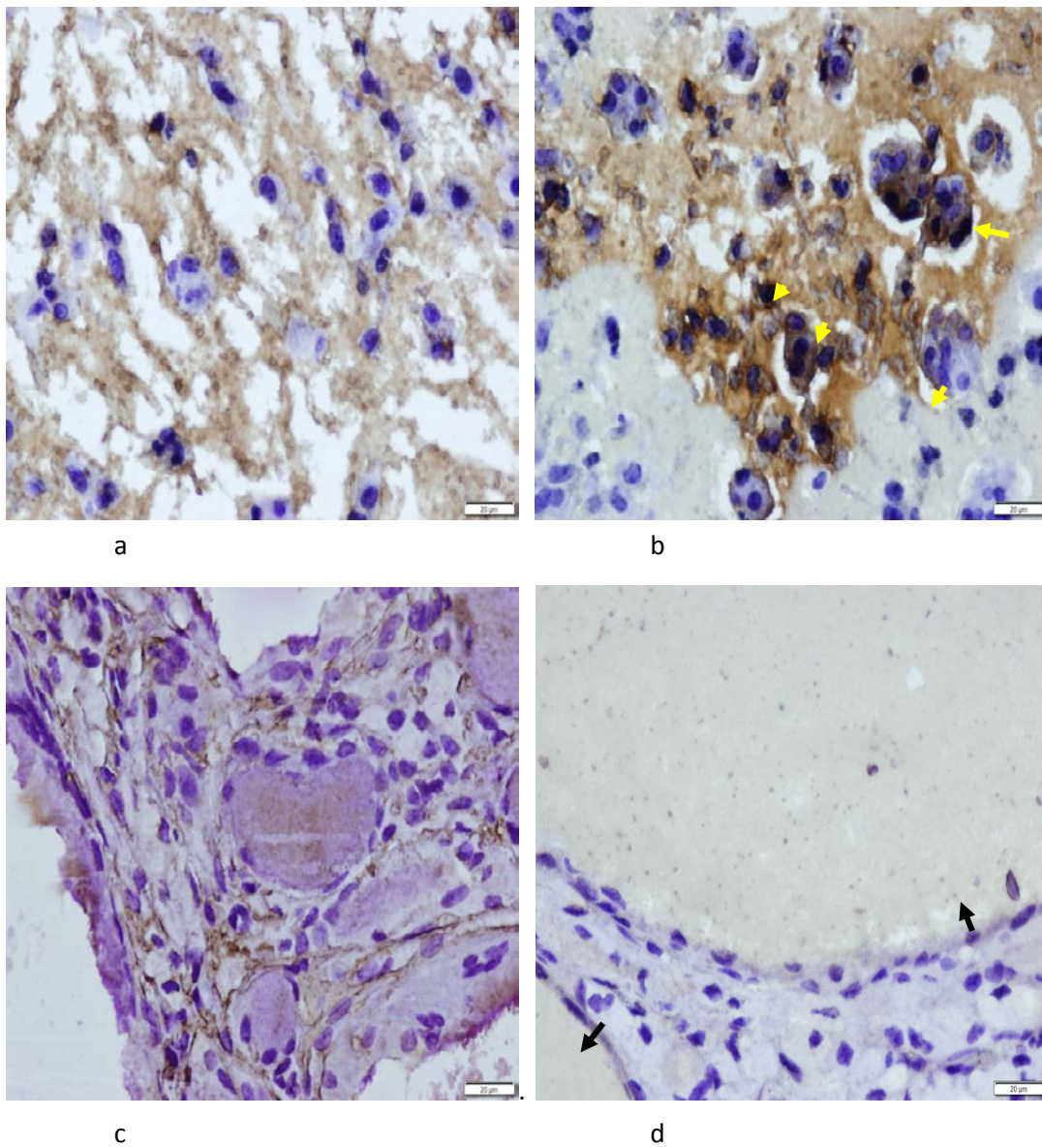


Figure 38. Immunostaining of alginate bead implant paraffin sections for bone marker alkaline phosphatase (ALP) in the four different groups.

Key: a) alginate beads with pigment epithelium-derived factor (PEDF), b) alginate beads with mesenchymal stem cells (MSCs), c) alginate beads with MSCs and PEDF, d) alginate beads. *Arrows:* black, acellular alginate bead matrix, yellow, positive staining. *Scale bar* = 20µm.

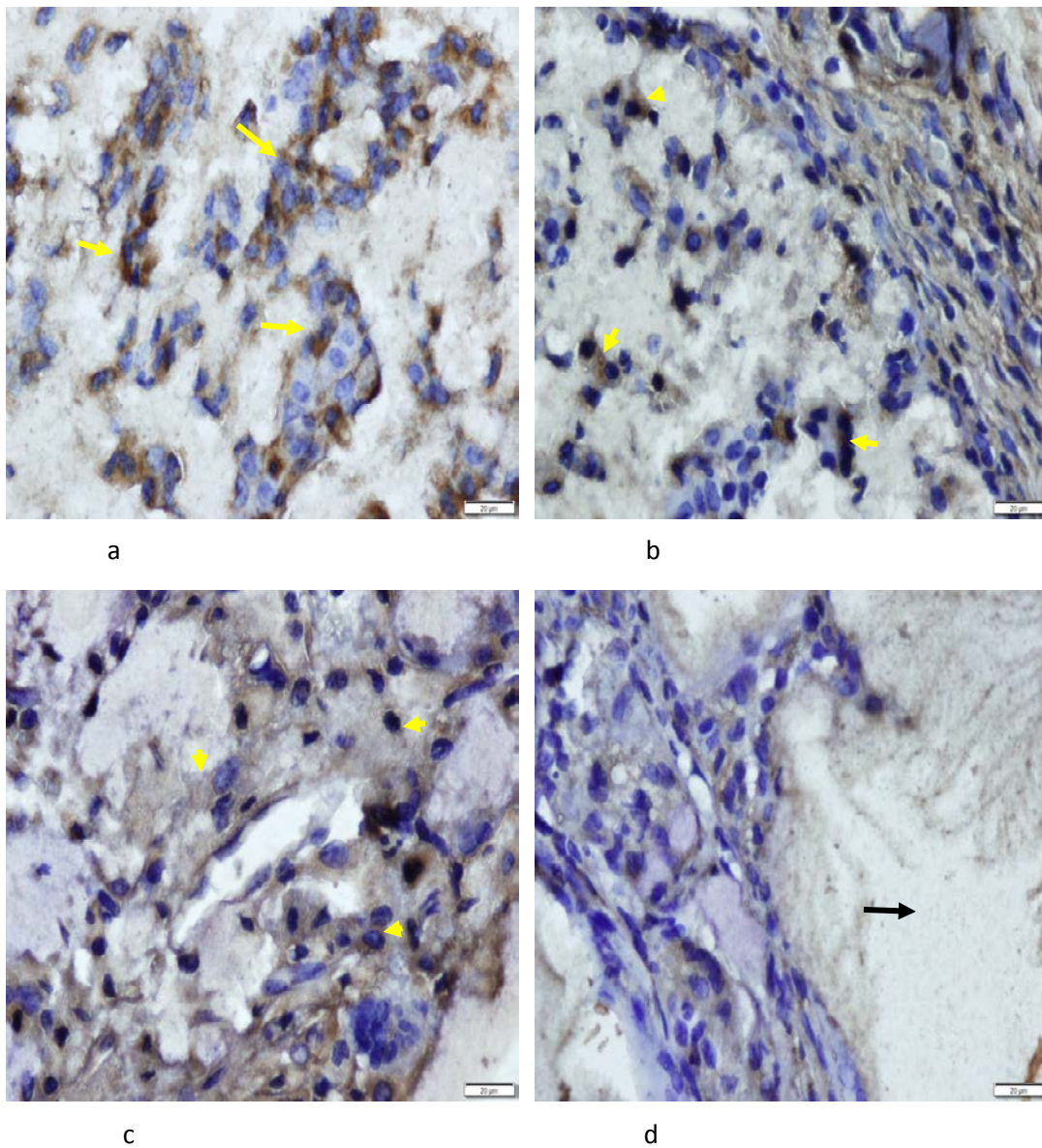


Figure 39. Immunostaining of alginate bead implant paraffin sections for bone marker collagen-I (Col-I) in the four different groups.
 Key: a) alginate beads with pigment epithelium-derived factor (PEDF), b) alginate bead with MSCs), c) alginate beads with MSCs and PEDF, d) alginate beads. Arrows: *black*, acellular alginate bead matrix; *yellow*, positive staining. Scale bar = 20 μ m.

In addition to bone forming markers, bone matrix markers were also investigated. Pro-col-I was most abundant in the MSCs with PEDF in beads group (**Figure 39-c**) compared to the PEDF in alginate beads group (**Figure 39-a**), which showed low and localised expression of pro-col-I (yellow arrows). The MSCs in alginate group (**Figure 39-b**) showed no staining for this marker. The alginate beads group (**Figure 39-d**) was acellular in appearance (black arrow) and showed no staining. The staining for HSP47 was more intense for the MSCs with PEDF in beads group (**Figure 40-c**) in comparison with the PEDF in alginate beads (**Figure 40-a**) and MSCs in alginate groups (**Figure 40-b**), which showed very low expression of HSP47 (yellow arrow). No staining was observed for the alginate beads alone group (**Figure 40-d**). A relatively similar amount of staining was observed for MT-MMP1 (yellow arrow) in the PEDF in alginate beads (**Figure 41-a**), MSCs in alginate (**Figure 41-b**), and MSCs with PEDF in beads groups (**Figure 41-c**). No staining was observed for the alginate beads alone group (**Figure 41-d**) and also, there was no staining observed for MMP-2 in this cohort (**Figure 42 a-d**).

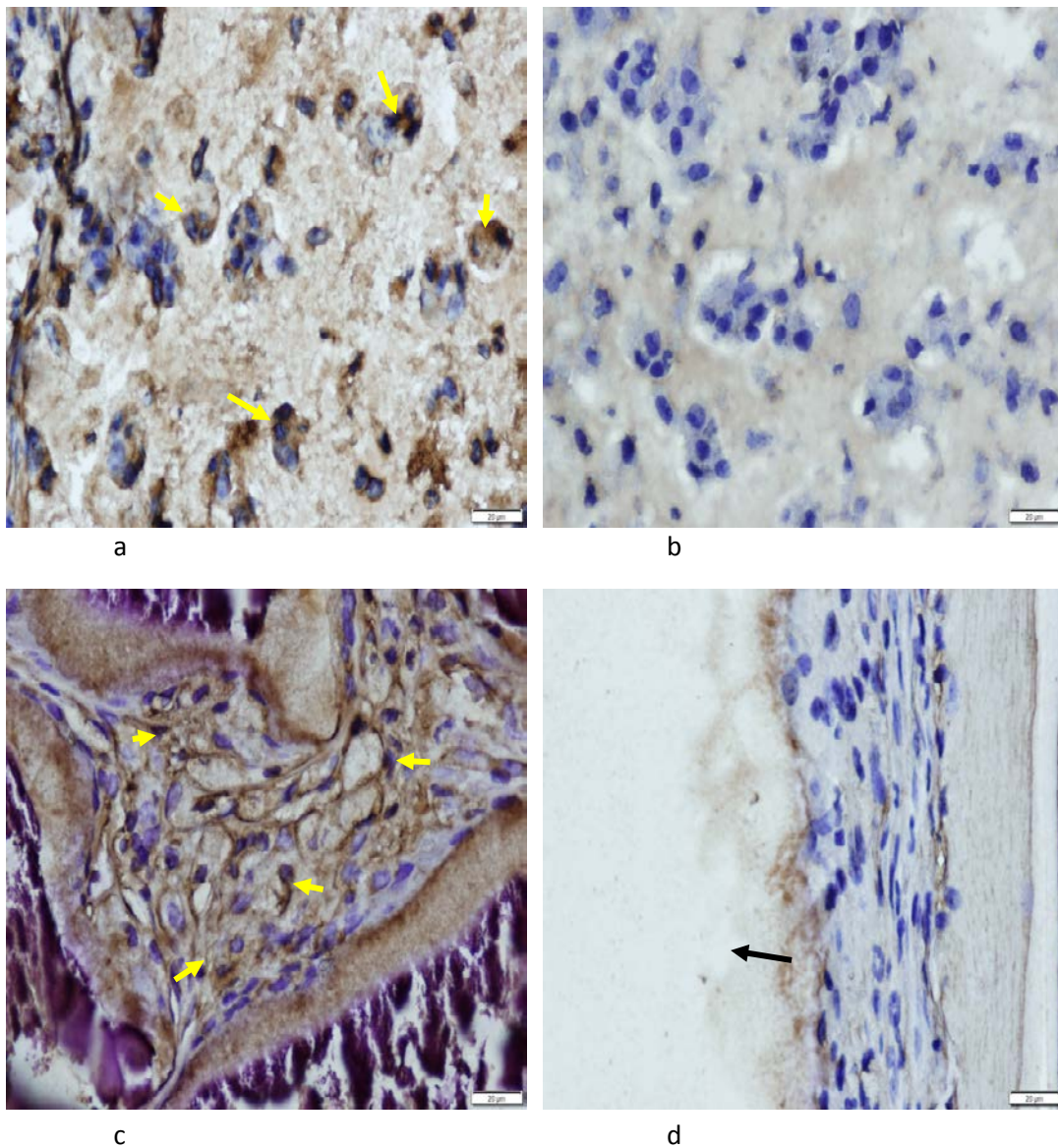


Figure 40. Immunostaining of alginate bead implant paraffin sections for bone matrix marker pro-collagen-I (pro-col-I) in four different groups.

Key: a) alginate bead with pigment epithelium-derived factor (PEDF), b) alginate bead with mesenchymal stem cells (MSCs), c) alginate bead with MSCs and PEDF, d) alginate bead. *Arrows:* black, acellular alginate bead matrix, yellow, positive staining. *Scale bar* = 20µm.

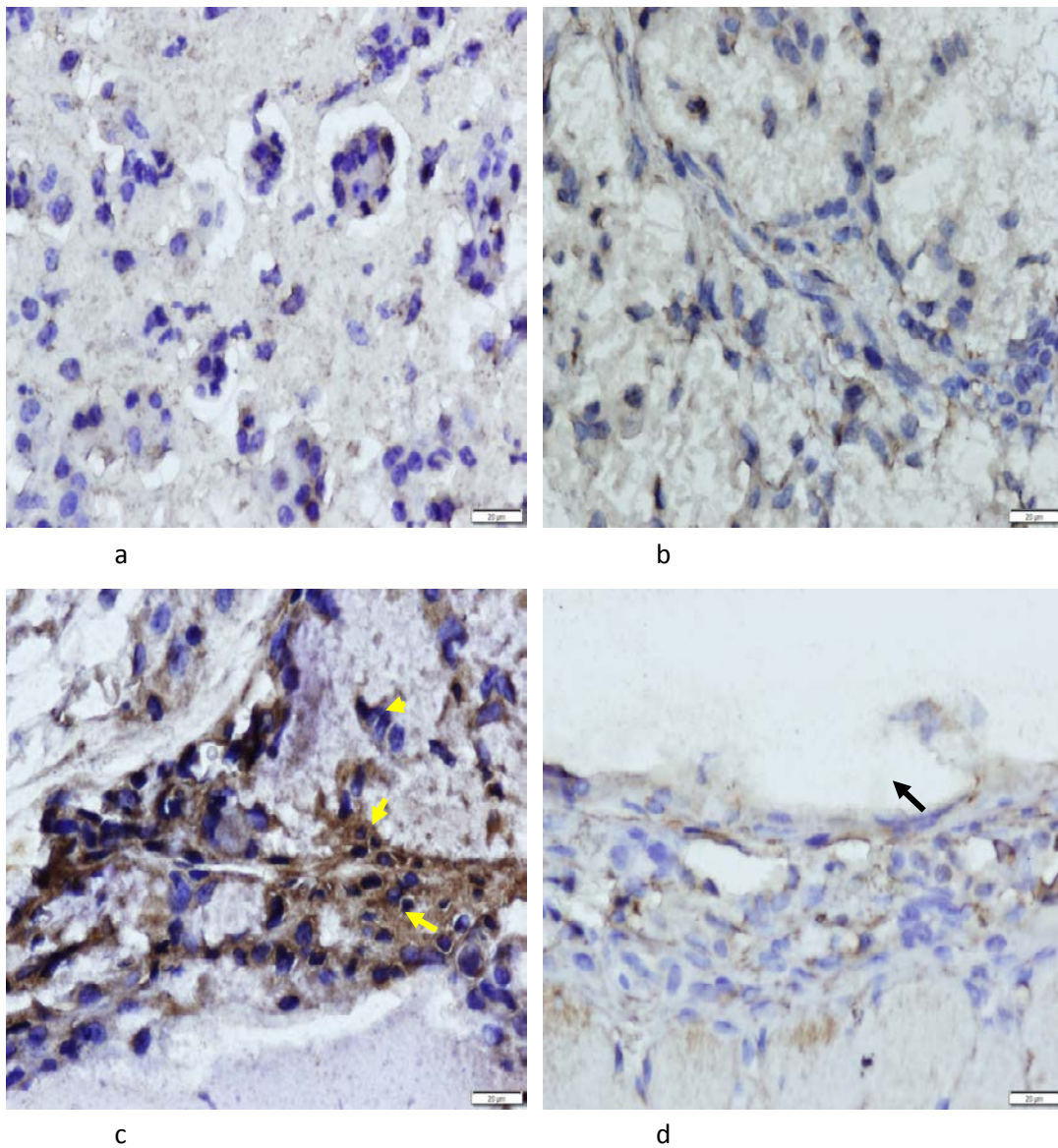


Figure 41. Immunostaining of alginate bead implant paraffin sections for bone matrix marker heat shock protein 47 (HSP47) in four different groups.

Key: a) alginate bead with pigment epithelium-derived factor (PEDF), b) alginate bead with mesenchymal stem cells (MSCs), c) alginate bead with MSCs and PEDF, d) alginate bead. *Arrows:* *black*, acellular alginate bead matrix, *yellow*, positive staining. *Scale bar* = 20µm.

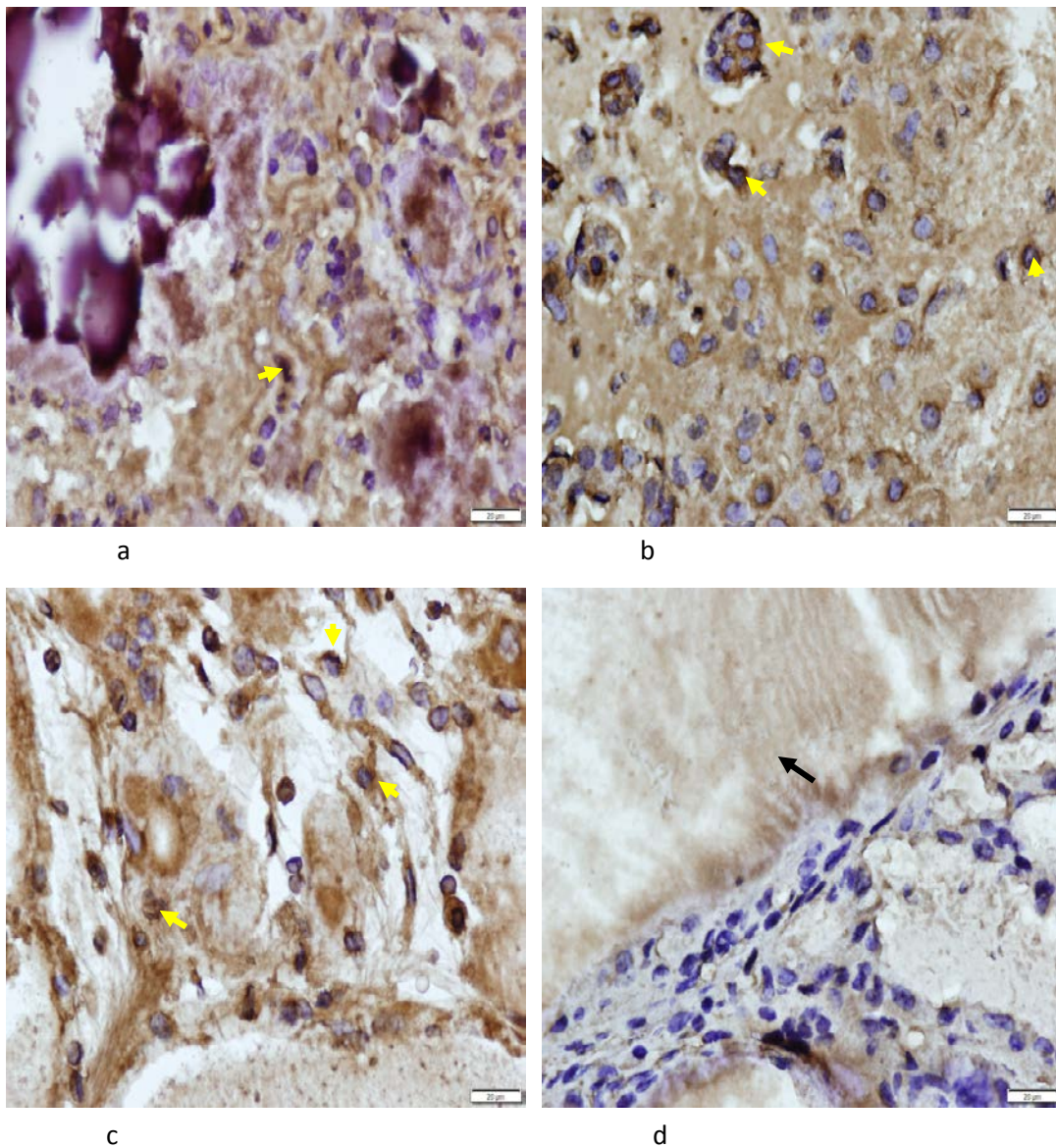


Figure 42. Immunostaining of alginate bead implant paraffin sections for bone matrix marker membrane-type matrix metalloproteinase (MT1-MMP) in the four different groups.

Key: a) alginate beads with pigment epithelium-derived factor (PEDF), b) alginate beads with mesenchymal stem cells (MSCs), c) alginate beads with MSCs and PEDF, d) alginate beads. Arrows: black, acellular alginate bead matrix; yellow, positive staining. Scale bar = 20µm.

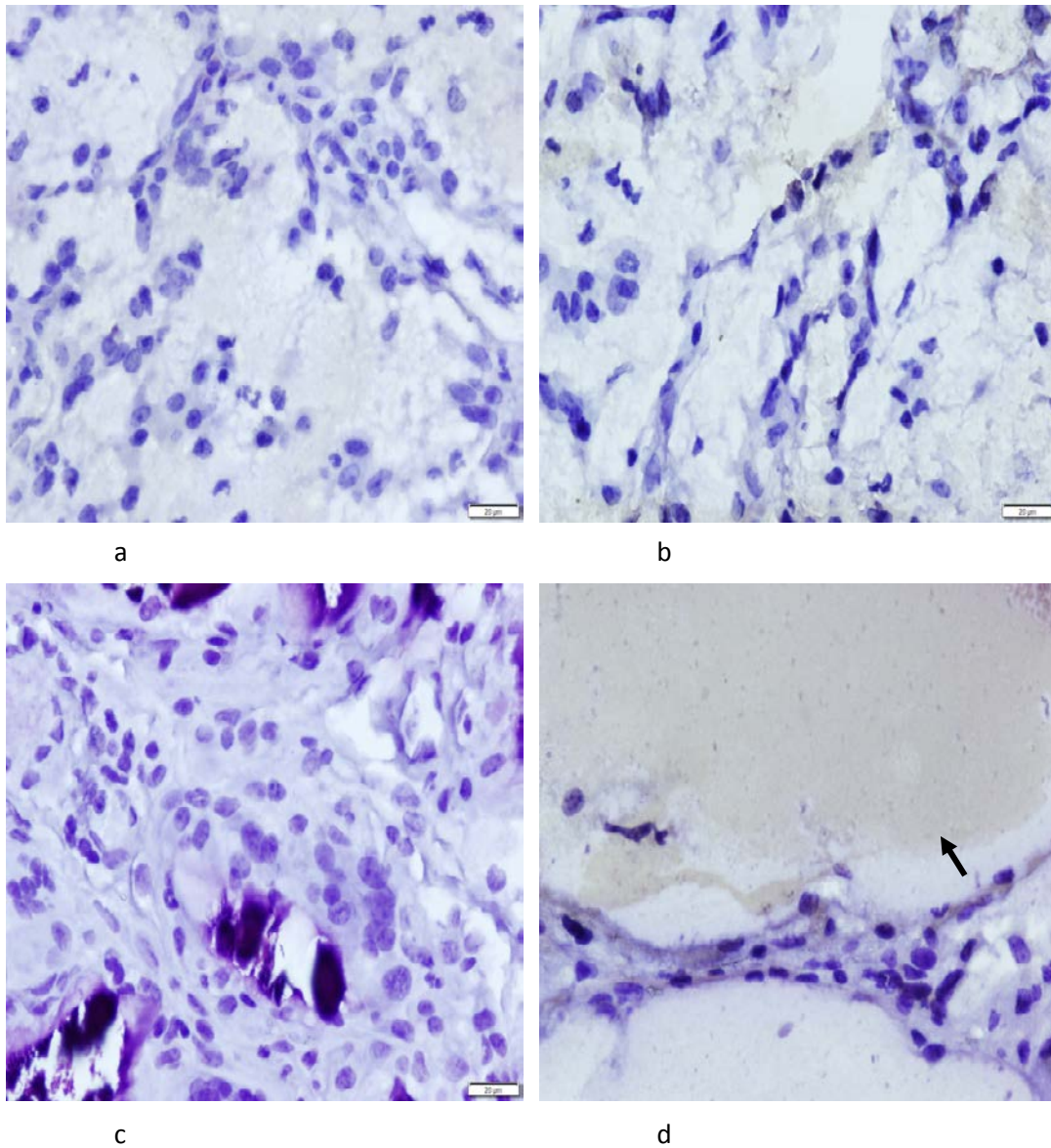


Figure 43. Immunostaining of alginate bead implant paraffin sections for bone matrix marker matrix metalloproteinase 2 (MMP-2) in the four different groups.

Key: a) alginate beads with pigment epithelium-derived factor (PEDF), b) alginate beads with mesenchymal stem cells (MSCs), c) alginate beads with MSCs and PEDF, d) alginate beads. *Arrows: black*, acellular alginate bead matrix. *Scale bar* = 20µm.

Chapter Four

4. Discussion

4.1. *In vitro* study

Previously it has been shown that PEDF protein is expressed by osteoblasts and osteoclasts [198]. PEDF has also been detected in areas of endochondral ossification and active bone remodelling [196]. Endochondral ossification is one of the main processes that MSCs go through for bone tissue formation [56]. The role of MSCs during bone formation is far from clear. The osteogenic potential of these cells makes them suitable candidates for bone tissue engineering. It is also suggested that these cells may have a role as pericytes in support of newly formed blood vessels, which is a very active process during endochondral ossification [201, 202]. While adipose-derived MSCs can be differentiated to osteoblasts at the expense of adipocytes by PEDF [219], and PEDF can differentiate bone marrow-derived MSCs to osteoblasts grown in osteogenic medium [220], no reports of differentiation of bone marrow-derived MSCs by PEDF in the absence of osteogenic supplements are available. This is critical if PEDF is to be used clinically in future for bone tissue engineering *in situ*. All these facts led to the hypothesis for the present study that PEDF might have a pre-osteoblastic differentiation effect on MSCs in the absence of osteogenic supplements.

A natural osteogenic supplement would be desirable for bone tissue engineering, and in the case of PEDF, not only it is naturally expressed at high levels in the active bone forming site, it also has a high affinity binding to glycosaminoglycans and collagens in

the ECM [196]. To support this hypothesis, after isolation of MSCs from bone marrow, four of the recommended surface markers for stem cells were used for stem cell identification. Our results were consistent with previous reports [25, 221] and expression for two positive markers (CD73 and CD105) was detected whereas no expression for CD34 and CD19 was observed *via* immunocytochemistry. Consistent with our immunocytochemistry findings, FACS results also showed a similar expression of MSC-characteristic surface markers (CD73 and CD105) and the absence of haematopoietic markers (CD34 and CD19), indicating that the isolated cells had no haematopoietic cell contamination [27, 222]. The tri-lineage differentiation, which is one of the important characteristics of MSCs [223], were replicated in our results here, demonstrating that these cells have the capacity to be induced to differentiate into bone, fat, and cartilage. Before testing the osteogenic potential of PEDF, stem cell survival in the presence and absence of PEDF was studied. Previous studies have shown that PEDF supports cell survival and proliferation of human embryonic stem cells [224, 225]. It also induces self-renewal, activates cell division, and plays a role in the maintenance of multipotency in neural stem cells [226] and self-renewal and cell expansion in retinal stem cells [227, 228]. Consistent with these studies, results of this study show that PEDF helps MSC survival in a monolayer culture after seven days in the absence of other pro-differentiation factors.

The encapsulation of stem cells for cell delivery and tissue engineering purposes is now being increasingly performed [146, 229-234]. There are a significant number of studies

that have utilised fast-degradable hydrogels such as gelatine and collagen. Degradation and cell release are two important parameters in successful bone tissue formation. A fast degradation rate (degradation in less than 6 days) will lead to minimum bone formation by transplanted stem cells and loss of support for cell proliferation. On the other hand, slow degradation of beads may inhibit cell proliferation and matrix formation [235, 236]. Co-immobilising stem cells with endothelial cells in alginate beads [146], and arginine-glycine-aspartate (RGD)-grafted alginate beads [237], and a blend of alginate-fibrin [109] and alginate co-encapsulation with anti-BMP2 monoclonal antibody [238] were shown to increase the rate of alginate degradation, cell release, and differentiation. Our study showed that encapsulating PEDF and stem cells in alginate beads (treatments B and in some cases treatment A) improves degradation of and cell release from alginate beads significantly ($p < 0.05$) compared to encapsulation of stem cells alone in alginate beads (treatments C and D). It has also been observed that the cells released from alginate beads with PEDF treatment (both treatments A and B) differentiated into osteoblasts as exemplified by von Kossa staining. The significant difference in degradation rate of alginate beads in comparison to treatments B, E, and F might be due to the presence of CaCl_2 (which is the active factor in alginate polymerisation) in treatments A and C.

Staining for osteogenic markers in the monolayer study showed a similar increasing trend in expression of late differentiation markers including osteocalcin (OCN) and osteopontin (OPN) in all osteogenic treatments (A, B, E, and F) from day 7 to

day 21 [118, 209]. The expression of ALP was also observed in these treatments with strong staining at day 14 and a gradual reduction in expression afterward. The same trend was also observed in ALP activity, which was evaluated for the monolayer cultures in osteogenic plates during the course of differentiation for days 7, 14, and 21. Increased enzyme activity at day 14 was observed in treatments A, B, E, and F, followed by a decreasing trend until day 21 as cells differentiate; the expression and activity of ALP would reduce (day 14 onward). In contrast, in treatments C and D, no significant difference was observed at the different timepoints and is consistent with findings from previous studies [118, 239, 240].

Collagen I expression also expectedly had an increasing trend, which would be due to assembly of a collagen matrix for pre-osteoblast cells. At day 21, a decrease in collagen I was observed that is consistent with the fact that day 21 is close to the maturation point of osteoblasts, when the expression of collagen decreases and matrix mineralisation is initiated. These results also have been confirmed using whole cell protein content, which was shown by immunoblotting at day 14. Overall, the increased amount of the four osteoblast-specific proteins (ALP, Col-1, OCN, and OPN) observed after day 14 indicates the presence of post-proliferative osteoblast cells in the culture.

Alizarin red [109, 241] and von Kossa [118, 146] staining were performed in order to monitor the calcium and phosphate mineralisation respectively. The significant amount of mineralisation in both treatments A and B compared to controls (treatments C and D) indicates the successful osteogenic effect of PEDF in both normal and

osteogenic plates. The sudden increase in mineral concentration in treatment C (complete media + 10 mM β -GP + 1.4 mM CaCl_2) above baseline and treatment D (complete media) may be due to cell-associated, non-HA precipitates that form in the presence of β -GP [210]. Considering other results from immunocytochemistry, von Kossa staining, and immunoblotting, which showed negative results with treatments C and D, this mineral staining is not likely to be representative of bone-like matrix mineralisation [210].

4.2. *In vivo* study

To investigate the bone formation potential of any engineered construct *in vivo*, one of the commonly used methods is intramuscular (muscle pouch) implantation [242-246]. This model can be used in nearly any animal model and, in fact, it was also tested on a human patient in 2004 [247]. The promising *in vitro* results of osteoblastic differentiation of MSCs *via* PEDF observed in both monolayer cultures and encapsulation in alginate beads, leads to the further step of testing the hypothesis in an animal model. The micro-CT images show formation of osteoid tissue in all three groups (PEDF in alginate beads, MSCs in alginate beads, and MSCs with PEDF in alginate beads) with no osteoid tissue found in the alginate alone beads group. However the amount of formed osteoid tissue varied, and the highest amount was observed in the MSCs with PEDF in alginate beads group followed by PEDF in alginate beads group and

MSCs in alginate beads group. The quantitative analysis on bone parameters acquired from micro-CT such as bone volume, structural thickness, and tissue mineral density [248, 249] also confirm the formation of bone tissue in this cohort for the mentioned groups. The micro-CT also showed a morphologically different mass in the alginate alone group. Further parameter analysis for this group showed no data representing osteoid tissue formation, which might be due to the presence of CaCl₂ in the polymer structure of alginate as well as the formation of a necrotic collagen capsule as part of the animal's foreign body reaction [148, 250]. Along with micro-CT findings, immunohistology results showed high expression of OCN - a late osteoblastic marker - in MSCs with PEDF in alginate beads group, followed by PEDF in alginate beads group, and finally with the MSCs in the alginate beads group. These results indicate that the cells in the MSCs with PEDF in alginate beads group were in a later stage of osteoblastic differentiation compared to the other two groups. Additionally, immunostaining also showed that expression of OPN, a mid-late osteogenic marker was as follows: PEDF in alginate beads > MSCs with PEDF in alginate beads > MSCs in alginate beads. These observation stating that the involving in alginate beads with PEDF also going through differentiation but in earlier stage than MSCs with PEDF in alginate beads. The expression of col-I can also be summarised as follows: PEDF in alginate beads > MSCs in alginate beads = MSCs with PEDF in alginate beads. Expression of ALP - a mid osteogenic marker - however, was higher in the MSCs in alginate beads group, followed by the PEDF in alginate beads group and lastly, a very weak level of expression was

observed in the MSCs with PEDF in alginate beads group. The interesting finding regarding the expression of col-I was that col-I appeared to be more localised in the MSCs in alginate beads and PEDF in alginate groups compared to MSCs with PEDF in alginate beads group. When cells are traversing the late stage of differentiation, col-I diffuses from the cytoplasm to the ECM to form a matrix that is replaced during ossification. In regard to pro-col-I, less expression was observed in differentiated cells (MSCs with PEDF in alginate beads) as this protein is the precursor of col-I. HSP47 expression on the other hand, was the highest in MSCs with PEDF in alginate beads group in comparison to the other groups as it is the active chaperone for col-I folding. These observations of pro-col-I, col-I, and HSP47 coincide with the high amount of expression of MT1-MMP observed in the MSCs with PEDF in alginate beads group. In bone, collagen-I can be degraded by MT1-MMP, which is critical for growth plate function and secondary ossification [251-254]. Moreover, in the Alcian blue staining, the glycosaminoglycan-rich matrix seems weak and was only observed in the MSCs with PEDF in alginate beads group, which could represent the late, hypertrophic stage of ossification.

Taking micro-CT and immunohistology data together, it can be postulated that PEDF differentiated the alginate encapsulated MSCs toward an osteoblastic lineage and produced osteoid tissue (**Figure 28-c**). The most intriguing finding was that the PEDF without MSCs in alginate beads group also produced bone tissue (**Figure 28-a**) by utilising cells seconded from the surrounding tissue. However, it seems that these cells

are in earlier stage of differentiation, as demonstrated by immunohistology for the majority of the cells. It has been suggested that these PEDF-attracted migrating cells are derived from the adjacent adipose tissue, as these adipose-derived stromal cells can be channelled towards the osteoblastic lineage [255, 256], as can cells from the *spatium intermuscular* [257]. It is unlikely that inflammatory cells were the predominant cells migrating into the alginate bead scaffolds since osteoblastic markers stained a clear majority of cells resident in implant sites in this cohort. One interesting observation was the presence of blood vessels in implants that contained PEDF; one possible explanation can be that PEDF function is to restore a balance in pathological angiogenesis by counteracting excessive VEGF activity. It is not known to block or destroy normal blood vessel formation rather it destroys leaky blood vessels. It is found early in embryogenesis when blood vessels are developing so unlikely to affect normal angiogenesis event.

Bone morphogenic proteins (BMPs), especially (rh) BMP-2 and (rh) BMP-7, have been used widely in the clinic and orthopaedic surgery to enhance bone growth. Several studies carried out in different animal models have concluded that BMPs have a species-specific osteo-inductive dose. For example, in non-human primates, the minimum required dose of BMP-2 to induce bone formation is substantially higher than in rodents [258]. The wide range of species-specific differential in the osteo-conductive BMP-2 dose may account for the lack of evidence of BMP2-related side effects in animal models such as rodents, where the lower doses will result in bone formation

with no significant side-effects [259]. However, due to high dose requirements of BMP in human treatment, several adverse side effects have been documented including ectopic bone formation with spinal cord impingement, osteoclast activation with transiently elevated bone resorption, cyst-like bone void formation, and life-threatening cervical swelling [260-263]. Interestingly, in most cases the swelling was due to inflammation and soft tissue swelling rather than fluid accumulation such as seen with haematoma [260]. The inflammatory response is not unexpected, as BMP2 is a known chemoattractant for lymphocytes, monocytes, and macrophages [263]. One of the suggested solutions to address this issue is combining BMPs with other growth factors to dampen the unwanted inflammatory reaction. The other strategy is to suppress the natural antagonist of the BMPs such as noggin and inhibit them from blocking BMPs. In that case, the required dose would decrease [264]. Nevertheless, these invasive strategies have to be investigated thoroughly for potential side-effects and interference with other biological reactions before they can become clinically applicable. In this study, the osteogenic potential of PEDF encapsulated in alginate with or without stem cells provides us with a new technique for bone tissue engineering. In this method, PEDF induces osteogenesis *in vitro* when co-encapsulated with MSCs, and *in vivo* using cells present endogenously in the body (that is without the need for co-encapsulation of MSCs). Considering the fact that PEDF has inflammation-dampening effects in tissues such as the eye (retinal pericytes) [265] and has a protective effect on cerebellum granule cells [266], as well as an inhibitory effect on

pro-inflammatory cytokine production in neonatal astrocytes and cultured microglia [267, 268], make this protein a suitable candidate for further investigation in the field of bone tissue engineering for potential clinical use.

Chapter Five

5. Conclusions, limitations and future directions

5.1 Conclusions

In the present study, the effects of a cell-based technique were tested *in vitro* and investigated ectopically in a mouse model. Alginate beads were used for scaffold fabrication in combination with mesenchymal stem cells and PEDF as the sole osteogenic supplement. Mineral deposition representing bone tissue was found *in vitro* along with a mineral structure similar to bone *in vivo*. Interestingly, in the *in vivo* model, the MSCs plus PEDF was not the only group able to produce bone and the group with alginate supplemented only with PEDF also produced bone in a comparable manner. A noteworthy observation in this case is the ability of PEDF to recruit cells and directly contribute to ectopic bone formation *in vivo*.

Bone morphogenic protein is a clinically used factor in several orthopaedic scenarios. However, the safety of this powerful biological product is debatable based on recent clinical trials. Several studies showed that a super physiological dose of BMPs is required to induce bone formation. The high-dose of BMP2 not only induces significant tissue inflammation (that explains the clinically observed cervical swelling), but also increases osteoclastogenesis that may manifest clinically as vertebral subsidence or collapse and excessive bone resorption. PEDF, a naturally available protein during bone formation and remodelling, with anti-inflammatory effects can be a suitable candidate for future studies in the field of bone tissue engineering. As shown

by this study, a biological dose of PEDF (100nM) successfully formed bone mass in an ectopic animal model.

5.2 Limitations and future directions:

So far the focus on PEDF has been limited to its anticancer potential and anti-angiogenic properties. Thus, several molecular mechanisms in those areas are known. However, in the last couple of years, other properties of PEDF have come to light especially as a differentiation factor. There are only two other reports on the *in vitro* osteoblastic effect of PEDF. The present study is one of the first studies looking at osteogenic differentiation of PEDF *in vitro* and *in vivo*. Hence, the knowledge on the molecular mechanisms is yet scarce in this field. One possible pathway which might be involved in the osteogenic differentiation via PEDF is ERK/MAPK. However, there might be other pathways involved and more study is warranted.

PEDF-R is the general receptor identified for PEDF in several different cell lines. Other receptors such as plexin domain containing 1 (PLXDC1), plexin domain containing 2 (PLXDC2), laminin receptor and membrane linked F1-ATP synthase have also been recognised for PEDF, however, the involvement and role of these receptors in PEDF osteogenic pathways need to be investigated as this is uncharted territory.

Murine MSCs were used in this study and showed promising results to take the hypothesis further to other animal models and possibly clinical trial. However, to explore the efficacy and feasibility (relative potential) of this technique for its future

clinical application, additional comparative studies are needed. First of all, it is of great importance to introduce hMSCs and hESCs to this system with the objective of final clinical application. Following this, systematic studies are crucial using optimised alginate bead size (in micro scale) *in vitro* accompanied with relative assessments, as well as *in vivo* studies using different animal models with defects of critical size before its introduction to clinical trials. Alginate has been used in clinical trials since 2006 for different tissue engineering purposes such as bone and periodontal tissue repair, as well as a vehicle for cell therapy. However, microbead handling might be a problem despite its easy use, especially when it comes to CSD healing, fracture, or tumour resection defect area.

The safety of using hMSC and hESCs in combination of PEDF should be verified, as these cells might provoke inflammatory and/or immune adverse reactions while going through differentiation and transformation, even though PEDF has an anti-inflammatory and protective effect. Utilising PEDF knock-out animal model would help to investigate the effect of endogenous PEDF on MSCs and their behaviour.

Finally, with regard to the possibility of immune rejection and the need for immune suppression, it is striking to consider a “patient-specific” cell-scaffold for personal bone tissue engineering. In this case, the patient’s stem cells can be used for personalised tissue regeneration with the advantage of minimizing the risk of immune rejection.

6. References

1. Si, Y.L., et al., *MSCs: Biological characteristics, clinical applications and their outstanding concerns*. Ageing Research Reviews, 2011. **10**(1): p. 93-103.
2. Weissman, I.L., *Stem Cells: Units of Development, Units of Regeneration, and Units in Evolution*. Cell, 2000. **100**(1): p. 157-168.
3. Evans, M.J. and M.H. Kaufman, *Establishment in culture of pluripotential cells from mouse embryos*. Nature, 1981. **292**(5819): p. 154-156.
4. Martin, G.R., *Isolation of a pluripotent cell line from early mouse embryos cultured in medium conditioned by teratocarcinoma stem cells*. Proceedings of the National Academy of Sciences of the United States of America, 1981. **78**(12 II): p. 7634-7638.
5. Thomson, J.A., *Embryonic stem cell lines derived from human blastocysts*. Science, 1998. **282**(5391): p. 1145-1147.
6. Wilson, A., et al., *Hematopoietic Stem Cells Reversibly Switch from Dormancy to Self-Renewal during Homeostasis and Repair*. Cell, 2008. **135**(6): p. 1118-1129.
7. Walker, M.R., K.K. Patel, and T.S. Stappenbeck, *The stem cell niche*. Journal of Pathology, 2009. **217**(2): p. 169-180.
8. Schofield, R., *The relationship between the spleen colony-forming cell and the haemopoietic stem cell. A hypothesis*. Blood Cells, 1978. **4**(1-2): p. 7-25.
9. Verga Falzacappa, M.V., et al., *Regulation of self-renewal in normal and cancer stem cells*. FEBS Journal, 2012. **279**(19): p. 3559-3572.
10. Yamashita, Y.M., M.T. Fuller, and D.L. Jones, *Signaling in stem cell niches: Lessons from the Drosophila germline*. Journal of Cell Science, 2005. **118**(4): p. 665-672.
11. Lu, W., et al., *Niche-associated activation of rac promotes the asymmetric division of Drosophila female germline stem cells*. PLoS Biology, 2012. **10**(7).
12. Yamashita, Y.M. and M.T. Fuller, *Asymmetric stem cell division and function of the niche in the Drosophila male germ line*. International Journal of Hematology, 2005. **82**(5): p. 377-380.
13. Cheng, J., et al., *Asymmetric division of cyst stem cells in Drosophila testis is ensured by anaphase spindle repositioning*. Development, 2011. **138**(5): p. 831-837.
14. Gönczy, P. and L.S. Rose, *Asymmetric cell division and axis formation in the embryo*. WormBook : the online review of C. elegans biology, 2005: p. 1-20.
15. Tsunekawa, Y. and N. Osumi, *How to keep proliferative neural stem/progenitor cells: A critical role of asymmetric inheritance of cyclin D2*. Cell Cycle, 2012. **11**(19): p. 3550-3554.
16. Sousa-Nunes, R. and W.G. Somers, *Mechanisms of asymmetric progenitor divisions in the Drosophila central nervous system*. 2013. p. 79-102.
17. Friedenstein, A.J., U.F. Gorskaja, and N.N. Kulagina, *Fibroblast precursors in normal and irradiated mouse hematopoietic organs*. Experimental Hematology, 1976. **4**(5): p. 267-274.
18. Friedenstein, A.J., R.K. Chailakhjan, and K.S. Lalykina, *The development of fibroblast colonies in monolayer cultures of guinea-pig bone marrow and spleen cells*. Cell and Tissue Kinetics, 1970. **3**(4): p. 393-403.
19. Prockop, D.J., *Marrow stromal cells as stem cells for nonhematopoietic tissues*. Science, 1997. **276**(5309): p. 71-74.

20. Pittenger, M.F., et al., *Multilineage potential of adult human mesenchymal stem cells*. Science, 1999. **284**(5411): p. 143-7.
21. Caplan, A.I. and S.P. Bruder, *Mesenchymal stem cells: Building blocks for molecular medicine in the 21st century*. Trends in Molecular Medicine, 2001. **7**(6): p. 259-264.
22. Mezey, E., et al., *Turning blood into brain: Cells bearing neuronal antigens generated in vivo from bone marrow*. Science, 2000. **290**(5497): p. 1779-1782.
23. Horwitz, E.M., et al., *Clarification of the nomenclature for MSC: The International Society for Cellular Therapy position statement*. Cytotherapy, 2005. **7**(5): p. 393-395.
24. Dominici, M., et al., *Minimal criteria for defining multipotent mesenchymal stromal cells. The International Society for Cellular Therapy position statement*. Cytotherapy, 2006. **8**(4): p. 315-317.
25. De Schauwer, C., et al., *Markers of stemness in equine mesenchymal stem cells: A plea for uniformity*. Theriogenology, 2011. **75**(8): p. 1431-1443.
26. Phinney, D.G., et al., *Plastic adherent stromal cells from the bone marrow of commonly used strains of inbred mice: Variations in yield, growth, and differentiation*. Journal of Cellular Biochemistry, 1999. **72**(4): p. 570-585.
27. Peister, A., et al., *Adult stem cells from bone marrow (MSCs) isolated from different strains of inbred mice vary in surface epitopes, rates of proliferation, and differentiation potential*. Blood, 2004. **103**(5): p. 1662-8.
28. Da Silva Meirelles, L. and N.B. Nardi, *Murine marrow-derived mesenchymal stem cell: Isolation, in vitro expansion, and characterization*. British Journal of Haematology, 2003. **123**(4): p. 702-711.
29. Beers, J., et al., *Passaging and colony expansion of human pluripotent stem cells by enzyme-free dissociation in chemically defined culture conditions*. Nature Protocols, 2012. **7**: p. 2029–2040).
30. Ashton, B.A., et al., *Distribution of fibroblastic colony-forming cells in rabbit bone marrow and assay of their osteogenic potential by an in vivo diffusion chamber method*. Calcif Tissue Int, 1984. **36**(1): p. 83-6.
31. Wilschut, K.J., et al., *Approaches to isolate porcine skeletal muscle stem and progenitor cells*. 2010.
32. Sivasubramaniyan, K., et al., *Phenotypic and functional heterogeneity of human bone marrow– and amnion-derived MSC subsets*. Annals of the New York Academy of Sciences, 2012. **1266**(1): p. 94-106.
33. Harichandan, A., K. Sivasubramaniyan, and H.J. Buhring, *Prospective Isolation and Characterization of Human Bone Marrow-Derived MSCs*. Adv Biochem Eng Biotechnol, 2013. **129**: p. 1-17.
34. Krishnappa, V., S.V. Boregowda, and D.G. Phinney, *The peculiar biology of mouse mesenchymal stromal cells - Oxygen is the key*. Cytotherapy, 2013. **15**(5): p. 536-541.
35. Prowse, K.R. and C.W. Greider, *Developmental and tissue-specific regulation of mouse telomerase and telomere length*. Proceedings of the National Academy of Sciences, 1995. **92**(11): p. 4818-4822.
36. Rosca, A.M. and A. Burlacu, *Isolation of a mouse bone marrow population enriched in stem and progenitor cells by centrifugation on a Percoll gradient*. Biotechnology and Applied Biochemistry, 2010. **55**(4): p. 199-208.

37. Shainer, R., et al., *Efficient isolation and chondrogenic differentiation of adult mesenchymal stem cells with fibrin microbeads and micronized collagen sponges*. Regenerative Medicine, 2010. **5**(2): p. 255-265.
38. Soleimani, M. and S. Nadri, *A protocol for isolation and culture of mesenchymal stem cells from mouse bone marrow*. Nature Protocols, 2009. **4**(1): p. 102-106.
39. Fulzele, K., et al., *Insulin Receptor Signaling in Osteoblasts Regulates Postnatal Bone Acquisition and Body Composition*. Cell, 2010. **142**(2): p. 309-319.
40. Clemens, T.L. and G. Karsenty, *The osteoblast: An insulin target cell controlling glucose homeostasis*. Journal of Bone and Mineral Research, 2011. **26**(4): p. 677-680.
41. Nather, A., Z. Aziz, and H.J.C. Ong, *Structure of Bone*, in *Bone Grafts and Bone Substitutes*. p. 3-17.
42. Taichman, R.S., *Blood and bone: two tissues whose fates are intertwined to create the hematopoietic stem-cell niche*. Blood, 2005. **105**(7): p. 2631-2639.
43. Rodan, G.A., *Bone homeostasis*. Proceedings of the National Academy of Sciences, 1998. **95**(23): p. 13361-13362.
44. Robey, P.G., et al., *Thrombospondin is an osteoblast-derived component of mineralized extracellular matrix*. J Cell Biol, 1989. **108**(2): p. 719-27.
45. Ganss, B., R.H. Kim, and J. Sodek, *Bone sialoprotein*. Crit Rev Oral Biol Med, 1999. **10**(1): p. 79-98.
46. Bonucci, E., G. Silvestrini, and P. Bianco, *Extracellular alkaline phosphatase activity in mineralizing matrices of cartilage and bone: ultrastructural localization using a cerium-based method*. Histochemistry, 1992. **97**(4): p. 323-327.
47. Termine, J.D., et al., *Osteonectin, a bone-specific protein linking mineral to collagen*. Cell, 1981. **26**(1 Pt 1): p. 99-105.
48. Hauschka, P.V., et al., *Osteocalcin and matrix Gla protein: vitamin K-dependent proteins in bone*. Physiol Rev, 1989. **69**(3): p. 990-1047.
49. Rey, C., et al., *Bone mineral: update on chemical composition and structure*. Osteoporosis International, 2009. **20**(6): p. 1013-1021.
50. Tang, Y., et al., *TGF- β 1-induced migration of bone mesenchymal stem cells couples bone resorption with formation*. Nature Medicine, 2009. **15**(7): p. 757-765.
51. *Wheeless' Textbook of Orthopaedics*, ed. C. Wheeless. 1996: Duke University Medical Center's Division of Orthopedic Surgery, Data Trace Internet Publishing.
52. Gaur, T., et al., *Canonical WNT Signaling Promotes Osteogenesis by Directly Stimulating Runx2 Gene Expression*. Journal of Biological Chemistry, 2005. **280**(39): p. 33132-33140.
53. Nakashima, K., et al., *The Novel Zinc Finger-Containing Transcription Factor Osterix Is Required for Osteoblast Differentiation and Bone Formation*. Cell, 2002. **108**(1): p. 17-29.
54. Hall, B.K. and T. Miyake, *All for one and one for all: Condensations and the initiation of skeletal development*. BioEssays, 2000. **22**(2): p. 138-147.
55. Nishi, M., et al., *Effects of implantation of three-dimensional engineered bone tissue with a vascular-like structure on repair of bone defects*. Applied Surface Science, 2012.
56. Sundelacruz, S. and D.L. Kaplan, *Stem cell- and scaffold-based tissue engineering approaches to osteochondral regenerative medicine*. Seminars in Cell and Developmental Biology, 2009. **20**(6): p. 646-655.
57. Fox, J.M., et al., *Recent advances into the understanding of mesenchymal stem cell trafficking*. British Journal of Haematology, 2007. **137**(6): p. 491-502.

58. Schindeler, A., et al., *Bone remodeling during fracture repair: The cellular picture*. Seminars in Cell and Developmental Biology, 2008. **19**(5): p. 459-466.
59. Mackie, E.J., et al., *Endochondral ossification: How cartilage is converted into bone in the developing skeleton*. International Journal of Biochemistry and Cell Biology, 2008. **40**(1): p. 46-62.
60. Ortega, N., D.J. Behonick, and Z. Werb, *Matrix remodeling during endochondral ossification*. Trends in Cell Biology, 2004. **14**(2): p. 86-93.
61. Oh, J., et al., *Mutations in two matrix metalloproteinase genes, MMP-2 and MT1-MMP, are synthetic lethal in mice*. Oncogene, 2004. **23**(29): p. 5041-8.
62. Zhou, Z., et al., *Impaired endochondral ossification and angiogenesis in mice deficient in membrane-type matrix metalloproteinase I*. Proc Natl Acad Sci U S A, 2000. **97**(8): p. 4052-7.
63. Oblander, S.A., et al., *Distinctive functions of membrane type 1 matrix-metalloprotease (MT1-MMP or MMP-14) in lung and submandibular gland development are independent of its role in pro-MMP-2 activation*. Dev Biol, 2005. **277**(1): p. 255-69.
64. Strongin, A.Y., et al., *Mechanism of cell surface activation of 72-kDa type IV collagenase. Isolation of the activated form of the membrane metalloprotease*. J Biol Chem, 1995. **270**(10): p. 5331-8.
65. Sato, H., et al., *A matrix metalloproteinase expressed on the surface of invasive tumour cells*. Nature, 1994. **370**(6484): p. 61-5.
66. Arthur, A., A. Zannettino, and S. Gronthos, *The therapeutic applications of multipotential mesenchymal/stromal stem cells in skeletal tissue repair*. Journal of Cellular Physiology, 2009. **218**(2): p. 237-245.
67. Little, N., B. Rogers, and M. Flannery, *Bone formation, remodelling and healing*. Surgery, 2011. **29**(4): p. 141-145.
68. Tuan, R.S., *Biology of developmental and regenerative skeletogenesis*. Clinical Orthopaedics and Related Research, 2004(427 SUPPL.): p. S105-S117.
69. Fayaz, H.C., et al., *The role of stem cells in fracture healing and nonunion*. International Orthopaedics, 2011. **35**(11): p. 1587-1597.
70. O'Keeffe, R.M., Jr., B.L. Riemer, and S.L. Butterfield, *Harvesting of autogenous cancellous bone graft from the proximal tibial metaphysis. A review of 230 cases*. J Orthop Trauma, 1991. **5**(4): p. 469-74.
71. Tashjian, R.Z. and D.S. Horwitz, *Healing and graft-site morbidity rates for midshaft clavicle nonunions treated with open reduction and internal fixation augmented with iliac crest aspiration*. American journal of orthopedics (Belle Mead, N.J.), 2009. **38**(3): p. 133-136.
72. Tressler, M.A., et al., *Bone morphogenetic protein-2 compared to autologous iliac crest bone graft in the treatment of long bone nonunion*. Orthopedics, 2011. **34**(12): p. e877-e884.
73. Nowicki, P.D., et al., *Structural bone allograft in pediatric foot surgery*. American journal of orthopedics (Belle Mead, N.J.), 2010. **39**(5): p. 238-240.
74. Nelson, E.R., et al., *New bone formation by murine osteoprogenitor cells cultured on corticocancellous allograft bone*. Journal of Orthopaedic Research, 2008. **26**(12): p. 1660-1664.
75. Schlegel, A.K. and K. Donath, *BIO-OSS® - A resorbable bone substitute?* Journal of Long-Term Effects of Medical Implants, 1998. **8**(3-4): p. 201-209.

76. Block, M.S., C.W. Ducote, and D.E. Mercante, *Horizontal Augmentation of Thin Maxillary Ridge With Bovine Particulate Xenograft Is Stable During 500 Days of Follow-Up: Preliminary Results of 12 Consecutive Patients*. Journal of Oral and Maxillofacial Surgery, 2012. **70**(6): p. 1321-1330.
77. Suckow, M.A., et al., *Enhanced bone regeneration using porcine small intestinal submucosa*. Journal of Investigative Surgery, 1999. **12**(5): p. 277-287.
78. Di Stefano, D.A., et al., *Alveolar ridge regeneration with equine spongy bone: A clinical, histological, and immunohistochemical case series*. Clinical Implant Dentistry and Related Research, 2009. **11**(2): p. 90-100.
79. Shafiei-Sarvestani, Z., et al., *The effect of hydroxyapatite-hPRP, and coral-hPRP on bone healing in rabbits: Radiological, biomechanical, macroscopic and histopathologic evaluation*. International Journal of Surgery, 2012. **10**(2): p. 96-101.
80. Yukna, R.A. and C.N. Yukna, *A 5-year follow-up of 16 patients treated with coralline calcium carbonate (Biocoral™) bone replacement grafts in infrabony defects*. Journal of Clinical Periodontology, 1998. **25**(12): p. 1036-1040.
81. Pryor, L.S., et al., *Review of Bone Substitutes*. Cranial Maxillofac Trauma Reconstruction, 2009. **2**(EFirst): p. 151-160.
82. Mittermayer, F., et al., *Long-term followup of uncemented tumor endoprostheses for the lower extremity*. Clinical Orthopaedics and Related Research, 2001(388): p. 167-177.
83. Navarro, M., et al., *Biomaterials in orthopaedics*. Journal of The Royal Society Interface, 2008. **5**(27): p. 1137-1158.
84. De la Torre, B., et al., *10 years results of an uncemented metaphyseal fit modular stem in elderly patients*. Vol. 45. 2011. 351-358.
85. Hench, L.L. and I. Thompson, *Twenty-first century challenges for biomaterials*. Journal of The Royal Society Interface, 2010. **7**(Suppl 4): p. S379-S391.
86. Díaz-Prado, S., et al., *Potential use of the human amniotic membrane as a scaffold in human articular cartilage repair*. Cell and Tissue Banking, 2010. **11**(2): p. 183-195.
87. Macchiarini, P., et al., *Clinical transplantation of a tissue-engineered airway*. The Lancet, 2008. **372**(9655): p. 2023-2030.
88. Zhao, Y., et al., *The development of a tissue-engineered artery using decellularized scaffold and autologous ovine mesenchymal stem cells*. Biomaterials, 2010. **31**(2): p. 296-307.
89. Lu, Z., et al., *Bone biomimetic microenvironment induces osteogenic differentiation of adipose tissue-derived mesenchymal stem cells*. Nanomedicine: Nanotechnology, Biology, and Medicine, 2011.
90. Carter, P. and N. Bhattarai, *Chapter 7 - Bioscaffolds: Fabrication and Performance*, in *Engineered Biomimicry*, A. Lakhtakia and R.J. Martín-Palma, Editors. 2013, Elsevier: Boston. p. 161-188.
91. Xia, Y., et al., *Bone tissue engineering using bone marrow stromal cells and an injectable sodium alginate/gelatin scaffold*. Journal of Biomedical Materials Research - Part A, 2012. **100 A**(4): p. 1044-1050.
92. Bellucci, D., et al., *Processing and characterization of innovative scaffolds for bone tissue engineering*. Journal of Materials Science: Materials in Medicine, 2012: p. 1-13.
93. Dias, M.R., et al., *Permeability analysis of scaffolds for bone tissue engineering*. Journal of Biomechanics, 2012. **45**(6): p. 938-944.

94. Pek, Y.S., A.C.A. Wan, and J.Y. Ying, *The effect of matrix stiffness on mesenchymal stem cell differentiation in a 3D thixotropic gel*. *Biomaterials*, 2010. **31**(3): p. 385-391.
95. Frosch, K.-H. and K. Stürmer, *Metallic Biomaterials in Skeletal Repair*. *European Journal of Trauma*, 2006. **32**(2): p. 149-159.
96. Petite, H., et al., *Tissue-engineered bone regeneration*. *Nature Biotechnology*, 2000. **18**(9): p. 959-963.
97. Runyan, C.M., et al., *Porcine allograft mandible revitalization using autologous adipose-derived stem cells, bone morphogenetic protein-2, and periosteum*. *Plastic and Reconstructive Surgery*, 2010. **125**(5): p. 1372-1382.
98. Tilley, S., et al., *Taking tissue-engineering principles into theater: augmentation of impacted allograft with human bone marrow stromal cells*. *Regenerative medicine*, 2006. **1**(5): p. 685-692.
99. Aarvold, A., et al., *Taking tissue engineering principles into theatre: Retrieval analysis from a clinically translated case*. *Regenerative medicine*, 2011. **6**(4): p. 461-467.
100. Isenberg, B.C., C. Williams, and R.T. Tranquillo, *Small-diameter artificial arteries engineered in vitro*. *Circulation Research*, 2006. **98**(1): p. 25-35.
101. Kim, B.S., et al., *Optimizing seeding and culture methods to engineer smooth muscle tissue on biodegradable polymer matrices*. *Biotechnology and Bioengineering*, 1998. **57**(1): p. 46-54.
102. Cai, X., et al., *Preparation and characterization of homogeneous chitosan-poly(lactic acid)/hydroxyapatite nanocomposite for bone tissue engineering and evaluation of its mechanical properties*. *Acta Biomaterialia*, 2009. **5**(7): p. 2693-2703.
103. Hutmacher, D.W., *Scaffolds in tissue engineering bone and cartilage*. *Biomaterials*, 2000. **21**(24): p. 2529-2543.
104. Cohn, D. and A. Hotovely Salomon, *Designing biodegradable multiblock PCL/PLA thermoplastic elastomers*. *Biomaterials*, 2005. **26**(15): p. 2297-2305.
105. Connelly, J.T., et al., *Fibronectin- and collagen-mimetic ligands regulate bone marrow stromal cell chondrogenesis in three-dimensional hydrogels*. *European cells & materials*, 2011. **22**: p. 168-176; discussion 176-177.
106. Lee, H.J., S.H. Ahn, and G.H. Kim, *Three-dimensional collagen/alginate hybrid scaffolds functionalized with a drug delivery system (DDS) for bone tissue regeneration*. *Chemistry of Materials*, 2012. **24**(5): p. 881-891.
107. Ng, K.K., H.S. Thatte, and M. Spector, *Chondrogenic differentiation of adult mesenchymal stem cells and embryonic cells in collagen scaffolds*. *Journal of Biomedical Materials Research - Part A*, 2011. **99 A**(2): p. 275-282.
108. Zhang, L., et al., *In vivo alveolar bone regeneration by bone marrow stem cells/fibrin glue composition*. *Archives of Oral Biology*, 2012. **57**(3): p. 238-244.
109. Zhou, H. and H.H.K. Xu, *The fast release of stem cells from alginate-fibrin microbeads in injectable scaffolds for bone tissue engineering*. *Biomaterials*, 2011. **32**(30): p. 7503-7513.
110. Dozza, B., et al., *Mesenchymal stem cells and platelet lysate in fibrin or collagen scaffold promote non-cemented hip prosthesis integration*. *Journal of Orthopaedic Research*, 2011. **29**(6): p. 961-968.
111. Mendonça-Caridad, J., et al., *A novel approach to human cranial tissue regeneration and frontal sinus obliteration with an autogenous platelet-rich/fibrin-rich composite*

- matrix: 10 patients with a 6-10year follow-up.* Journal of Tissue Engineering and Regenerative Medicine, 2012.
112. Roohani-Esfahani, S.I., et al., *Effect of self-assembled nanofibrous silk/polycaprolactone layer on the osteoconductivity and mechanical properties of biphasic calcium phosphate scaffolds.* Acta Biomaterialia, 2012. **8**(1): p. 302-312.
 113. Moisenovich, M.M., et al., *Tissue regeneration in vivo within recombinant spidroin 1 scaffolds.* Biomaterials, 2012. **33**(15): p. 3887-3898.
 114. Rockwood, D.N., et al., *Ingrowth of human mesenchymal stem cells into porous silk particle reinforced silk composite scaffolds: An in vitro study.* Acta Biomaterialia, 2011. **7**(1): p. 144-151.
 115. Park, J.K., et al., *Solid free-form fabrication of tissue-engineering scaffolds with a poly(lactic-co-glycolic acid) grafted hyaluronic acid conjugate encapsulating and intact bone morphogenetic protein-2/poly(ethylene glycol) complex.* Advanced Functional Materials, 2011. **21**(15): p. 2906-2912.
 116. Lungu, A., et al., *The effect of BMP-4 loaded in 3D collagen-hyaluronic acid scaffolds on biocompatibility assessed with MG 63 osteoblast-like cells.* Digest Journal of Nanomaterials and Biostructures, 2011. **6**(4): p. 1897-1908.
 117. Costa-Pinto, A.R., et al., *Chitosan-poly(butylene succinate) scaffolds and human bone marrow stromal cells induce bone repair in a mouse calvaria model.* Journal of Tissue Engineering and Regenerative Medicine, 2012. **6**(1): p. 21-28.
 118. Cruz, D.M.G., et al., *Differentiation of mesenchymal stem cells in chitosan scaffolds with double micro and macroporosity.* Journal of Biomedical Materials Research - Part A, 2010. **95**(4): p. 1182-1193.
 119. Kolambkar, Y.M., et al., *An alginate-based hybrid system for growth factor delivery in the functional repair of large bone defects.* Biomaterials, 2011. **32**(1): p. 65-74.
 120. Lee, G.S., et al., *Alginate combined calcium phosphate cements: Mechanical properties and in vitro rat bone marrow stromal cell responses.* Journal of Materials Science: Materials in Medicine, 2011. **22**(5): p. 1257-1268.
 121. Petrenko, Y.A., et al., *Comparison of the methods for seeding human bone marrow mesenchymal stem cells to macroporous alginate cryogel carriers.* Bulletin of Experimental Biology and Medicine, 2011: p. 1-4.
 122. Turco, G., et al., *Alginate/hydroxyapatite biocomposite for bone ingrowth: A trabecular structure with high and isotropic connectivity.* Biomacromolecules, 2009. **10**(6): p. 1575-1583.
 123. Boccaccini, A.R., et al., *Biodegradable and bioactive polymer/bioglass® composite foams for tissue engineering scaffolds.* 2005: Herceg Novi. p. 499-506.
 124. Day, R.M., et al., *In vitro and in vivo analysis of macroporous biodegradable poly(D,L-lactide-co-glycolide) scaffolds containing bioactive glass.* Journal of Biomedical Materials Research - Part A, 2005. **75**(4): p. 778-787.
 125. Wang, L., et al., *Porous bioactive scaffold of aliphatic polyurethane and hydroxyapatite for tissue regeneration.* Biomedical Materials, 2009. **4**(2).
 126. Wu, Y.C., et al., *A comparative study of the physical and mechanical properties of three natural corals based on the criteria for bone-tissue engineering scaffolds.* Journal of Materials Science: Materials in Medicine, 2009. **20**(6): p. 1273-1280.
 127. Temenoff, J.S. and A.G. Mikos, *Injectable biodegradable materials for orthopedic tissue engineering.* Biomaterials, 2000. **21**(23): p. 2405-2412.

128. Cai, Q., et al., *A novel porous cells scaffold made of polylactide-dextran blend by combining phase-separation and particle-leaching techniques*. *Biomaterials*, 2002. **23**(23): p. 4483-4492.
129. Ciardelli, G., et al., *Blends of poly-(ϵ -caprolactone) and polysaccharides in tissue engineering applications*. *Biomacromolecules*, 2005. **6**(4): p. 1961-1976.
130. Tramper, J. and A.W.A. De Man, *Characterization of Nitrobacter agilis immobilized in calcium alginate*. *Enzyme and Microbial Technology*, 1986. **8**(8): p. 472-476.
131. Wang, X., et al., *Gelcasting of silicon carbide based on gelation of sodium alginate*. *Ceramics International*, 2002. **28**(8): p. 865-871.
132. Goh, C.H., P.W.S. Heng, and L.W. Chan, *Alginates as a useful natural polymer for microencapsulation and therapeutic applications*. *Carbohydrate Polymers*, 2012. **88**(1): p. 1-12.
133. Arica, M.Y., Y. Kaçar, and Ö. Genç, *Entrapment of white-rot fungus Trametes versicolor in Ca-alginate beads: Preparation and biosorption kinetic analysis for cadmium removal from an aqueous solution*. *Bioresource Technology*, 2001. **80**(2): p. 121-129.
134. Sun, A.M., *Microencapsulation of pancreatic islet cells: A bioartificial endocrine pancreas*. *Methods in Enzymology*, 1988. **137**: p. 575-580.
135. Purcell, E.K., A. Singh, and D.R. Kipke, *Alginate composition effects on a neural stem cell-seeded scaffold*. *Tissue Eng Part C Methods*, 2009. **15**(4): p. 541-50.
136. Constantinidis, I., et al., *Effects of alginate composition on the metabolic, secretory, and growth characteristics of entrapped β TC3 mouse insulinoma cells*. *Biomaterials*, 1999. **20**(21): p. 2019-2027.
137. Kong, H.J., M.K. Smith, and D.J. Mooney, *Designing alginate hydrogels to maintain viability of immobilized cells*. *Biomaterials*, 2003. **24**(22): p. 4023-4029.
138. West, E.R., et al., *Physical properties of alginate hydrogels and their effects on in vitro follicle development*. *Biomaterials*, 2007. **28**(30): p. 4439-4448.
139. Augst, A.D., H.J. Kong, and D.J. Mooney, *Alginate hydrogels as biomaterials*. *Macromolecular Bioscience*, 2006. **6**(8): p. 623-633.
140. Dhoot, N.O., et al., *Peptide-modified alginate surfaces as a growth permissive substrate for neurite outgrowth*. *Journal of Biomedical Materials Research - Part A*, 2004. **71**(2): p. 191-200.
141. Prang, P., et al., *The promotion of oriented axonal regrowth in the injured spinal cord by alginate-based anisotropic capillary hydrogels*. *Biomaterials*, 2006. **27**(19): p. 3560-3569.
142. Bidarra, S.I.J., et al., *Immobilization of Human Mesenchymal Stem Cells within RGD-Grafted Alginate Microspheres and Assessment of Their Angiogenic Potential*. *Biomacromolecules*, 2010. **11**(8): p. 1956-1964.
143. Huang, X., et al., *Microenvironment of alginate-based microcapsules for cell culture and tissue engineering*. *Journal of Bioscience and Bioengineering*, 2012. **114**(1): p. 1-8.
144. Arica, M.Y., et al., *Ca-alginate as a support for Pb(II) and Zn(II) biosorption with immobilized Phanerochaete chrysosporium*. *Carbohydrate Polymers*, 2003. **52**(2): p. 167-174.
145. Stabler, C., et al., *The effects of alginate composition on encapsulated β TC3 cells*. *Biomaterials*, 2001. **22**(11): p. 1301-1310.

146. Grellier, M., et al., *The effect of the co-immobilization of human osteoprogenitors and endothelial cells within alginate microspheres on mineralization in a bone defect*. Biomaterials, 2009. **30**(19): p. 3271-3278.
147. Ben-David, D., et al., *Cell-scaffold transplant of hydrogel seeded with rat bone marrow progenitors for bone regeneration*. Journal of Cranio-Maxillofacial Surgery, 2011. **39**(5): p. 364-371.
148. Poldervaart, M.T., et al., *Sustained release of BMP-2 in bioprinted alginate for osteogenicity in mice and rats*. PLoS ONE, 2013. **8**(8): p. e72610.
149. Lim, H., et al., *Controlled release of BMP-2 from alginate nanohydrogels enhanced osteogenic differentiation of human bone marrow stromal cells*. Macromolecular Research, 2010. **18**(8): p. 787-792.
150. Wegman, F., et al., *Osteogenic differentiation as a result of BMP-2 plasmid DNA based gene therapy in vitro and in vivo*. European Cells and Materials, 2011. **21**: p. 230-42; discussion 242.
151. Axelrad, T.W. and T.A. Einhorn, *Bone morphogenetic proteins in orthopaedic surgery*. Cytokine & Growth Factor Reviews, 2009. **20**(5-6): p. 481-488.
152. Cheung, A. and A.M. Phillips, *Bone morphogenetic proteins in orthopaedic surgery*. Current Orthopaedics, 2006. **20**(6): p. 424-429.
153. Burkus, J.K., et al., *Anterior lumbar interbody fusion using rhBMP-2 with tapered interbody cages*. Journal of Spinal Disorders and Techniques, 2002. **15**(5): p. 337-49.
154. Friedlaender, G.E., et al., *Osteogenic protein-1 (bone morphogenetic protein-7) in the treatment of tibial nonunions*. J Bone Joint Surg Am, 2001. **83-A Suppl 1**(Pt 2): p. S151-8.
155. Nauth, A., et al., *Growth factors and bone regeneration: How much bone can we expect?* Injury, 2011. **42**(6): p. 574-579.
156. Carragee, E.J., E.L. Hurwitz, and B.K. Weiner, *A critical review of recombinant human bone morphogenetic protein-2 trials in spinal surgery: emerging safety concerns and lessons learned*. The Spine Journal, 2011. **11**(6): p. 471-491.
157. Branch Jr, C.L., *Physician-directed (off-label) use of recombinant bone morphogenetic protein-2: let us do it well!* The Spine Journal, 2011. **11**(6): p. 469-470.
158. Carragee, E.J., et al., *A challenge to integrity in spine publications: years of living dangerously with the promotion of bone growth factors*. The Spine Journal, 2011. **11**(6): p. 463-468.
159. Carragee, E.J., et al., *Retrograde ejaculation after anterior lumbar interbody fusion using rhBMP-2: a cohort controlled study*. The Spine Journal, 2011. **11**(6): p. 511-516.
160. Dmitriev, A.E., R.A. Lehman Jr, and A.J. Symes, *Bone morphogenetic protein-2 and spinal arthrodesis: the basic science perspective on protein interaction with the nervous system*. The Spine Journal, 2011. **11**(6): p. 500-505.
161. Jeong, G.K. and H.S. Sandhu, *Applications of Recombinant Human Bone Morphogenetic Protein-2 (rhBMP-2) in Spinal Surgery*. Seminars in Spine Surgery, 2006. **18**(1): p. 15-21.
162. Kang, J.D., *Commentary: Another complication associated with rhBMP-2?* The Spine Journal, 2011. **11**(6): p. 517-519.
163. Mirza, S.K., *Commentary: Folly of FDA-approval studies for bone morphogenetic protein*. The Spine Journal, 2011. **11**(6): p. 495-499.
164. Spengler, D.M., *Commentary: Resetting standards for sponsored research: do conflicts influence results?* The Spine Journal, 2011. **11**(6): p. 492-494.

165. Woo, E.J., *Adverse Events Reported After the Use of Recombinant Human Bone Morphogenetic Protein 2*. Journal of Oral and Maxillofacial Surgery, 2012. **70**(4): p. 765-767.
166. Bell, R.B. and C. Gregoire, *Reconstruction of Mandibular Continuity Defects Using Recombinant Human Bone Morphogenetic Protein 2: A Note of Caution in an Atmosphere of Exuberance*. Journal of Oral and Maxillofacial Surgery, 2009. **67**(12): p. 2673-2678.
167. Carragee, E.J., et al., *A biologic without guidelines: the YODA project and the future of bone morphogenetic protein-2 research*. The Spine Journal, 2012. **12**(10): p. 877-880.
168. Carragee, E.J., C.M. Bono, and G.J. Scuderi, *Pseudomorbidity in iliac crest bone graft harvesting: the rise of rhBMP-2 in short-segment posterior lumbar fusion*. The Spine Journal, 2009. **9**(11): p. 873-879.
169. Carragee, E.J., et al., *Future directions for The Spine Journal: managing and reporting conflict of interest issues*. The Spine Journal, 2011. **11**(8): p. 695-697.
170. Glassman, S.D., et al., *Complications with recombinant human bone morphogenetic protein-2 in posterolateral spine fusion associated with a dural tear*. The Spine Journal, 2011. **11**(6): p. 522-526.
171. Haid Jr, R.W., et al., *Posterior lumbar interbody fusion using recombinant human bone morphogenetic protein type 2 with cylindrical interbody cages*. The Spine Journal, 2004. **4**(5): p. 527-538.
172. Smoljanovic, T. and I. Bojanic, *Commentary: An evolving perception of the risk of rhBMP-2 use for anterior spinal interbody fusions*. The Spine Journal, 2011. **11**(6): p. 520-521.
173. Marx, R.E., et al., *Platelet-rich plasma: Growth factor enhancement for bone grafts*. Oral Surgery, Oral Medicine, Oral Pathology, Oral Radiology, and Endodontology, 1998. **85**(6): p. 638-646.
174. Weibrich, G., et al., *Effect of platelet concentration in platelet-rich plasma on peri-implant bone regeneration*. Bone, 2004. **34**(4): p. 665-671.
175. van den Dolder, J., et al., *Platelet-rich plasma: quantification of growth factor levels and the effect on growth and differentiation of rat bone marrow cells*. Tissue Engineering, 2006. **12**(11): p. 3067-73.
176. Caplan, A.I. and D. Correa, *PDGF in bone formation and regeneration: New insights into a novel mechanism involving MSCs*. Journal of Orthopaedic Research, 2011. **29**(12): p. 1795-1803.
177. Salgado, R., et al., *Platelets and vascular endothelial growth factor (VEGF): a morphological and functional study*. Angiogenesis, 2001. **4**(1): p. 37-43.
178. Pintucci, G., et al., *Trophic effects of platelets on cultured endothelial cells are mediated by platelet-associated fibroblast growth factor-2 (FGF-2) and vascular endothelial growth factor (VEGF)*. Thromb Haemost, 2002. **88**(5): p. 834-42.
179. Zhang, Y.D., et al., *Combination of platelet-rich plasma with degradable bioactive borate glass for segmental bone defect repair*. Acta Orthop Belg, 2011. **77**(1): p. 110-5.
180. Hakimi, M., et al., *Combined use of platelet-rich plasma and autologous bone grafts in the treatment of long bone defects in mini-pigs*. Injury, 2010. **41**(7): p. 717-723.
181. Kanthan, S.R., et al., *Platelet-rich plasma (PRP) enhances bone healing in non-union critical-sized defects: A preliminary study involving rabbit models*. Injury, 2011. **42**(8): p. 782-789.

182. Yamada, Y., et al., *Autogenous injectable bone for regeneration with mesenchymal stem cells and platelet-rich plasma: tissue-engineered bone regeneration*. Tissue Engineering, 2004. **10**(5-6): p. 955-64.
183. Yoon, J.-S., S.-H. Lee, and H.-J. Yoon, *The influence of platelet-rich fibrin on angiogenesis in guided bone regeneration using xenogenic bone substitutes: A study of rabbit cranial defects*. Journal of Cranio-Maxillofacial Surgery, 2014(0).
184. Sanchez, M., et al., *Nonunions treated with autologous preparation rich in growth factors*. J Orthop Trauma, 2009. **23**(1): p. 52-9.
185. Cancedda, R., P. Giannoni, and M. Mastrogiacomo, *A tissue engineering approach to bone repair in large animal models and in clinical practice*. Biomaterials, 2007. **28**(29): p. 4240-4250.
186. Sanchez, A.R., P.J. Sheridan, and L.I. Kupp, *Is platelet-rich plasma the perfect enhancement factor? A current review*. Int J Oral Maxillofac Implants, 2003. **18**(1): p. 93-103.
187. Xu, Z., et al., *Combination of pigment epithelium-derived factor with radiotherapy enhances the antitumor effects on nasopharyngeal carcinoma by downregulating vascular endothelial growth factor expression and angiogenesis*. Cancer Sci, 2011.
188. Gong, Q., et al., *Expression and purification of functional epitope of pigment epithelium-derived factor in E. coli with inhibiting effect on endothelial cells*. Protein Journal, 2010. **29**(3): p. 167-173.
189. Tombran-Tink, J., et al., *PEDF and the serpins: Phylogeny, sequence conservation, and functional domains*. Journal of Structural Biology, 2005. **151**(2): p. 130-150.
190. Samkharadze, T., et al., *Pigment epithelium-derived factor associates with neuropathy and fibrosis in pancreatic cancer*. Am J Gastroenterol, 2011. **106**(5): p. 968-80.
191. Olson, S.T. and P.G. Gettins, *Regulation of proteases by protein inhibitors of the serpin superfamily*. Prog Mol Biol Transl Sci, 2011. **99**: p. 185-240.
192. Akiyama, T., et al., *PEDF regulates osteoclasts via osteoprotegerin and RANKL*. Biochemical and Biophysical Research Communications, 2010. **391**(1): p. 789-794.
193. Sanchez-Sanchez, F., et al., *Expression and purification of functional recombinant human pigment epithelium-derived factor (PEDF) secreted by the yeast Pichia pastoris*. J Biotechnol, 2008. **134**(1-2): p. 193-201.
194. Broadhead, M.L., C.R. Dass, and P.F. Choong, *In vitro and in vivo biological activity of PEDF against a range of tumors*. Expert Opinion on Therapeutic Targets, 2009. **13**(12): p. 1429-1438.
195. Elahy, M., S. Baidur-Hudson, and C.R. Dass, *The emerging role of PEDF in stem cell biology*. Journal of Biomedicine and Biotechnology, 2012. **2012**.
196. Quan, G.M.Y., et al., *Localization of pigment epithelium-derived factor in growing mouse bone*. Calcified Tissue International, 2005. **76**(2): p. 146-153.
197. Sarojini, H., et al., *PEDF from mouse mesenchymal stem cell secretome attracts fibroblasts*. J Cell Biochem, 2008. **104**(5): p. 1793-802.
198. Tombran-Tink, J. and C.J. Barnstable, *Osteoblasts and osteoclasts express PEDF, VEGF-A isoforms, and VEGF receptors: possible mediators of angiogenesis and matrix remodeling in the bone*. Biochemical and Biophysical Research Communications, 2004. **316**(2): p. 573-579.
199. Chiellini, C., et al., *Characterization of human mesenchymal stem cell secretome at early steps of adipocyte and osteoblast differentiation*. BMC Mol Biol, 2008. **9**: p. 26.

200. Fan, W., R. Crawford, and Y. Xiao, *The ratio of VEGF/PEDF expression in bone marrow mesenchymal stem cells regulates neovascularization*. *Differentiation*, 2011. **81**(3): p. 181-91.
201. Bexell, D., et al., *Bone marrow multipotent mesenchymal stroma cells act as pericyte-like migratory vehicles in experimental gliomas*. *Molecular Therapy*, 2009. **17**(1): p. 183-190.
202. Bergers, G. and S. Song, *The role of pericytes in blood-vessel formation and maintenance*. *Neuro-Oncology*, 2005. **7**(4): p. 452-464.
203. Ahmadbeigi, N., et al., *Dormant phase and multinuclear cells: two key phenomena in early culture of murine bone marrow mesenchymal stem cells*. *Stem Cells Dev*, 2011. **20**(8): p. 1337-47.
204. Dass, C.R., et al., *Dz13 induces a cytotoxic stress response with upregulation of E2F1 in tumor cells metastasizing to or from bone*. *Oligonucleotides*, 2010. **20**(2): p. 79-91.
205. Yang, M.T., et al., *Assaying stem cell mechanobiology on microfabricated elastomeric substrates with geometrically modulated rigidity*.
206. Li, X., et al., *Culture of neural stem cells in calcium alginate beads*. *Biotechnology Progress*, 2006. **22**(6): p. 1683-1689.
207. Nadiminty, N., et al., *Prostate-Specific Antigen Modulates Genes Involved in Bone Remodeling and Induces Osteoblast Differentiation of Human Osteosarcoma Cell Line SaOS-2*. *Clinical Cancer Research*, 2006. **12**(5): p. 1420-1430.
208. Langenbach, F. and J. Handschel, *Effects of dexamethasone, ascorbic acid and β -glycerophosphate on the osteogenic differentiation of stem cells in vitro*. *Stem Cell Research & Therapy*, 2013. **4**(5): p. 117-117.
209. Choong, P.F.M., et al., *The molecular pathogenesis of osteosarcoma: A review*. *Sarcoma*, 2011. **2011**.
210. Hoemann, C.D., H. El-Gabalawy, and M.D. McKee, *In vitro osteogenesis assays: Influence of the primary cell source on alkaline phosphatase activity and mineralization*. *Pathologie Biologie*, 2009. **57**(4): p. 318-323.
211. Tan, M.L., P.F. Choong, and C.R. Dass, *Anti-chondrosarcoma effects of PEDF mediated via molecules important to apoptosis, cell cycling, adhesion and invasion*. *Biochemical and Biophysical Research Communications*, 2010. **398**(4): p. 613-8.
212. Dass, C.R. and P.F. Choong, *uPAR mediates anticancer activity of PEDF*. *Cancer Biology and Therapy*, 2008. **7**(8): p. 1262-70.
213. Gregory, C.A., et al., *An Alizarin red-based assay of mineralization by adherent cells in culture: Comparison with cetylpyridinium chloride extraction*. *Analytical Biochemistry*, 2004. **329**(1): p. 77-84.
214. Dass, C.R., et al., *A novel orthotopic murine model provides insights into cellular and molecular characteristics contributing to human osteosarcoma*. *Clinical and Experimental Metastasis*, 2006. **23**(7-8): p. 367-380.
215. Ek, E.T.H., et al., *Pigment epithelium-derived factor overexpression inhibits orthotopic osteosarcoma growth, angiogenesis and metastasis*. *Cancer Gene Therapy*, 2007. **14**(7): p. 616-626.
216. Petersen, S.V., Z. Valnickova, and J.J. Enghild, *Pigment-epithelium-derived factor (PEDF) occurs at a physiologically relevant concentration in human blood: purification and characterization*. *Biochem J*, 2003. **374**(Pt 1): p. 199-206.

217. Rennert, R.C., et al., *Stem cell recruitment after injury: lessons for regenerative medicine*. *Regenerative medicine*, 2012. **7**(6): p. 833-850.
218. Hou, H.-Y., et al., *A Therapeutic Strategy for Choroidal Neovascularization Based on Recruitment of Mesenchymal Stem Cells to the Sites of Lesions*. *Mol Ther*, 2010. **18**(10): p. 1837-1845.
219. Gattu, A.K., et al., *Determination of mesenchymal stem cell fate by pigment epithelium-derived factor (PEDF) results in increased adiposity and reduced bone mineral content*. *FASEB J*, 2013. **27**(11): p. 4384-94.
220. Li, F., et al., *Pigment Epithelium Derived Factor Enhances Differentiation and Mineral Deposition of Human Mesenchymal Stem Cells*. *Stem Cells*, 2013.
221. Ahmadbeigi, N., et al., *Dormant phase and multinuclear cells: Two key phenomena in early culture of murine bone marrow mesenchymal stem cells*. *Stem Cells and Development*, 2011. **20**(8): p. 1337-1347.
222. Wegmeyer, H., et al., *Mesenchymal stromal cell characteristics vary depending on their origin*. *Stem Cells and Development*, 2013. **22**(19): p. 2606-2618.
223. Chamberlain, G., et al., *Concise Review: Mesenchymal Stem Cells: Their Phenotype, Differentiation Capacity, Immunological Features, and Potential for Homing*. *Stem Cells*, 2007. **25**(11): p. 2739-2749.
224. Anisimov, S.V., et al., *Identification of molecules derived from human fibroblast feeder cells that support the proliferation of human embryonic stem cells*. *Cellular and Molecular Biology Letters*, 2011. **16**(1): p. 79-88.
225. Zhu, D., et al., *Polarized secretion of PEDF from human embryonic stem cell-derived RPE promotes retinal progenitor cell survival*. *Investigative Ophthalmology and Visual Science*, 2011. **52**(3): p. 1573-1585.
226. Ramírez-Castillejo, C., et al., *Pigment epithelium-derived factor is a niche signal for neural stem cell renewal*. *Nature Neuroscience*, 2006. **9**(3): p. 331-339.
227. Andreu-Agulló, C., et al., *Vascular niche factor PEDF modulates notch-dependent stemness in the adult subependymal zone*. *Nature Neuroscience*, 2009. **12**(12): p. 1514-1523.
228. Tong, J.P. and Y.F. Yao, *Contribution of VEGF and PEDF to choroidal angiogenesis: A need for balanced expressions*. *Clinical Biochemistry*, 2006. **39**(3): p. 267-276.
229. Trotman, R.J., et al., *Calcium alginate bead immobilization of cells containing tyrosine ammonia lyase activity for use in the production of p-hydroxycinnamic acid*. *Biotechnology Progress*, 2007. **23**(3): p. 638-644.
230. Weir, M.D. and H.H.K. Xu, *Human bone marrow stem cell-encapsulating calcium phosphate scaffolds for bone repair*. *Acta Biomaterialia*, 2010. **6**(10): p. 4118-4126.
231. Wang, N., et al., *Alginate encapsulation technology supports embryonic stem cells differentiation into insulin-producing cells*. *Journal of Biotechnology*, 2009. **144**(4): p. 304-312.
232. Leslie, S.K., et al., *Controlled release of rat adipose-derived stem cells from alginate microbeads*. *Biomaterials*, 2013. **34**(33): p. 8172-8184.
233. Moshaverinia, A., et al., *Alginate hydrogel as a promising scaffold for dental-derived stem cells: An in vitro study*. *Journal of Materials Science: Materials in Medicine*, 2012. **23**(12): p. 3041-3051.

234. Moshaverinia, A., et al., *Dental mesenchymal stem cells encapsulated in an alginate hydrogel co-delivery microencapsulation system for cartilage regeneration*. Acta Biomaterialia, 2013.
235. Alsberg, E., et al., *Regulating bone formation via controlled scaffold degradation*. Journal of Dental Research, 2003. **82**(11): p. 903-908.
236. Lee, K.Y., E. Alsberg, and D.J. Mooney, *Degradable and injectable poly(aldehyde guluronate) hydrogels for bone tissue engineering*. Journal of Biomedical Materials Research, 2001. **56**(2): p. 228-233.
237. Bidarra, S.J., et al., *Immobilization of human mesenchymal stem cells within RGD-grafted alginate microspheres and assessment of their angiogenic potential*. Biomacromolecules, 2010. **11**(8): p. 1956-1964.
238. Moshaverinia, A., et al., *Co-encapsulation of anti-BMP2 monoclonal antibody and mesenchymal stem cells in alginate microspheres for bone tissue engineering*. Biomaterials, 2013. **34**(28): p. 6572-6579.
239. Lee, W.Y., et al., *The effect of bone marrow transplantation on the osteoblastic differentiation of human bone marrow stromal cells*. J Clin Endocrinol Metab, 2002. **87**(1): p. 329-35.
240. Thibault, R.A., et al., *Osteogenic differentiation of mesenchymal stem cells on pregenerated extracellular matrix scaffolds in the absence of osteogenic cell culture supplements*. Tissue Engineering. Part A, 2010. **16**(2): p. 431-40.
241. Srouji, S., S. Maurice, and E. Livne, *Microscopy analysis of bone marrow-derived osteoprogenitor cells cultured on hydrogel 3-D scaffold*. Microscopy Research and Technique, 2005. **66**(2-3): p. 132-138.
242. Hulsart-Billström, G., et al., *Calcium phosphates compounds in conjunction with hydrogel as carrier for BMP-2: A study on ectopic bone formation in rats*. Acta Biomaterialia, 2011. **7**(8): p. 3042-3049.
243. Yu, P.B., et al., *BMP type I receptor inhibition reduces heterotopic [corrected] ossification*. Nat Med, 2008. **14**(12): p. 1363-9.
244. Lee, J.H., et al., *Combined effects of porous hydroxyapatite and demineralized bone matrix on bone induction: in vitro and in vivo study using a nude rat model*. Biomed Mater, 2011. **6**(1): p. 015008.
245. Luca, L., et al., *Injectable rhBMP-2-loaded chitosan hydrogel composite: Osteoinduction at ectopic site and in segmental long bone defect*. Journal of Biomedical Materials Research Part A, 2011. **96A**(1): p. 66-74.
246. Qu, D., et al., *Ectopic osteochondral formation of biomimetic porous PVA-n-HA/PA6 bilayered scaffold and BMSCs construct in rabbit*. Journal of Biomedical Materials Research Part B: Applied Biomaterials, 2011. **96B**(1): p. 9-15.
247. Warnke, P.H., et al., *Growth and transplantation of a custom vascularised bone graft in a man*. The Lancet, 2004. **364**(9436): p. 766-770.
248. Luan, H.Q., et al., *The application of micro-CT in monitoring bone alterations in tail-suspended rats in vivo*. Advances in Space Research, 2014. **53**(11): p. 1567-1573.
249. Taiani, J.T., et al., *Embryonic stem cell therapy improves bone quality in a model of impaired fracture healing in the mouse; tracked temporally using in vivo micro-CT*. Bone, 2014. **64**: p. 263-272.
250. Zhang, L., et al., *Zwitterionic hydrogels implanted in mice resist the foreign-body reaction*. 2013.

251. Holmbeck, K., et al., *MT1-MMP-Deficient Mice Develop Dwarfism, Osteopenia, Arthritis, and Connective Tissue Disease due to Inadequate Collagen Turnover*. Cell, 1999. **99**(1): p. 81-92.
252. Kulkarni, R.N., et al., *MT1-MMP modulates the mechanosensitivity of osteocytes*. Biochemical and Biophysical Research Communications, 2012. **417**(2): p. 824-829.
253. Lieu, S., et al., *Impaired remodeling phase of fracture repair in the absence of matrix metalloproteinase-2*. Disease Models and Mechanisms, 2011. **4**(2): p. 203-211.
254. Karsdal, M.A., et al., *Matrix Metalloproteinase-dependent Activation of Latent Transforming Growth Factor- β Controls the Conversion of Osteoblasts into Osteocytes by Blocking Osteoblast Apoptosis*. Journal of Biological Chemistry, 2002. **277**(46): p. 44061-44067.
255. Lu, Z., et al., *Bone biomimetic microenvironment induces osteogenic differentiation of adipose tissue-derived mesenchymal stem cells*. Nanomedicine: Nanotechnology, Biology and Medicine, 2012. **8**(4): p. 507-515.
256. Cowan, C.M., et al., *Adipose-derived adult stromal cells heal critical-size mouse calvarial defects*. Nat Biotechnol, 2004. **22**(5): p. 560-7.
257. Wu, X., X. Liu, and S. Wang, *Implantation of biomaterial as an efficient method to harvest mesenchymal stem cells*. Experimental Biology and Medicine, 2011. **236**(12): p. 1477-1484.
258. Boden, S.D., et al., *Use of recombinant human bone morphogenetic protein-2 to achieve posterolateral lumbar spine fusion in humans: a prospective, randomized clinical pilot trial: 2002 Volvo Award in clinical studies*. Spine (Phila Pa 1976), 2002. **27**(23): p. 2662-73.
259. Vaidya, R., et al., *Complications of anterior cervical discectomy and fusion using recombinant human bone morphogenetic protein-2*. European Spine Journal, 2007. **16**(8): p. 1257-1265.
260. Smucker, J.D., et al., *Increased swelling complications associated with off-label usage of rhBMP-2 in the anterior cervical spine*. Spine (Phila Pa 1976), 2006. **31**(24): p. 2813-9.
261. Mroz, T.E., et al., *Complications related to osteobiologics use in spine surgery: a systematic review*. Spine (Phila Pa 1976), 2010. **35**(9 Suppl): p. S86-104.
262. Perri, B., et al., *Adverse swelling associated with use of rh-BMP-2 in anterior cervical discectomy and fusion: a case study*. The spine journal : official journal of the North American Spine Society, 2007. **7**(2): p. 235-239.
263. Zara, J.N., et al., *High doses of bone morphogenetic protein 2 induce structurally abnormal bone and inflammation in vivo*. Tissue Eng Part A, 2011. **17**(9-10): p. 1389-99.
264. Fan, J., et al., *Enhanced Osteogenesis of Adipose Derived Stem Cells with Noggin Suppression and Delivery of BMP-2*. PLoS ONE, 2013. **8**(8): p. e72474.
265. Yamagishi, S. and T. Matsui, *Advanced glycation end products (AGEs), oxidative stress and diabetic retinopathy*. Current Pharmaceutical Biotechnology, 2011. **12**(3): p. 362-368.
266. Yabe, T., et al., *Pigment epithelium-derived factor Induces pro-inflammatory genes in neonatal astrocytes through activation of NF- κ B and CREB*. Glia, 2005. **50**(3): p. 223-234.
267. Yabe, T., et al., *Pigment epithelium-derived factor induces pro-survival genes through cyclic AMP-responsive element binding protein and nuclear factor kappa B activation in*

- rat cultured cerebellar granule cells: Implication for its neuroprotective effect.* Neuroscience, 2005. **133**(3): p. 691-700.
268. Sanagi, T., T. Yabe, and H. Yamada, *The regulation of pro-inflammatory gene expression induced by pigment epithelium-derived factor in rat cultured microglial cells.* Neuroscience Letters, 2005. **380**(1-2): p. 105-110.